Final Degree Project

Study of end-of-life disposal options for highly-inclined geosynchronous satellites

Author: Elisabeth Cabot Costa

Supervisor: Dr. Elena Fantino

Co-supervisors: Dr. Josep Mª Domènech i Mas;

Dr. Daniel Garcia-Almiñana

A thesis submitted in partial fulfillment of the requirements for the Bachelor Degree in Aerospace Technology Engineering

at

Physics Department

Aeronautical Engineering Division

Polytechnic University of Catalonia (UPC)

June 2016

This page intentionally left blank

Universitat Politècnica de Catalunya

Abstract

School of Industrial and Aeronautic Engineering of Terrassa

Physics Department

Aeronautical Engineering Division

Bachelor Degree of Aerospace Technology Engineering

Study of end-of-life disposal options for highly-inclined geosynchronous satellites

by Elisabeth Cabot Costa

In recent years, the growing volume of activities in the northern regions (Arctic, Canada, Northern Russia) has produced an increasing request for communications services. Several studies have concluded that there are already unsatisfied demands for communications services in the Arctic, and that adequate solutions must be developed to meet current and future requirements. Coverage of high-latitude regions (north of, say, 70º degrees) is not possible (or is seriously limited) from the geostationary orbit. On the other hand, low-altitude orbits require large constellations.

In previous investigations (Fantino et al. 2013, Fantino et al. 2015), a family of eccentric, highly-inclined geosyncronous orbits has been proposed and the maintenance (i.e., orbit station keeping) requirements have been analysed. Once the mission is concluded, the long-term, uncontrolled orbital evolution of these orbits inevitably makes them cross the geostationary ring, with consequent high collision danger for the many telecommunications satellites operating at such altitudes. As a result, a disposal strategy is mandatory and, in agreement with current international space policy, should be conceived and detailed as part of the mission design. In particular, an adequate amount of propellant should be available at mission termination to carry out the corresponding end-of-life operations.

The proposed study consists of the evaluation of the available options (maneuver strategy, propellant cost, type of engine, execution times and any other relevant aspect that may arise) for the disposal of this type of satellites. The scarcity of satellites operating in this class of orbits gives the work a strong character of originality. Furthermore, the growing commercial interest

in extending satellite telecommunications service to the high latitude regions gives the study a clear projection into the future of space exploitation.

The study aims at identifying and evaluating alternative options for satellite end-of-life disposal from an eccentric highly-inclined geosynchronous orbit. The issues to be considered are the maneuver strategy, the execution times, the requirements on propellant mass and the type of engine required for maneuver execution.

Acknowledgements

I would like to especially thank my director, Dr. Elena Fantino. Her motivation, enthusiasm and support have been a major encouragement not only during the project, but also on the academic subject imparted by her during the academic year. Moreover, her outstanding searching skills and expertise have proved to be exceedingly valuable during the development of the project. She performed an extremely helpful follow-up work which has been really useful. Finally, my most sincere gratitude to my family and friends for their patience and understanding.

Contents

List of Figures

List of Tables

Abbreviations

AGI	**A**nalytical **G**raphics, **I**nc
CNES	**C**entre **N**ational d'**É**tudes **S**patiales
EC	**E**nvironment **C**anada
ESA	**E**uropean **S**pace **A**gency
FDP	**F**inal **D**egree **P**roject
GEO	**Ge**ostationary **O**rbits
HEO	**H**igh **E**lliptical **O**rbit / **H**igh **E**arth **O**rbit
IADC	**I**nter-**A**gency Space **D**ebris **C**oordination Committee
LEO	**L**ow **E**arth **O**rbit
LT	**L**ow **T**hrust
NASA	**N**ational **A**eronautics and **S**pace **A**dministration
ODE	**O**rdinary **D**ifferential **E**quations
RAAN	**R**ight **A**scension of the **A**scending **N**ode
STK	**S**ystems **T**ool **K**it
UAV	**U**nmanned **A**erial **V**ehicle
UNOOSA	**U**nited **N**ations **O**ffice for **O**uter **S**pace **A**ffairs

Physical Constants

Earth's sidereal rotation rate	$n_E = 7.292 \cdot 10^{-5}\ rad/s.$
Gravitational constant	$G = 6.674 \cdot 10^{-11}\ N\ m^2/kg^2.$
Earth's mass	$M_E = 5.972 \cdot 10^{24}\ kg.$
Earth's gravitational parameter	$\mu = 4 \cdot 10^5\ km^3/s^2.$
Earth's radius	$R_E = 6.371\ km$

Introduction

The objective of the study is to identify and evaluate alternative options for satellite end-of-life disposal from an eccentric highly-inclined geosynchronous orbit.

Currently, numerous studies [1, 2, 3, 4] have identified telecommunications gaps in the northern regions, specifically in the Artic zone, Canada and northern Russia. The reason of the existence of these gaps is the current use of geostationary orbits (GEO) for telecommunications missions. GEO orbits cannot satisfy the coverage in latitudes approximately above 60^{o} because the elevation of these satellites at these latitudes is not sufficient.

To highlight some researches, it can be mentioned that the Arctic Marine Shipping Assessment [10] remarks the lack of radio and satellite communications for data and voice transmission in this area. Environment Canada (EC) and national funded studies, such as MarCom [11] and MarSafe [11], have also shown the increasing request for communications services in the Artic. Another study [4] developed by the Norwegian Space Centre reaches the same conclusion, emphasizing the amount of parties from different sectors that intend to increase the communications in this region. The noticeable intensification of aircraft operations at high latitudes and the increase of the commercial shipping activity in the North East Passage, create the need for enhancing aeronautical traffic services and operational communications. These outcomes show the increased demand for communications services in the Arctic.

As a result of this growing request for communications services at high latitudes, suitable solutions must be identified to achieve the present and upcoming goals. The conventional geostationary satellites cannot serve the mentioned demand, therefore some alternatives have been studied. Those that use low-altitude orbits involve large constellations [6]. More attractive possibilities are the Tundra and Molniya orbits [1, 7], characterized by critical inclination, moderate to high eccentricity and the apogee located at high latitudes.

In previous studies [8], a family of eccentric, highly-inclined geosynchronous orbits has been investigated and the maintenance requirements have been evaluated. In this final degree project (FDP), these investigations will be a reference.

Once the mission is completed, due to natural evolution, these orbits are pulled to cross the geostationary ring. This movement is extremely dangerous because of the high probability of impact with the many satellites operating at such altitudes.

Consequently, an end-of-life disposal strategy is required and shall be precisely designed as part of the mission project, in compliance with the current international space policy. According to an international treaty [24], when space objects within the geostationary (GEO) protected area conclude their mission, they have to be relocated to disposal orbits that guarantee the non-crossing of this dangerous region over the following 100 years.

An interesting point that should be considered is the clear usefulness of this study, due to the noticeable projection into the forthcoming space operations as a consequence of the increasing demand and interest in satellite communications services in the high latitude areas.

The selection of the adequate end-of-life disposal strategy is moderately simple for usual geostationary satellites. As opposed to GEO orbits, whose radius is effortlessly changed using Hohmann maneuvers, moderately to highly eccentric orbits imply high cost of circularization in the apogee. Consequently, in geosynchronous orbits at the geostationary altitude and with non-zero eccentricity, the disposal options are more complicated and, until now, they have been little investigated.

The operations are even more tedious in the case of high inclinations, due to the extreme eccentricity variations experienced in this type of orbits, which probably make the disposal orbit cross the GEO region. Another challenge is the scarcity of satellites operating in this critical orbit domain, the only example being the Sirius constellation of digital radio satellites [12]. This adds difficulty to the proposed study, but at the same time it makes it original, innovative and leaves space to creativity.

Numerous issues will be analysed to achieve the goals of this study. To sum up the main points, this FDP includes the maneuver strategy, the requirements on propellant mass, the execution times and the type of engine required for maneuver execution.

Scope

The scope of the project is to summarize the essential tasks that shall be developed in order to achieve the goal of the study. These chores are shown below:

- State of the art, i.e. a bibliographic study concerning orbit disposal strategies in geocentric orbit. The state of the art shall focus on geosynchronous orbits.
- Identification of candidate options for the maneuver strategy and the types of propulsion systems to accomplish them.
- Evaluation of the end-of-life disposal strategies, addressing the following aspects:
    - Detailed description of the maneuver strategy.
    - The amount of propellant mass that should be available at mission termination to carry out the corresponding end-of-life operations. Also, specify the corresponding cost and requirements.
    - Type of engine required for maneuver execution.
    - Execution times.
- Recommendations for end-of-life disposal.
- Simulations of the disposal maneuvers using Matlab.
- Optimization for low thrust maneuver during disposal strategy is out of scope since it would require the implementation of optimal control theory and calculus of variation.

Requirements

Certifications and regulations

Space is subject to increasingly stringent regulations as a consequence of the increasing use of it. To develop this project according to current space laws, first we must collect and summarize the general regulations that will limit this investigation focused on end-of life disposal strategies. Space law is generally divided into specific rules for launchers and for satellites. In this project, satellites are the objects of the study, therefore the regulations detailed here below are related with them.

The main organization that is responsible for space law is UNOOSA. For this reason, some of the following regulations are extracted from the document entitled *United Nations Treaties and Principles on Outer Space* [24]. Others are taken from some useful and reliable books and files related with space law [21, 22, 23, 25, 26].

First, a few general space laws are presented:

United Nations treaties	
Ibid., vol. 610, No. 8843: Treaty on principles governing the activities of states in the exploration and use of outer space, including the Moon and other celestial bodies.	
Article IX	- Any State Party to the Treaty have to evade damaging contamination of outer space, including the Moon and other celestial bodies, and adverse variations in the environment of the Earth. - Members have to notify the Secretary- General of the United Nations as well as the public and the international scientific community, as much as possible and practicable, of the nature, conduct, locations and results of such activities.
Article XI	- Any State Party to the Treaty have to promote international cooperation in the peaceful exploration and use of outer space.

***Ibid., vol. 672, No. 9574*:** Agreement on the rescue of astronauts, the return of astronauts and return of objects launched into outer space.	
Article 5	This article contains regulations related to recover and return a space object or its component parts considering the jurisdiction of any State and the ways to proceed.

***Ibid., vol. 961, No. 13810*:** Convention on international liability for damage caused by space objects.	
Article I	Important definitions: - *Damage* means loss of life, particular damage; or loss of or impairment to property of States or of persons, natural or juridical, or property of international intergovernmental organizations; - *Space object* includes component parts of a space object as well as its launch vehicle and parts thereof.
Other articles	In this section, the articles describe all the possible ways to proceed in the event of damage being caused by a space object to another space object, to a person or a thing; and who is liable to pay compensation and, in some cases, which compensation is.

***Ibid., vol. 1023, No. 15020*:** Convention on registration of objects launched into outer space	
Article IV	List of the information that should be provided to the Secretary-General of the United Nations.
Other articles	In this section it can be found: - Criteria of registration of objects launched into Earth Orbit or beyond and ways to proceed in each different case. - Each launching State should notify the Secretary-General of the United Nations of the establishment of such a registry

Table 1 *United Nations treaties.*

Principles adopted by the General Assembly
Resolution 1962 (XVIII) of 13 December 1963: Declaration of legal principles governing the activities of states in the exploration and use of outer space.
Resolution 41/65 of 3 December 1986: Principles relating to remote sensing of the earth from outer space.

Table 2 *Principles adopted by the General Assembly.*

To summarize the main points of these resolutions, each activity should be performed bearing in mind:

- The benefit and interests of all countries.

- The international law, including the Charter of the United Nations, the Treaty on Principles Governing the Activities of States in the Exploration and Use of Outer Space, including the Moon and Other Celestial Bodies.
- The interest of maintaining international peace and security and promoting international cooperation and understanding.

Related resolutions adopted by the General Assembly	
A/AC.105/738, annex III: Some aspects concerning the use of the geostationary orbit.	
a	The spacecraft orbits and radio frequency spectrum must be utilised efficiently, rationally, equitably and economically because they are limited natural resources.
d	The principle of "first come, first served" is followed in some frequency bands and services access to frequencies and spacecraft orbits, also considering the geostationary satellite orbit.
e	Difficult situations involving tough processes of coordination among developed and developing countries may appear as a consequence of the existing space laws on entry to frequencies and satellite orbits in respect of bands and services.

Table 3 Related resolutions concerning the use of the geostationary orbit.

Taking into account the aim of this study, the most important requirements to accomplish are the space debris mitigation guidelines. The Inter-Agency Space Debris Coordination Committee (IADC) [16] is an international governmental forum for the worldwide organization of activities associated with space debris that has collaborated in the establishment of important guidelines related to this topic.

Since 1987, some measurements have been established to catalogue and regulate the quantity of debris in space. The currently adopted document to mitigate space debris was approved in February 2007 and contains 7 guidelines. In the UNOOSA document, the mentioned guidelines are described.

United Nations publication	
A/62/20, annex: Space debris mitigation guidelines of the Committee on the peaceful uses of outer space.	
Guideline 1	During normal operations, it is necessary to minimize debris released.
Guideline 2	The probability of accidental fragmentation have to be less than 10 – 3 until the end–of-life of the space object. This regulation limits the potential for break-ups during operational stages.

Guideline 3	Minimize the probability of unintentional impact in orbit.
Guideline 4	Avoid accidental destruction and other damaging activities.
Guideline 5	Reduce to minimum the potential for post-mission fragmentation as a consequence of stored energy: - All the aboard energy reserves will be exhausted or placed in a state such that exhaustion of the energy is unavoidable or that there is no possible risk of releasing debris. - All the means of on-board energy production are going to be permanently defused.
Guideline 6	After the end of the mission of spacecraft and launch vehicle orbital stages, their long-term presence in the low-Earth orbit (LEO) region shall be limited.
Guideline 7	After the end of the mission of spacecraft and launch vehicle orbital stages, their long-term interference with the geosynchronous Earth orbit (GEO) region shall be limited.

***Table 4** Space debris mitigation guidelines [24].*

In these 7 guidelines there is no mention of the 25 years rule, which had a certain importance in the old space debris laws and it consists of a lifetime reduction rule for post-mission disposal performed in the LEO region.

Technical requirements

There are no technical requirements, except for the fact that the amount of propellant to be employed in the disposal maneuver shall be a small fraction of the total propellant mass at the beginning of the mission.

Economical requirements

In this study, at the beginning, we do not consider economical requirements.

I. State of the Art

In 1963, the SYNCOM 2 spacecraft [17] was the first operational man-made satellite orbiting in an almost circular, inclined geosynchronous orbit. A year after, the SYNCOM 3 [14] spacecraft was inserted into a geostationary orbit.

Since 1963 more than 230 launch vehicle stages and more than 900 satellites have been placed inside the useful geosynchronous orbit. Some of them were never placed into an exact geosynchronous orbit and others have been displaced to disposal regions. Focusing on the mitigation concern, more than 300 spacecraft have been moved into disposal orbits at the end of their operational life, in order to reduce the accumulation of objects in the GEO region.

To summarize some important data, the number of registered objects in 2011 within 200 km of the GEO altitude was about 650. Of this amount, only a few more than half were functional and the rest were non-operational satellites, smaller debris or forlorn propulsion stages. Moreover, practically another 700 catalogued objects were introduced in elliptical orbits which cross the GEO region. The number of operational spacecraft in GEO continues to raise. Currently, there are more than 400 operational spacecraft and this value is expected to increase.

Fig. 1 *Space debris seen from HEO. The two main debris fields are the ring of objects in GEO and the cloud of objects in LEO. [18]*

Furthermore, two break-ups are identified in this area [14]: the Ekran spacecraft and a Titan upper stage, whose remains are not registered. Several researches by NASA, ESA and CNES detect a noteworthy population of unknown debris objects between 20 cm and 100 cm of size. To obtain the information about meteoroids and micro-debris, dust detectors are used, such as GORID on Express-2 [13].

In addition, an increase of the frequency of utilization of eccentric and inclined geosynchronous orbits has been detected, which differ from the typical features of previous missions in GEO. Accordingly, the environment in the GEO altitude and its surroundings is changing.

The Inter-Agency Space Debris Coordination Committee (IADC) [16] conceived a GEO protected area in order to include the nominal operational altitude region of GEO, which was established as 75 km above and below the GEO altitude and 125 km on either side to provide a spacecraft displacement corridor. Later, this was turned into a volume of space within 200 km below and above the GEO altitude and 15 degrees on either side of the equator in latitude.

In 1977 an aerospace policy was requested to be implemented to move GEO spacecraft at end-of-mission to disposal regions in order to avoid their interference with operational satellites. In 1993 the International Telecommunications Union (ITU) [19] established its first formal recommendation about the topic. In 2007, after a long period of deliberations, the IADC simplified this GEO spacecraft disposal recommendation and concluded that spacecraft should be displaced to adequately high disposal orbits. This ensures that satellites remain above the GEO protected area, despite the effect of solar and lunar gravitational perturbations and solar radiation pressure.

NASA approved this recommendation [20] and took measures to prevent spacecraft going through the GEO region until, at least, 100 years after disposal. As a consequence of the intention of preserving this area, in 2001-2010, approximately 80% of the 160 GEO satellites which concluded their mission were moved into disposal orbits. An unexpected malfunction, which did not allow the implementation of a disposal strategy, was the cause of leaving the rest of spacecraft in the GEO area. This undesired fact occurred with TELSTAR 4, UFO 3, INTELSATs 511 and 804, ECHOSTAR 2, and GALAXY 3R, amongst others.

To reduce the number of collisions and avoid interference with spacecraft in geosynchronous transfer orbits, a general pact was reached to situate the disposal orbits above the GEO region, rather than below it.

Approximately 70% of the operational satellites were moved into regions at least 200km above the GEO altitude, and almost 50% of these were transferred to orbits at least 300km above the GEO altitude. The mass, shape, stability and size of them are the main variables that are responsible of altitude variations. Their original orbital plane with respect to the Moon and the Sun is another issue to take into account.

Currently, the scientific community is concerned about the high probabilities of creating a new region of derelict objects about 300 km above the GEO altitude. The main worry is the possibility of increasing the number of collisions and, consequently, more breakups whose remains would cross the GEO region creating even more danger. This disturbing future situation will probably occur if all GEO satellites are transferred to almost circular orbits at 300km above the GEO region. The positive side is that not all disposal orbits are the same, actually, there is a huge variety of orbits. Therefore, there is a certain dispersion of orbits, rather than a concentration, as shown in Figure 2.

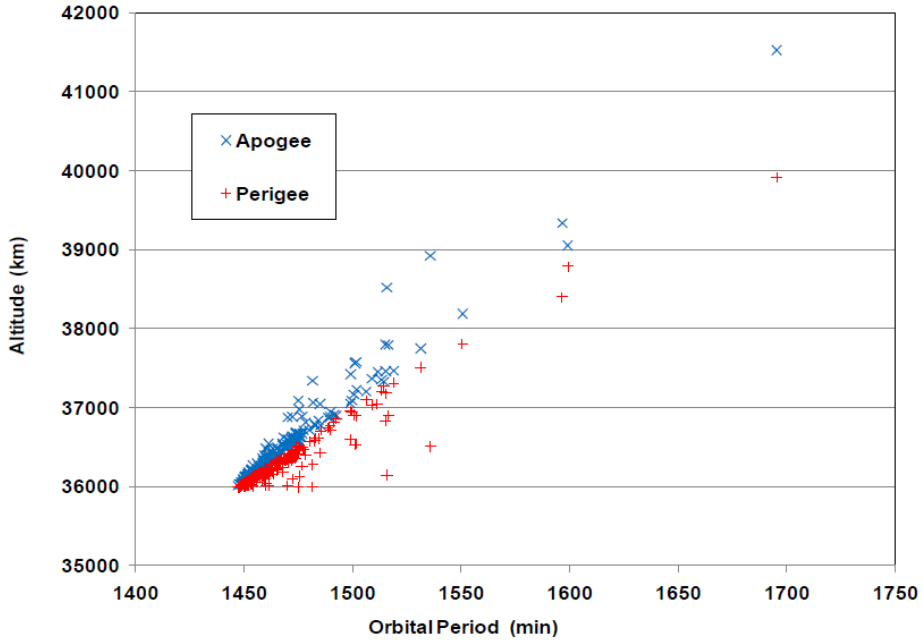

Fig. 2 Distribution of all registered objects with perigees at least 200km above the GEO altitude. [14]

Focusing on telecommunications services to high-latitude areas, the Sirius constellation of digital radio satellites provides this facility in the United States and Canada. These satellites operate in a geosynchronous highly elliptical orbit and their orbital period is approximately 23 hours and 56 minutes, one sidereal day. Each satellite of this constellation spends about 16 hours a day over the desired northern region.

II. Description of the Orbits

The disposal strategies that will be studied in this FDP will be applied to a specific group of spacecraft operating in orbits classified inside the family of eccentric, highly inclined geosynchronous orbits. This group of orbits was selected in previous studies [8] due to the benefits they provide to telecommunications services in the northern regions.

The choice of a geosynchronous orbit offers exceptional advantages for numerous missions, such as navigation, surveillance satellites, national defence, communications and scientific investigations. When a satellite is located in a geosynchronous orbit, it completes one orbit around the Earth in one sidereal day, which is the time it takes the Earth to make one revolution relative to the fixed stars. A sidereal day is about 23 hours, 56 minutes and 5.5 seconds. This gives the spacecraft a mean altitude of 35.786km. Therefore, a satellite in a geosynchronous orbit completes a revolution around the Earth every 1436 minutes.

Focusing on the inclination and eccentricity, a circular or almost circular geosynchronous orbit with zero inclination is called a geostationary orbit. A satellite in a geostationary orbit stays above the same ground area at all times. However, in this investigation, the studied orbits are eccentric and highly inclined, which adds complications but also offer some unique benefits.

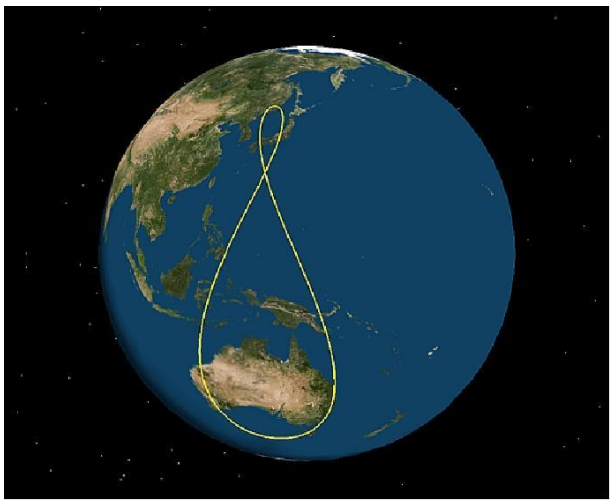

Fig. 3 The typical figure-eight ground track of an eccentric inclined geosynchronous orbit. [38].

A geosynchronous inclined orbit traces a specific figure-eight ground track (Figure 3) centred at the selected reference longitude. Moreover, if the orbit is highly eccentric, an interesting option is to situate the perigee at the point of lowest latitude, consequently, the apogee will be located at the northern hemisphere. This configuration allows to spend many hours per day over the

desired northern region (thanks to the "apogee dwell"), which means offering long uninterrupted links with the users.

In previous studies [8, 27, 28, 29, 30, 31], several satellite constellations were investigated, specifically a total of 15 highly inclined eccentric orbits were considered including periods of 12, 16, 18 and 24 hours. The study [8] reached the conclusion that the best solution consist of three satellites in three equally-spaced orbital planes and distinguished by a 24 hours period.

2.1. Characterization of the orbit

The selected constellation is made up of three satellites whose orbits trace the same ground track and their orbital planes are equally spaced in order to provide coverage at all times. Firstly, to define the orbits, their six orbital elements shall be established using a value or a range of values:

○ Semi-major axis (a_0):

The orbits are geosynchronous, hence their orbital mean motion n_0 equals the Earth's sidereal rotation rate n_E, and the orbital period T_0 is obtained directly from the previous parameter:

$$n_0 = n_E = 7.292 \cdot 10^{-5}\ rad/s \implies T_0 = \frac{2\pi}{n_0} = 86165.5\ s. \qquad (1)$$

The semi-major axis a_0 can be easily calculated using the third Kepler's law:

$$2\pi\sqrt{\frac{a_0^3}{\mu}} = T_0 \implies \boldsymbol{a_0} = \sqrt[3]{\frac{\mu\, T_0^2}{4\,\pi^2}} = \mathbf{42164.6\ km}, \qquad (2)$$

where μ is the Earth's gravitational parameter, defined as $\mu = G(M+m)$ and equal to $4 \cdot 10^5 km^3/s^2$; G is the gravitational constant; and $M+m$ is the combined mass of the central body (in this case the Earth) and the satellite. Commonly the mass of the central body is much bigger than the mass of the satellite, therefore: $\mu = G(M+m) \approx GM$.

○ Eccentricity (e_0) and inclination (i_0):

This orbits are characterized by values of eccentricity and inclination that have been selected bearing in mind the purpose of providing an adequate coverage of the specific region. Following the requirement adopted in the case of the Sirius satellites, the minimum elevation over the horizon is 60º for telecommunications operations. By satisfying this requirement, general users

will be able to use radio and television signals or voice and data transmission because of the successful connexion. Moreover, this limitation allows also other services such as maritime connections, aircraft on routes through the northern region and even in the polar areas, and the incoming industry of UAVs, because their requirements are less restrictive due to the scarcity of obstacles in their areas of performance.

Previous studies [8] have analysed the points on the Earth's surface to maximize the coverage over the desired region. To achieve this goal, a Matlab script was programmed. It considers the three satellite ground tracks and imposes that the elevation requirement must be satisfied by at least one satellite at all times.

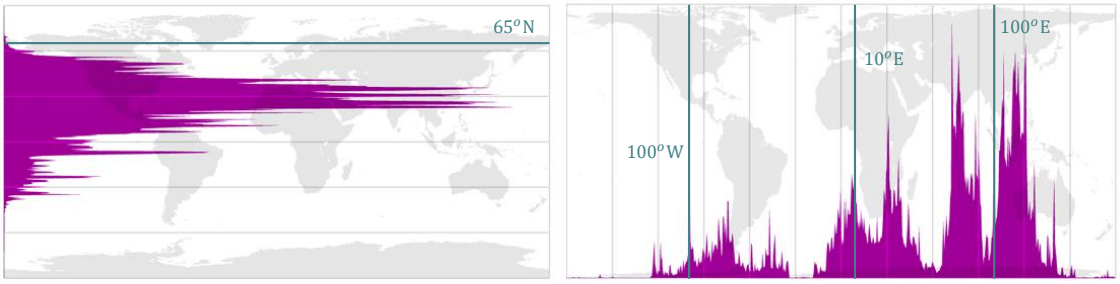

Fig. 4 Distribution of world population by latitude (left) and by longitude (right) as of 2000. [37]

To design the most efficient constellation, the population distribution was also investigated (Figure 4) and the results obtained show the scarcity of people above 55^{o}N latitude and the almost absence of population living in regions beyond 65^{o}N. Consequently, coverage in regions above 65^{o}N does not provide economic benefits, therefore this area has not been considered. Respect to the world population distribution in longitude, in the northern hemisphere the most populated areas are centered around 100^{o}E (between China and Russia), 10^{o}E (Europe) and 100^{o}W (North America). These longitudes are considered the most economically sensible regions for operation of telecommunications satellites. Figure 4 shows the upper limit of latitude and the three selected longitudes.

Bearing in mind all these points, a variety of combinations of e_0 and i_0 have been studied and those listed in Table 5 are considered the best choice to satisfy the requirements and maximize the coverage. The critical inclination (i.e., 63.4^{o}) has been considered because it offers the possibility of comparing the Tundra with other geosynchronous highly inclined orbits. Moreover, the Tundra orbit is well known inside the space community, therefore their orbit features are also familiar.

Combinations	**1**	**2**	**3**	**4**	**5**	**6**	**7**	**8**	**9**
Eccentricity e_0	0.25	0.25	0.30	0.25	0.30	0.35	0.40	0.35	0.40
Inclination i_0 *(deg)*	55.0	60.0	60.0	63.4	63.4	63.4	63.4	70.0	70.0

Table 5 *Selected combinations of initial eccentricities and inclinations (in degrees) [8].*

○ Right ascension of ascending node (Ω_0):

The selected constellation is constituted by three satellites whose orbital planes shall be equally spaced in order to satisfy the coverage at all times. Therefore, there is a 120º of ascending node separation between them. Five equally-spaced values for the initial right ascension of the ascending node (Ω_0) are assigned to each of the nine combinations of initial eccentricity and inclination:

$$\boldsymbol{\Omega_0 = 0^o; 60^o; 120^o; 180^o; 240^o}. \quad (3)$$

○ Argument of perigee (ω_0):

The aim is to provide coverage at all times to high-latitudes users. To fulfil this goal, the perigee is placed in the point of lowest latitude, hence, the argument of perigee is:

$$\boldsymbol{\omega_0 = 270^o}. \quad (4)$$

○ True anomaly (θ_0):

When the simulation starts, the satellite is supposed to be at perigee, therefore the value of initial true anomaly is:

$$\boldsymbol{\theta_0 = 0^o}. \quad (5)$$

Considering the nine selected combinations of initial eccentricities and inclinations and the five designated values for the initial right ascension of the ascending node, there are **45 suitable sets of initial orbital elements**. These combinations were used in the previous study [8] to investigate the orbital evolution of the satellites.

2.2. Orbit simulation

Considering the description of the constellation and the values of the six orbital elements, it is possible to write a Matlab script to simulate the constellation and represent their three ground tracks. As it has been explained before, the three orbits trace the same ground track and their orbital planes are equally spaced in order to guarantee continuous coverage.

To fulfil these requirements, we impose a separation $\Delta\Omega = 120^o$ between the orbital planes of the constellation. Then, it is necessary to know the initial position (at $t = 0$) of the three satellites of the constellation. We could use true anomaly (θ_0), but since the variable is time, an angular variable that grows linearly with time is more suitable. For this reason, the position along the orbit is described by the mean anomaly M_0.

As an example, we let the reference longitude of the ground track be zero (Greenwich meridian). Therefore, perigee ($\theta = 0^o$) is placed at zero longitude ($\lambda = 0^o$). The three satellites of the constellation trace a specific figure-eight ground track centered at the selected reference longitude. Consequently, the ground track crosses the reference meridian at four points: perigee, apogee and the node of the eight (which corresponds to two passages).

To obtain the described constellation, the position of these points have to be known. Firstly, three values of initial right ascension of the ascending node (Ω_0) are chosen bearing in mind the requirements ($\Delta\Omega = 120^o$). Then, a Matlab script is programed and, by using these Ω_0 values, a specific value of the initial mean anomaly (M_0) are computed for each orbit. Once the values of M_0 and Ω_0 are known, the ground track of each orbit can be drawn.

2.2.1. Constellation construction

Firstly, the Earth's parameters, namely the Earth's radius R_E, the Earth's gravitational parameter μ and the Earth's sidereal rotation rate n_E, are introduced. The spacecraft's orbital elements a_0, e_0, i_0 and ω_0 are also input. Then, the period is computed. The starting time, the initial right ascension of the ascending node Ω_0 and the initial mean anomaly M_0 are initialized to zero. A tolerance, a step in mean anomaly and a time increment are selected.

The initial values of Ω_0 and M_0 define the reference longitude. If, as in the example, we select 0^o to be the reference longitude, then:

$$\Omega_0 = 0^o \text{ and } M_0 = 90^o \implies \text{Reference longitude} = 0^o \text{ (Greenwich)}.$$

The script consist of three big loops:

- The first loop varies the right ascension of the ascending node Ω_0 between 0º and 360º.
- For each value of Ω_0, the second loop goes through all the values of the initial mean anomaly M_0 (from 0º to 360º).
- For each value of Ω_0 and M_0, the third loop is used to count time, which varies between the initial time (generally zero) and one period.

Inside the most internal loop, the following calculations are carried out:

1. Given t, the mean anomaly M is computed:

$$M = n_0\,(t - T_\pi) \tag{6}$$

   where T_π is the epoch of passing through perigee.

2. The true anomaly theta is determined. The studied orbit is an eccentric orbit, hence, the true anomaly θ is determined through Kepler's equation:

$$M = E - e_0\,sinE, \tag{7}$$

$$\cos\theta = \frac{e_0 - cosE}{e_0\,cosE - 1} \quad \text{and} \quad sin\theta = \frac{\sqrt{1 - e_0^2}sinE}{1 - e_0\,cosE}, \tag{8}$$

   where E is the eccentric anomaly. In the script, the first step consists of obtaining the eccentric anomaly E from Kepler's equation using an iterative algorithm (such as Newton Raphson). Then, the true anomaly is calculated by using the obtained value of the eccentric anomaly inside Eqs. 8.

3. The orbital position and velocity in geocentric equatorial coordinates are computed. By using the vector of the six orbital elements (semi-major axis, eccentricity, inclination, right ascension of the ascending node, argument of perigee and true anomaly), it is possible to obtain the state vector of six elements (position $\boldsymbol{r}$ and velocity $\boldsymbol{v}$).

   Considering:

$$p = a_0(1 - e_0^2)\,, \tag{9}$$

$$r = \frac{p}{1 + e_0\cos(\theta)}, \tag{10}$$

$$f_x = \cos(\Omega)\ \cos(\omega + \theta) - \sin(\Omega)\sin(\omega + \theta)\cos(i_0)\,, \tag{11}$$

$$f_y = \sin(\Omega)\cos(\omega+\theta) - \cos(\Omega)\sin(\omega+\theta)\cos(i_0)\,, \quad (12)$$

$$f_z = \sin(\omega+\theta)\sin(i_0)\,. \quad (13)$$

In the above formulas, p is the semi latus rectum, r is the distance to the centre of the Earth and f_x, f_y and f_z are the direction cosines of $\boldsymbol{r}$. The position components (r_x, r_y and r_z) of the state vector are:

$$r_x = r\, f_x\,, \quad (14)$$

$$r_y = r\, f_y\,, \quad (15)$$

$$r_z = r\, f_z\,. \quad (16)$$

Considering:

$$v_r = \sqrt{\frac{\mu}{p}}\, e_0 \sin(\theta)\,, \quad (17)$$

$$v_u = \sqrt{\frac{\mu}{p}}\, (1 + e_0\cos(\theta)), \quad (18)$$

where v_r is the radial velocity of the spacecraft and v_u is the tangential velocity, the velocity components (v_x, v_y and v_z) of the state vector are:

$$v_x = v_r\, f_x - v_u\,(\cos(\Omega)\sin(\omega+\theta) + \sin(\Omega)\cos(\omega+\theta)\cos(i_0))\,, \quad (19)$$

$$v_y = v_r\, f_y - v_u\,(\sin(\Omega)\sin(\omega+\theta) - \cos(\Omega)\cos(\omega+\theta)\cos(i_0))\,, \quad (20)$$

$$v_z = v_r\, f_z + v_u\cos(\omega+\theta)\sin(i_0)\,. \quad (21)$$

4. By using the position components of the state vector, it is possible to compute the geographical longitude λ and latitude ϕ of the spacecraft at the given time t:

$$\beta = \mathrm{n_E} t\,, \quad (22)$$

$$r = \sqrt{r_x^2 + r_y^2 + r_z^2}\,, \quad (23)$$

$$\lambda = \arctan\left(\frac{-r_x\, sin(\beta) + r_y\, cos(\beta)}{r_x\, cos(\beta) + r_y\, sin(\beta)}\right), \quad (24)$$

$$\phi = \arcsin\left(\frac{r_z}{r}\right). \quad (25)$$

β is the angle by which the Earth has rotated since the beginning of the simulation.

5. Finally, the combination of Ω_0 and M_0 for which the value of the true anomaly is zero (to within the given tolerance) when the longitude is zero, is selected.

If the tolerance is correct, the algorithm provides three sets of values of Ω_0 and M_0, one for each satellite of the constellation, as it can be seen in Figure 5.

To show an example, if we select the following eccentricity and inclination,

$$e_0 = 0.25 \;\; ; \;\; i_0 = 55.0^o, \tag{26}$$

the (Ω_0, M_0) points are those shown in Figure 5 and reported in Table 6.

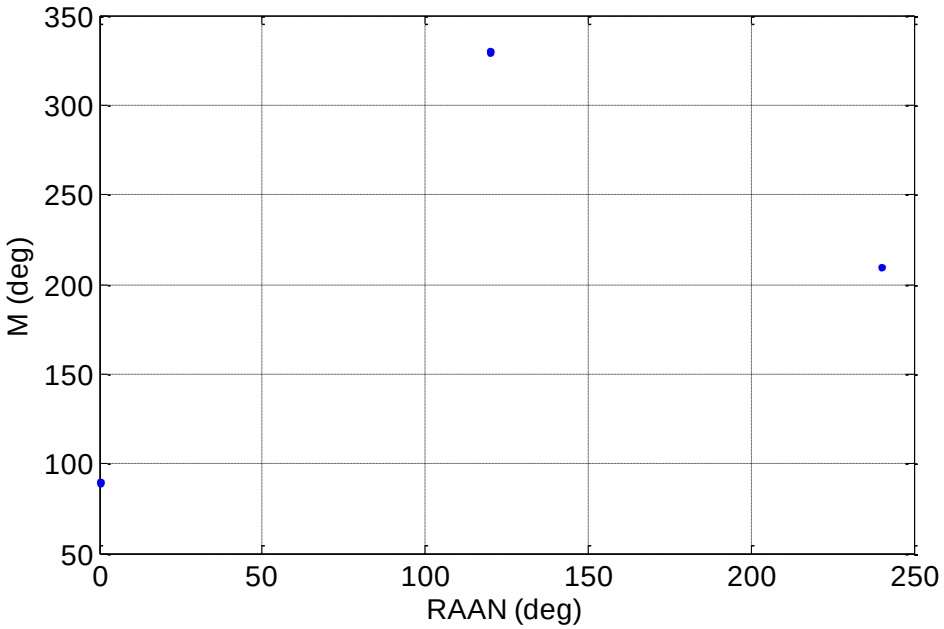

Fig. 5 *M_0 vs Ω_0 plot obtained by Matlab using the values e_0=0.25; i_0=55.0º.*

Satellite	Initial Mean Anomaly M_0	Initial ascending node Ω_0
1	90.0º	0.0º
2	330.0º	120.0º
3	210.0º	240.0º

Table 6 *M_0 vs Ω_0 values for the three satellites of the constellation.*

2.2.2. Ground-track Matlab script

Another Matlab script has been written in order to represent the ground track of the three orbits of the constellation. This program allows to check the orbital characteristics. Moreover, it offers the possibility to check that the three satellites trace the same ground track, as required. The coast line is needed to visualize the exact location of ground-tracks and satellites. Therefore, the script uses the function *"load('coast')"*.

The Earth's parameters (R_E, μ and n_E) and spacecraft's parameters (a_0, e_0, i_0, ω_0) are introduced and the period is computed. The values of Ω_0 and M_0 as obtained in the previous script are also introduced. The starting time is initialized to zero.

The script consists of one loop over time. It varies between zero and one orbital period. By using the same formulae and procedure as in the constellation script, given a particular value of time, the mean anomaly M is computed and the true anomaly θ as well. The next step consists of computing the state vector which contains orbital position and velocity in the geocentric equatorial reference. Then, by using the previous parameters, longitude and latitude can be found, which allows to plot the current position. The set of all points thus obtained forms the ground track of the satellite.

By using the values of Ω_0 and M_0 extracted from Table 6, it is possible to show the ground-tracks of this specific constellation and the initial position of each satellite. Figures 6 to 8 illustrate the three ground tracks of the constellation with $e_0 = 0.25$ and $i_0 = 55.0^o$.

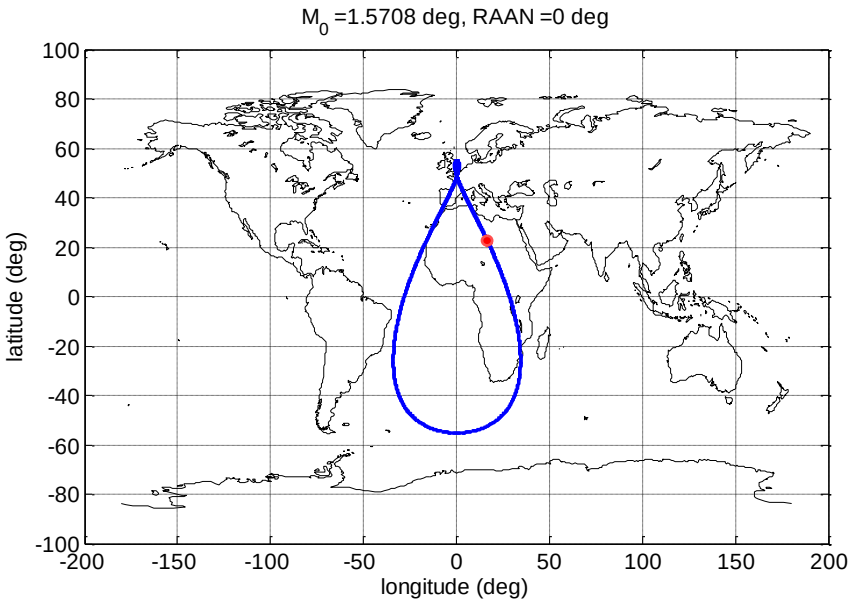

***Fig. 6** Ground track of the orbit (blue) and initial position (red circle) of the satellite 1 of the constellation with the values e_0=0.25 and i_0=55.0º.*

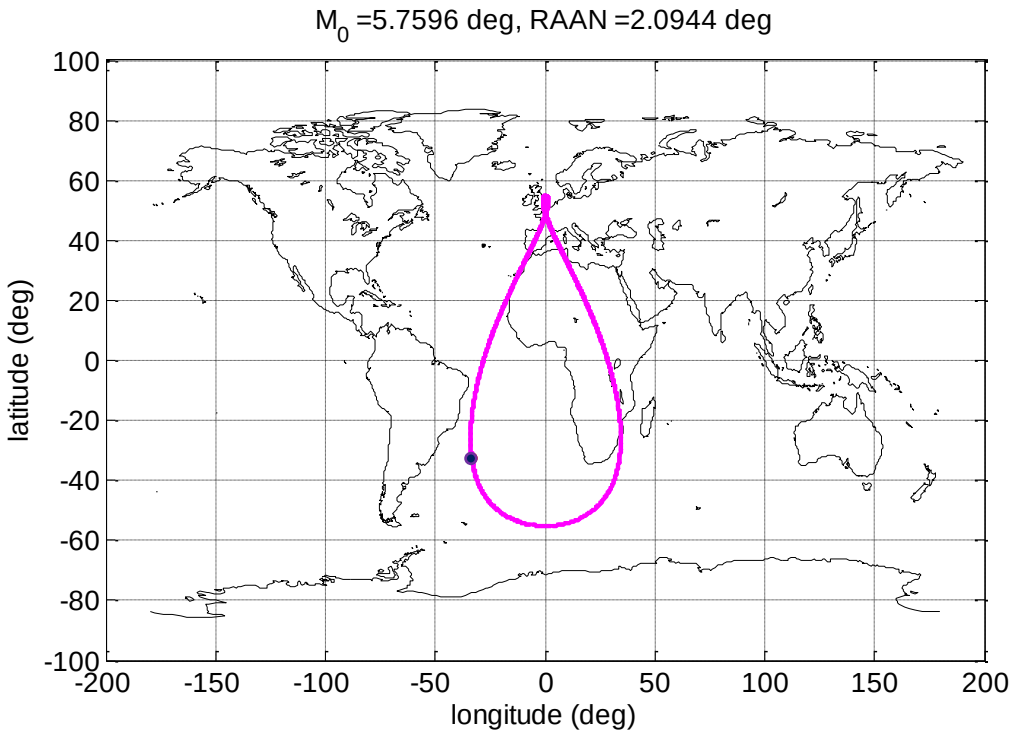

Fig. 7 *Ground track of the orbit (magenta) and initial position (purple circle) of the satellite 2 of the constellation with the values e_0=0.25 and i_0=55.0º.*

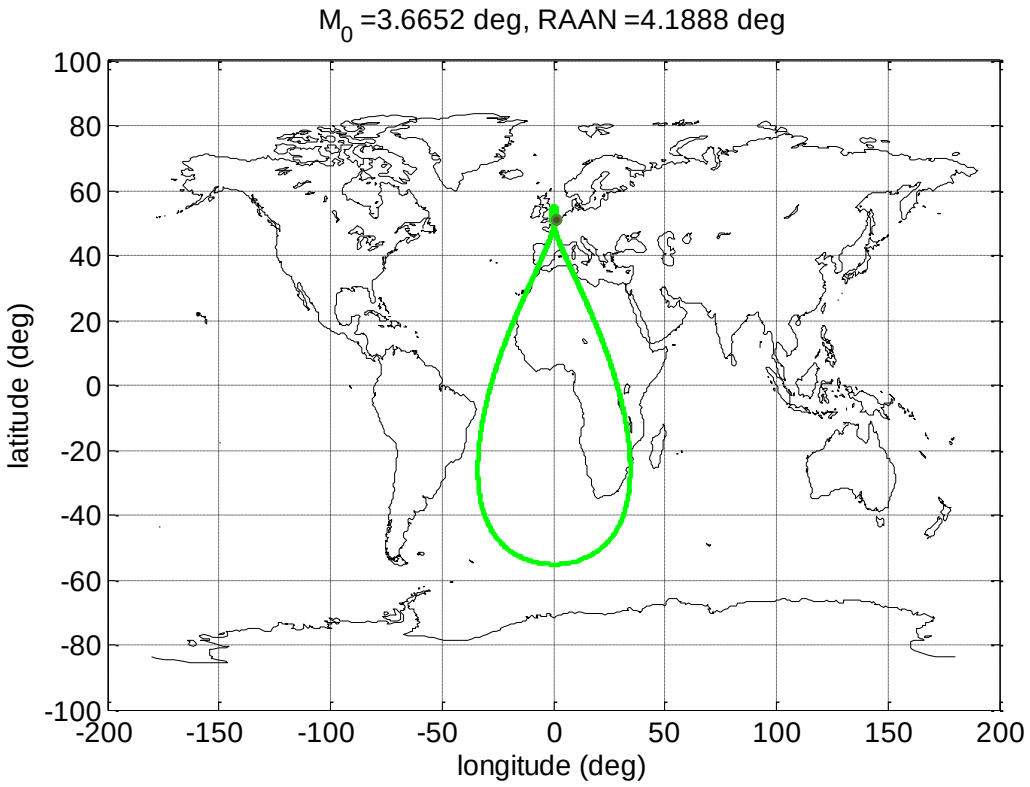

Fig. 8 *Ground track of the orbit (green) and initial position (green circle) of the satellite 3 of the constellation with the values e_0=0.25 and i_0=55.0º.*

To compare the three satellite ground tracks of the constellation, it is needed to show all of them in the same figure. Figure 9 shows the superposition of the three ground tracks. The three curves coincide, as they should.

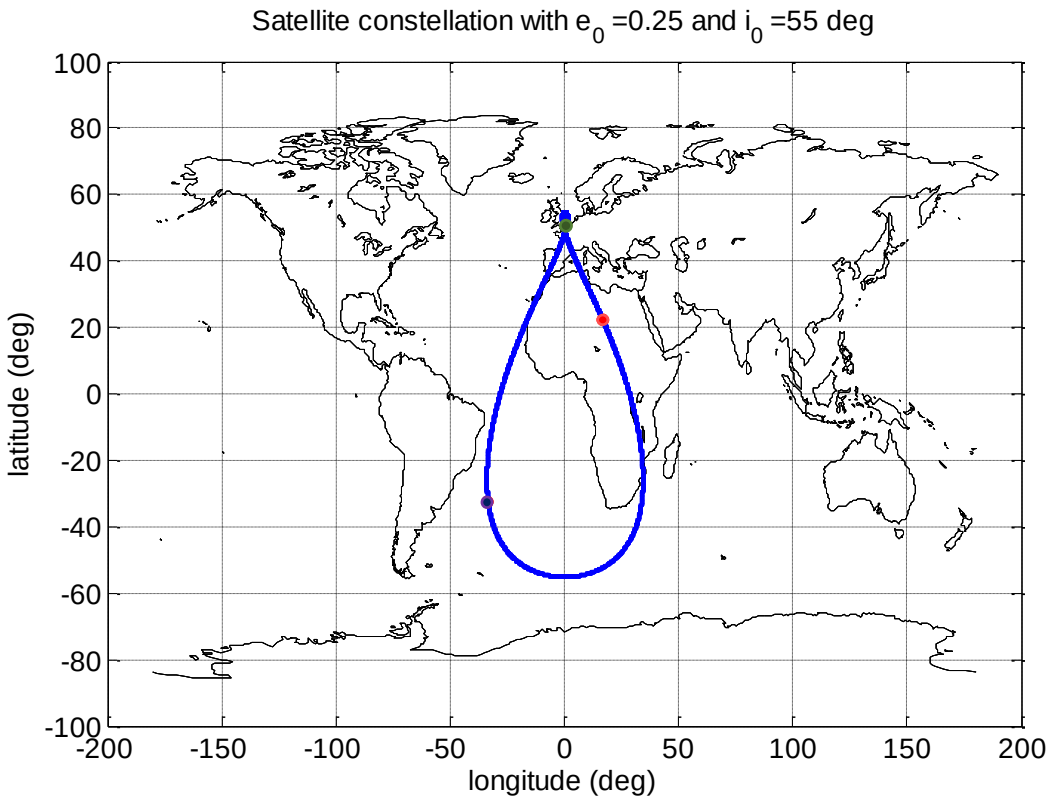

Fig. 9 *Satellite constellation with e_0=0.25 and i_0=55.0º. There appear the three ground tracks in blue and the initial position of the three satellites (satellite 1 in red, satellite 2 in purple and satellite 3 in green).*

2.3. Orbital perturbations

To guarantee the success of any space mission, a study of the orbital perturbations must be developed. In the vicinity of the Earth, the satellite orbits experience some perturbations which are responsible of severe deviations from theoretical keplerian motion.

2.3.1. Acceleration perturbations

Firstly, to analyse the evolution of a particular satellite, the main perturbations that affect its acceleration must be identified. These are:

- Earth's gravitational potential.
- Third-body perturbations.
- Solar radiation pressure.

- Atmospheric drag.
- Relativistic corrections to gravity.

In the previous study [8], the truncation error for the magnitudes of the considered perturbations was fixed by means of the determination of a tolerance, which is the maximum accepted deviation of the ground track. The studied orbits are characterized by a coverage area of approximately several thousand kilometres. Consequently, a spacecraft angular shift of 1º, which means a modification of 100 km in the ground track, is a small displacement in comparison with the global area. Therefore, an accuracy of 1º is adequate. Then, in the mentioned study [8], this displacement was transformed into an acceleration value and the obtained lower limit was $10^{-8}\ m/s^2$.

Drag takes energy away from the orbit due to friction with the atmosphere, which produces a non-conservative force. As a result, the semimajor axis and the eccentricity decrease. The orbit progressively circularizes. The orbits studied in this FDP develop well beyond the upper limit of the atmosphere since their perigees have altitudes of 1000km. The acceleration due to atmospheric drag can be neglected.

The effects of general relativity can be computed by adding a correction expressed as a perturbation δV to the Newtonian gravity potential with the formula:

$$\delta V = -\frac{GM_E L^2}{c^2 r^3}, \qquad (27)$$

where L is the specific angular momentum of the satellite and c is the speed of light in vacuum. For the orbits under study, the relativistic term is lower than $10^{-10} m/s^2$ which makes it negligible.

2.3.1.1. Earth's gravitational potential

The traditional form to express the Earth's gravitational potential at an external point of spherical coordinates $r,\ \varphi,\ \lambda$ is by means of spherical harmonics:

$$U(r,\varphi,\lambda) = \frac{\mu_E}{r}\left[1 + \sum_{n=2}^{\infty}\left(\frac{R_E}{r}\right)^n \sum_{m=0}^{n} \overline{P_n}^m(sin\varphi)(\bar{C}_{nm}\cos m\lambda + \bar{S}_{nm}\sin m\lambda)\right]. \qquad (28)$$

Here,

- $\bar{C}_{nm}$ and $\bar{S}_{nm}$ are the Stokes coefficients which describe the mass distribution within the Earth and decrease in magnitude as n (= degree) and m (= order) grow. Each spherical harmonic characterizes a specific deviation from the zero-order model (keplerian orbits).
- r, φ and λ are the radial distance, latitude and longitude from the reference meridian, respectively (Earth-centred spherical equatorial coordinates).
- R_E is the mean Earth's radius.
- $\overline{P_n}^m$ are the associated Legendre functions of the second kind.
- The bar above the Stokes coefficients and the Pnm's indicates that full normalization has been applied.

The Earth's shape and mass distribution are responsible for the existence of important perturbations. As a matter of fact, the Earth is not a perfect sphere. As an example, the equatorial radius is about 22 km longer than the polar radius. In other words, in first approximation the Earth is an oblate ellipsoid. The Stokes coefficient which describes the polar flattening is C_{20} (also referred to as J_2, although the two are not exactly identical, but can be derived one from the other). Similarly, C_{22} and S_{22} or, equivalently, J_{22} $\left(=\sqrt{{C_{22}}^2 + {S_{22}}^2}\right)$ describe the fact that the equator of the Earth is not circular but rather elliptical. Depending on the required accuracy, higher-order terms can be included in the model.

The secular effects of J_2 over the angular elements, particularly the right ascension of the ascending node, is especially relevant for the present study. For this reason, we give a brief description of them.

○ Precession of the right ascension of the ascending node:

The bulge produces a torque that rotates the angular momentum vector. Consequently, the plane of the orbit experience a precession which changes the right ascension of the ascending node linearly with time. The direction of precession is westward for prograde orbits ($0 \leq i < 90^o$) and eastward for retrograde orbits ($90^o < i \leq 180^o$).

$$\Omega_{J_2} = \Omega_0 + \dot{\Omega}_{J_2}(t - t_0)\,; \tag{29}$$

$$\dot{\Omega}_{J_2} = -\frac{3}{2} n J_2 \left(\frac{R_E}{a}\right)^2 \cos(i)\,(1 - e^2)^{-2}\,. \tag{30}$$

The greatest effect arises at low inclinations and low altitudes. Focusing on altitude, gravity is reduced with the inverse square of the distance, therefore, the higher the spacecraft is, the less effect the bulge has on the ascending node. Considering inclination, if the orbit has low values of this orbital element, spacecraft perform closer to the bulge and, hence, it is more pulled by it. Polar orbits have zero regression of the ascending node. Moreover, by increasing the values of eccentricity, the nodal regression rate is augmented too.

From the point view of satellite's operation, the placement of the ground track is essential and is much more important than the location of the orbital plane. This undesired perturbation is responsible for the modification of the right ascension of the ascending node. Then, the variation of the RAAN produces a change in the east-west placement of the ground track.

This linear effect of J_2 over the ground track can be removed by adjusting the orbital period before the propagation begins. Therefore, any east-west drift of the ground track can be neutralised by changing the orbital period. Consequently, this modification of the period overshadows the precession of the orbital plane. The resulting correction is usually of the order of 1 s. To change the orbital period before the propagation begins, the only orbital element that has to be adjusted is the semi-major axis.

- Precession of the line of apsides:

The major axis rotates in the plane of the orbit, therefore, the line of apsides, which joins perigee and apogee, also rotates. Consequently, the argument of perigee changes, and according to first-order theory it does it linearly with time. If the inclination is less than 63.4º or greater than 116.6º, the line of apsides spins in the direction of satellite motion, and, if the inclination is between 63.4º and 116.6º, it rotates in the opposite direction. This precession can be expressed by using the formula:

$$\omega_{J_2} = \omega_0 + \dot{\omega}_{J_2}(t - t_0) \tag{31}$$

$$\dot{\omega}_{J_2} = \frac{3}{4} n J_2 \left(\frac{R_E}{a}\right)^2 (4 - 5\sin^2 i)(1 - e^2)^{-2} \tag{32}$$

By using this formulae, a Matlab script was developed to study the changes in the argument of perigee related to the variation of the values of inclination, eccentricity and semi-major axis. Figure 10 is obtained from this script. It shows that this effect is greater for high eccentricity, low

inclination and low altitudes. To study the net effects that all the perturbations produce over the node and the perigee, a further analysis is needed. It is shown in section 2.3.3.

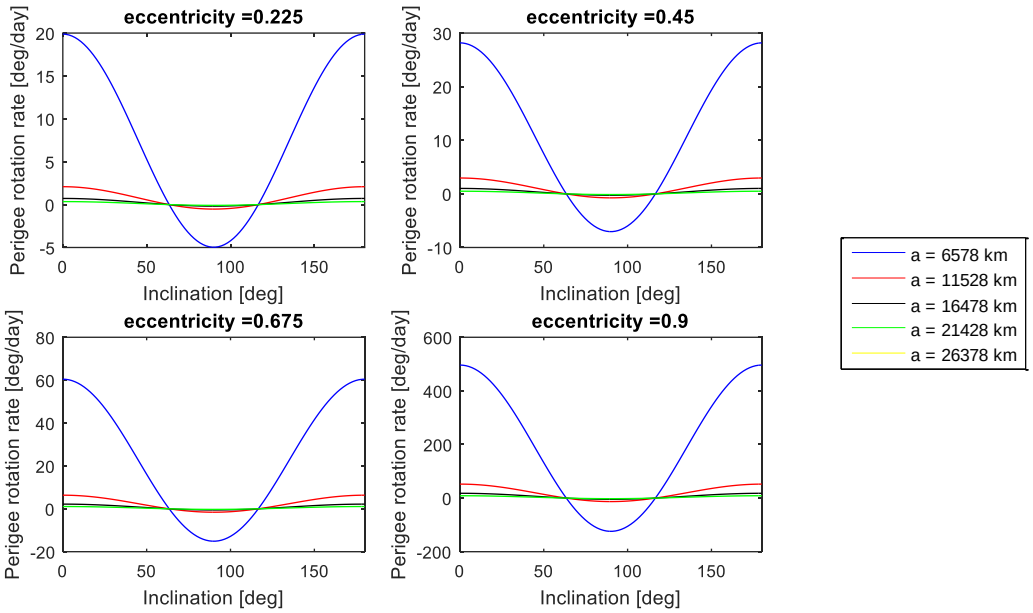

Fig. 10 Study of the precession of the line of apsides.

2.3.1.2. Third-body perturbations

The perturbations produced by the gravitational attraction of either the Sun or the Moon are known as third-body perturbations. They create an acceleration which can be mathematically described as:

$$\boldsymbol{a} = -GM_B\left[\frac{\boldsymbol{r}-\boldsymbol{r}_B}{|\boldsymbol{r}-\boldsymbol{r}_B|^3}+\frac{\boldsymbol{r}_B}{r_B^3}\right], \qquad (33)$$

where:

- M_B is the mass of the perturbing body.
- $\boldsymbol{r}$ is the geocentric position of the satellite.
- $\boldsymbol{r}_B$ is the geocentric position of the perturbing body.

The first term of Eqs. 33 is the gravitational attraction produced by the perturbing body B (the Moon or the Sun) acting on the satellite. The second term is the gravitational attraction produced by B acting on the Earth. The sum of both accelerations is the acceleration of the third-body perturbation.

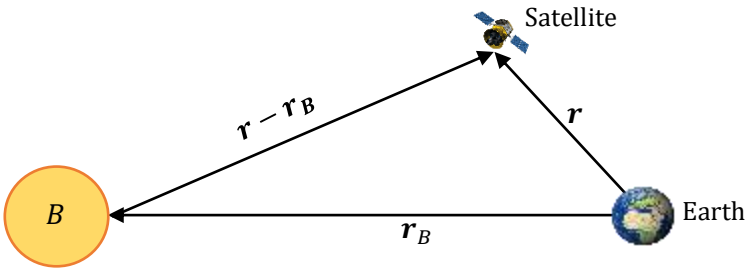

Fig. 11 Sketch of the distances considered to compute the acceleration produced by the third body perturbation.

This gravitational acceleration produces some forces that cause periodic variations in all the orbital elements and secular variations in the longitude of the ascending node, mean anomaly and argument of perigee. The secular variation in mean anomaly has little influence on the orbit because it is much smaller than the mean motion. However, the secular variations in the other two elements are significant, specifically for high altitude orbits like those dealt with in this study.

Some studies conclude that the orbital period and the argument of perigee are the key parameters in order to keep the same ground-track. Few modifications in the orbital period, typically caused by lunar perturbations, create a large east-west secular motion or drift of the ground-track which reduce the displacement produced by the regression of the ascending node.

2.3.1.3. Solar radiation pressure

The solar radiation pressure causes periodic variations in all of the orbital elements. These periodic variations are responsible for the acceleration that affects satellites, which can be described as:

$$\boldsymbol{a_R} = -f\left(\frac{P_s}{4\pi d_s^2 c}\right)\left(\frac{A}{m}\right)(1+k)\boldsymbol{u}_s\,, \qquad (34)$$

where:

- A is the cross-sectional area of the spacecraft exposed to the Sun.
- f is the shadow factor and it is equal to 0, if the satellite is in umbra; it is equal to 1, if the satellite is in sunlight; and its value is placed between 0 and 1, when it is in penumbra.
- P_s is the luminosity of the Sun and its value is: $P_s = 3.846 \cdot 10^{26} W$.
- d_s is the spacecraft-Sun distance.
- c is the speed of the light in vacuum.
- m is the mass of the spacecraft.

- k is the surface reflectivity, whose value range from 0 (complete absortion) and 1 (specular reflection).
- $\boldsymbol{u_s}$ spacecraft-Sun unit vector.

It is an important force for small particles, whereas it generates minor effects on large satellites. These are an oscillation in orbital inclination and in orbital eccentricity. The acceleration produced by the solar radiation pressure is usually of the order of $10^{-7}\ m/s^2$, therefore, for the present study it is considered.

2.3.2. Other perturbations

Any satellite orbiting the Earth can be affected by other perturbations than those described previously. The following are the main ones:

- Out-gassing can cause unexpected thrusting which can be responsible of an orbit perturbation and produce satellite rotation.
- Malfunctioning of thrusters

In this project, we are not going to develop a deeper study of the effects of these perturbations.

2.3.3. Orbital evolution

In this section, a study of the orbital evolution of an eccentric highly-inclined geosynchronous orbit is reported. The outcomes are analysed bearing in mind the previous analysis of the perturbations that can affect any satellite operating in such family of orbits.

Study [8] analyses the station-keeping requirements for these family of orbits over two years because this duration allows to obtain descriptive outcomes of the long-term progress. This is possible because two years include two periods of the solar perturbation, which is the slowest one. A 1º angular displacement per two years is equal to a shift of $1.4 \cdot 10^{-3}$ degrees per orbit. Considering the analysed orbits, this is interpreted as a change of more than 400 km per orbit. The error in the curve envelope propagation must be approximately ten times smaller (40 km per orbit).

Constant accelerations, such as those produced by drag and relativistic effects, with values $\leq 10^{-8}\ m/s^2$ are neglected because the perturbations are considerably minor. The main perturbations are those produced by the Earth's gravitational potential (precession of the line of

apsides and regression of the right ascension of the ascending node), and third-body perturbations. As commented previously, solar radiation pressure is usually of the order of $10^{-7}\ m/s^2$, consequently, for the present study it is marginal.

The accuracy level determines the expansion degree of spherical harmonics to retain when performing the Cartesian harmonic synthesis of the Earth's gravitational potential and its first-order gradient. To minimize the computation costs, the expansion degree to retain was dynamically determined while the curve envelope was being calculated. To cover the whole trajectory, several altitudes were analysed in steps of 2000 km. The orbit propagator used in study [8] incorporates a Runge-Kutta-Fehlberg integrator which uses a table containing the number of degrees to retain as a function of height. This procedure allows to compute the gravitational acceleration, maximize the efficiency of the computations and fulfil the accuracy requirement. Figure 12 plots the expansion degree as a function of height.

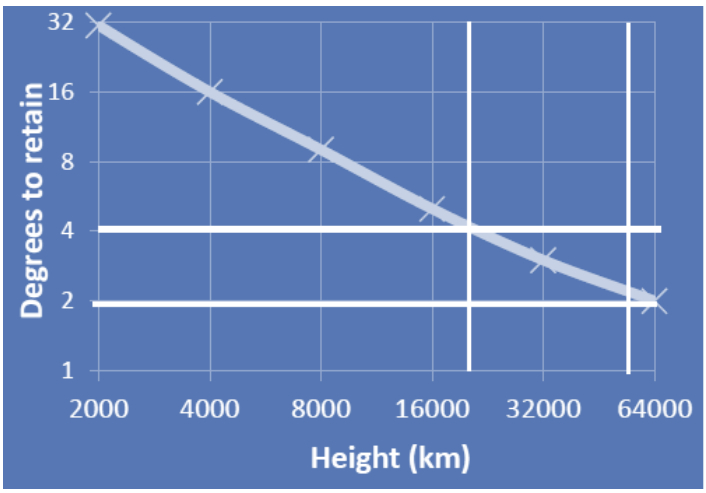

Fig. 12 Degrees of the Earth's gravity field to retain depending on height [8].

Figure 12 shows that the number of degrees to retain diminishes with altitude according to the relation between the orders of spherical harmonics and the satellite's altitude. The orbits under study have a height which varies approximately between 18,000 km and 56,000 km. Consequently, the degrees N to retain are:

$$2 < N \leq 4 \implies N \approx 3. \tag{35}$$

From the results obtained from the station-keeping strategy in study [8], the behaviour in front of these perturbations of some orbital elements can be analysed. Bearing in mind this purpose, the mentioned study have propagated the 45 sets of initial orbital conditions (described in

Section 2.1) over intervals of two years, to incorporate and analyse all the variations that orbital elements experience within this period of time.

To show the results, we choose as an example the orbits distinguished by $e_0 = 0.3$, $i_0 = 60^o$ and five values of the initial right ascension of the ascending node.

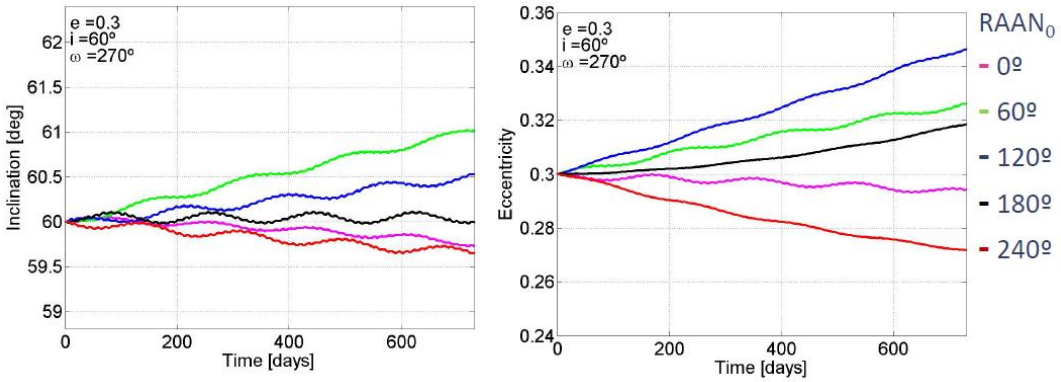

Fig. 13 *Behaviour of inclination and eccentricity over two years of propagation of the selected initial conditions [8].*

Figure 13 shows the variations of inclination and eccentricity over two years. Inclination changes at most ±1º. Eccentricity experiences bigger deviations. However, the variations of this orbital element have negligible effect on the ground track. Consequently, the variations of eccentricity and inclination do not need adjustment over a two-years period.

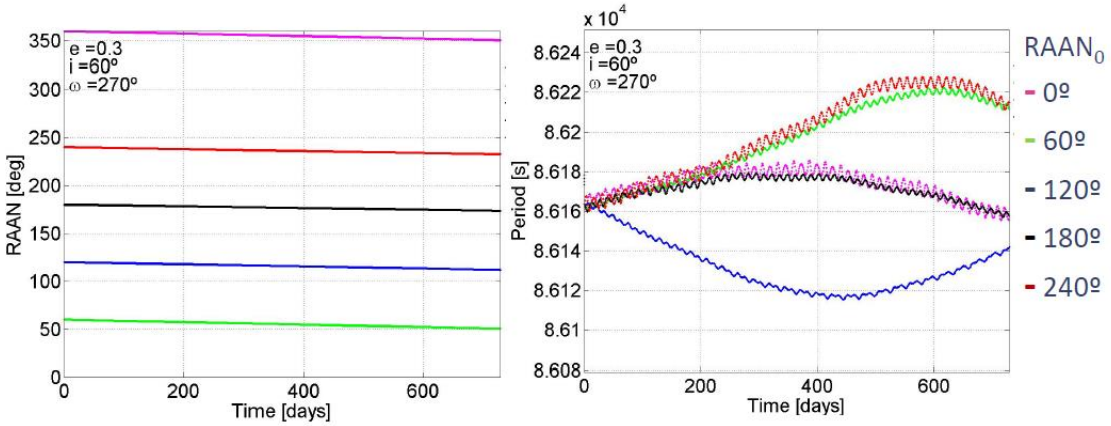

Fig. 14 *Behaviour of RAAN and period over two years of propagation of the selected initial conditions [8].*

Figure 14 shows the fluctuations of right ascension of the ascending node and period over two years. As it was explained, the linear effect of J_2 over the ground track can be counteracted by modifying the orbital period before the propagation begins. It is shown that the contribution of RAAN angular displacement is negligible. Moreover, Figure 14 supports the theory that low

order spherical harmonics of the Earth's gravitational potential field are responsible of long period fluctuations of the orbital period.

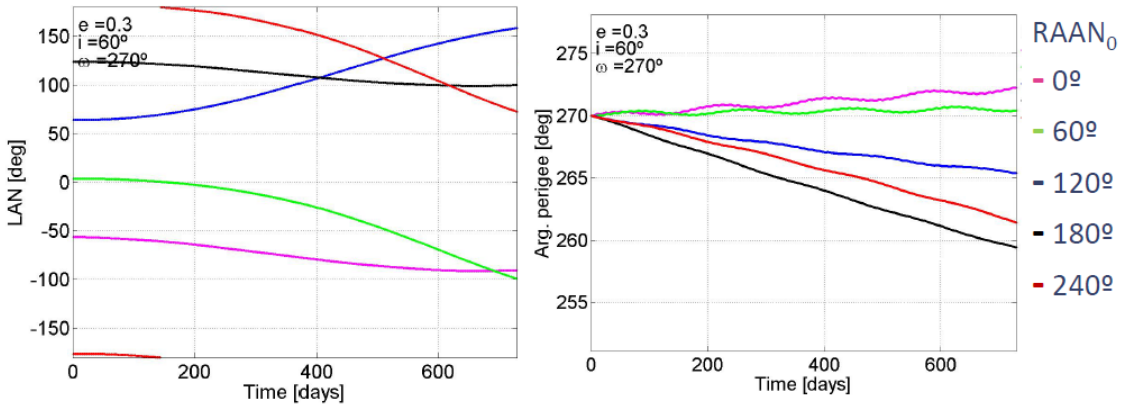

Fig. 15 Behaviour of longitude of ascending node and argument of perigee over two years of propagation of the selected initial conditions [8].

The Moon produce the greatest secular perturbation, which is responsible for the fluctuations of the orbital period. These variations produce a displacement of the ground track in the east-west direction. Figure 15 shows that this movement is of the order of hundreds of degrees in two years. Consequently, a major axis correction is needed in order to avoid this displacement and keep the ground track at the same position. Figure 15 also shows that the argument of perigee experiences a drift whose maximum is a change of approximately 20 degrees in two years. This variation is considerably high, therefore, the argument of perigee requires correction periodically.

Once the mission is ended, the station-keeping maneuvers, which are applied to the satellite during its operation with the aim of keeping the ground track fixed, are no longer applied. Therefore, if the satellite is left in its operational orbit, the orbit will develop freely under the perturbations described so far. Additionally, all the parameters that do not cause significant evolution of the trace over two years will inevitably go out of control. As a result, the orbit suffers modifications which cannot be predicted. In general, the probability that it crosses the GEO ring is not small and has to be considered. Considering the potential danger, a general pact was reached to situate the disposal orbits above the GEO region.

Consequently, an evaluation of alternative options for satellite end-of-life disposal from an eccentric highly-inclined geosynchronous orbit is required.

III. Possible Types of Propulsion Systems

To perform the disposal maneuvers, a propulsion system shall be selected. The performance of the propulsion system is typically the key factor in the global performance of the satellite's system, therefore it must be chosen bearing in mind all the consequences of this important decision. The satellite's propulsion system will affect the following parameters:

- Thrust.
- Specific impulse.
- Propellant mass, hence wet mass of the satellite.
- Power consumption.
- Cost.
- Lifetime.
- Complexity.
- Reliability.
- Maneuver execution time.
- Environmental issues.

To select the best option, a comparison between the main thrusters will be developed on the basis of their suitability to operate in the described orbit and their advantages and drawbacks. Two propulsion groups will be considered: chemical propulsion systems (including cold gas) and electrical propulsion systems.

3.1. Chemical thrusters

In chemical engines, pressure forces push the gas against the walls and they are also responsible for the gas acceleration produced in nozzle. Conventional chemical thrusters are characterized by fairly high thrust, but low exhaust velocities, consequently, they give a high specific power. There are different types of chemical thrusters (this study includes the cold gas type). The main ones are listed in Table 7 together with their advantages and disadvantages.

Engine	Advantages	Disadvantages
Monopropellant engine	○ High reliability due to large experience. ○ Simple system (no ignition system, only one set of plumbing). ○ Little weight. ○ Wide thrust range. ○ Modulable.	○ Little space (no need for oxider). ○ Low specific impulse (≈ 200-250 s). ○ Use of toxic fuels.
Bipropellant engine	○ High specific impulse in comparison with monopropellants (>300 s). ○ Large experience base (less than monopropellants). ○ Able to do re-starts. ○ Wide thrust range. ○ Modulable.	○ High complexity. ○ Short pulsing difficult. ○ High cost. ○ Heavy. ○ Use of toxic fuels.
Solid-fuel engine	○ Relatively high specific impulse (better than monopropellants and similar to bipropellants; ≈ 250-300 s). ○ Simple system. ○ Reliable (mainly because of their simple architecture). ○ Moderate-to-high cost. ○ High density of the propellant. ○ Low structural index ○ Compact size.	○ 1-5% dispersion in impulse direction, therefore trim engines are required in order to perform accurate maneuvers. ○ Non-restartable; one thruster per burn. ○ Total impulse fix. ○ Currently not suitable for long space missions.
Cold gas	○ Moderate-to-high cost. ○ Reliable (large experience base). ○ Safe. ○ Simple system. ○ Use of benign propellants. ○ Currently represent the smallest thruster technology available.	○ Low density of the propellant. ○ Propellant at high pressure. ○ Low thrust (≈10 mN). ○ Moderate impulse capability. ○ Severely limited in specific impulse (≈50 s). ○ Elevate risk of valve leakage problems.

Table 7 *Chemical thrusters performance.*

Considering a constant exhaust speed v_e, the increment in velocity experienced by the spacecraft can be calculated from:

$$m\frac{dv}{dt} = \frac{dm}{dt}v_e \quad \Rightarrow \quad \Delta v = v_e \ln\left(\frac{m_i}{m_f}\right). \tag{36}$$

where m is the mass, m_i its initial value, m_f its value at the end of the maneuver and Δv is the velocity variation caused. Eqs. 36 shows that Δv has a proportional relation with the exhaust velocity and it is logarithmically dependent on the fuel mass ejected. As chemical thrusters have low exhaust speeds, the velocity variation is also low.

This undesirable property of chemical thrusters becomes a considerable negative characteristic when spacecraft is operating in missions that require large velocity variations. This drawback, which derives from Newton's law of dynamics, appears due to the limitation in thermal transfer conditions and accessible reaction energies.

3.2. Electrical engines

An electrically-powered spacecraft propulsion system is used to produce thrust by means of electric and/or magnetic forces to accelerate a specific propellant. The common electric engines are electrostatic, electro-thermal or electromagnetic propulsion systems. Electro-thermal engines are based on chemical propulsion systems, but they are powered by electrical fields. Electrostatic and electromagnetic propellers are based on the direct application of body forces to accelerate particles through the propellant stream.

Consequently, the speed at which the propellant particles can be ejected has no physical limit, except reaching the speed of light. For this reason, electrical rockets are characterised by high exhaust speeds, which means operating at high specific impulse (of 500 to over 3000s), therefore they use much less propellant in comparison with classical propulsion systems. Nevertheless, these engines have a practical limitation because the fields are maintained by a power source, which is not unlimited.

The mass flow of this engines is considerably low, therefore the thrust is lower than the propulsion force obtained by chemical thrusters. The power consumption per thruster is considerable and the value is usually on the order of KWs. As a whole, electric thrusters can create small thrusts over long periods and they can operate at high speeds for a long time.

Currently, electric propulsion systems have a large experience base, hence, they are reliable and widely used on spacecraft. Their features make this type of rockets the most suitable for some deep space missions. Electric thrusters have been typically used for orbit raising, station keeping and primary propulsion. There are different types of electric thrusters, the main ones and their advantages and disadvantages are shown in Table 8.

Engine	Advantages	Disadvantages
Arcjet thruster	○ When fired with hydrazine, it can work together with a monopropellant AOCS by taking advantage of the same tank and propellant management system. ○ Use of non-flammable propellant (usually ammonia or hydrazine). ○ High specific impulse (600 – 1000 s). ○ Large lifetime (approximately above 1200 h). ○ Substantial propellant mass savings. The propellant mass flow is around 20 – 50 mg/s. ○ Reliable (large experience base).	○ Low thrust (100 – 250 mN). ○ Medium overall efficiency (up to 40%). ○ High power demand (750-2000 W). ○ Broadband noise. ○ Slight cathode and anode erosion. ○ High operating temperature. Consequently, there is thermal isolation difficulty (thermal radiation).
Resistojet	○ When fired with hydrazine, it can work together with a monopropellant AOCS by taking advantage of the same tank and propellant management system. ○ High specific impulse (300 – 1000 s). ○ High overall efficiency (up to 70%). ○ Substantial propellant mass savings. The propellant mass flow is around 100 mg/s. ○ Reliable (large experience base). ○ Propellant heated electrically. Exhaust velocity depends on temperature ($v_e \leq 10\ km/s$).	○ Low thrust (100 – 400 mN). ○ Lifetime (approximately above 400 h). ○ High power demand (500-600 W).
Hall effect thruster	○ High specific impulse (1600 – 2000 s). NASA achieved 3000 s. ○ Large lifetime (approximately above 7000 h). ○ Reasonable overall efficiency (up to 50%). ○ Substantial propellant mass savings. The propellant mass flow is around 5 – 10 mg/s.	○ Low thrust (80 – 100 mN). ○ High power demand (1300-1500 W). ○ Some concerns on pollution.

	○ Reliable (large experience base, mostly in Russia).	
Ion thruster	○ High specific impulse (2500 – 3800 s). NASA achieved 7000 s. ○ Large lifetime (approximately above 15000 h). ○ Medium-high overall efficiency (up to 60%). ○ Substantial propellant mass savings. The propellant mass flow is around 0.5 – 5 mg/s. ○ Reliable (large experience base).	○ Low thrust (5 – 40 mN). ○ High power demand (500-800 W). Also, there are some cases with 5000 W. ○ Broadband noise. ○ Slight cathode and anode erosion. ○ Moderately heavy engine.
Pulsed plasma thruster (PPT)	○ High specific impulse (up to 1000 s). ○ Reliable (large experience base). ○ Low power demand (10-100 W). Sometimes can be up to 200 W. ○ Non-toxic solid propellant (Teflon). ○ Various thrusters can be used by a shared capacitor.	○ Extremely low thrust (0.1 – 2 mN). ○ Low overall efficiency (below 20%).
Field emission electric propulsion (FEEP)	○ Extremely high specific impulse (6000 – 10000 s). ○ Reliable (large experience base). ○ Low power demand. ○ Possible spacecraft ground handling.	○ Extremely low thrust (0.001 – 2 mN). ○ Medium overall efficiency (up to 50%). ○ Moderately heavy auxiliary components.
Colloidal thruster	○ High specific impulse (500 – 1500 s). ○ Low power demand.	○ Extremely low thrust (0.001 – 1 mN). ○ Moderately heavy auxiliary components.
VASIMIR (variable impulse magneto-plasma rocket)	○ High thrust capability (in the order of 1N and above). ○ Extremely high exhaust velocity ($v_e \leq 290000\ m/s$). ○ Extremely high specific impulse (30000 s). ○ High energy-mass correlation (E/m = 43000 MJ/kg).	○ High power demand. ○ Limited development status.

Table 8 *Electrical thrusters performance.*

IV. Possible End-of-Life Disposal Strategies

To ensure the selection of a suitable, effective and efficient maneuver, an analysis of the possible disposal strategies must be developed, highlighting the positive and negative effects of each case. Figure 16 shows the main disposal regions for satellites. There exists two types of end-of-life disposal strategies:

- De-orbiting, i.e., moving the satellite to a lower orbit which will eventually make it re-enter into the atmosphere.
- Manoeuvring to a higher orbit.

The de-orbiting maneuvers consist of moving the satellite into an orbit with an altitude considerably below its operational orbit and, at that point, initialize either an uncontrolled or a controlled de-orbiting. To perform an uncontrolled de-orbiting maneuver, the satellite must be decelerated by means of either a moderately short impulse maneuver, which use chemical thrusters, or a long low-thrust maneuver of electrical thrusters. The purpose is to decrease the orbital lifetime by increasing the aerodynamic deceleration, therefore, the perigee altitude of the initial orbit must be reduced. The satellite will be placed into a disposal orbit. The atmospheric drag causes re-entry, and when the satellite flies through the densest layers it burns up, typically below 25 years.

If the atmospheric drag does not guarantee the complete destruction of the satellite, an uncontrolled disposal strategy must be replaced by a controlled re-entry to reduce the risk of risk in populated areas. To perform this strategy, the perigee altitude must be reduced to reach an adequate altitude which permits atmospheric capture. This re-entry maneuver requires exact computations to determine in advance the spot of impact on ground. This is needed because, during the re-entry, the structure parts that have endured the aerothermal heating start to disintegrate which creates an area of fragments in the zone of impact. For this reason, this area must be previously designated to minimize the risk to damage people.

Despite the benefits of the de-orbiting strategy, this re-entry maneuver hardly can be carried out from an eccentric highly-inclined geosynchronous orbit, like those studied in this FDP. This is because the propellant costs to perform a de-orbiting maneuver from this family of orbits are extremely high. Moreover, the analysed orbits are most of the time placed above the GEO protected area. Therefore, if the satellite have to perform a de-orbiting maneuver, it may cross

the GEO protected area and it may produce an impact with an operational satellite or any space object orbiting in this region. Although in several cases the satellite's orbit does not cross the GEO ring, to avoid this risk, a general pact was reached to situate the disposal orbits above the GEO region. Such region is called Super GEO Storage Orbit (Figure 16).

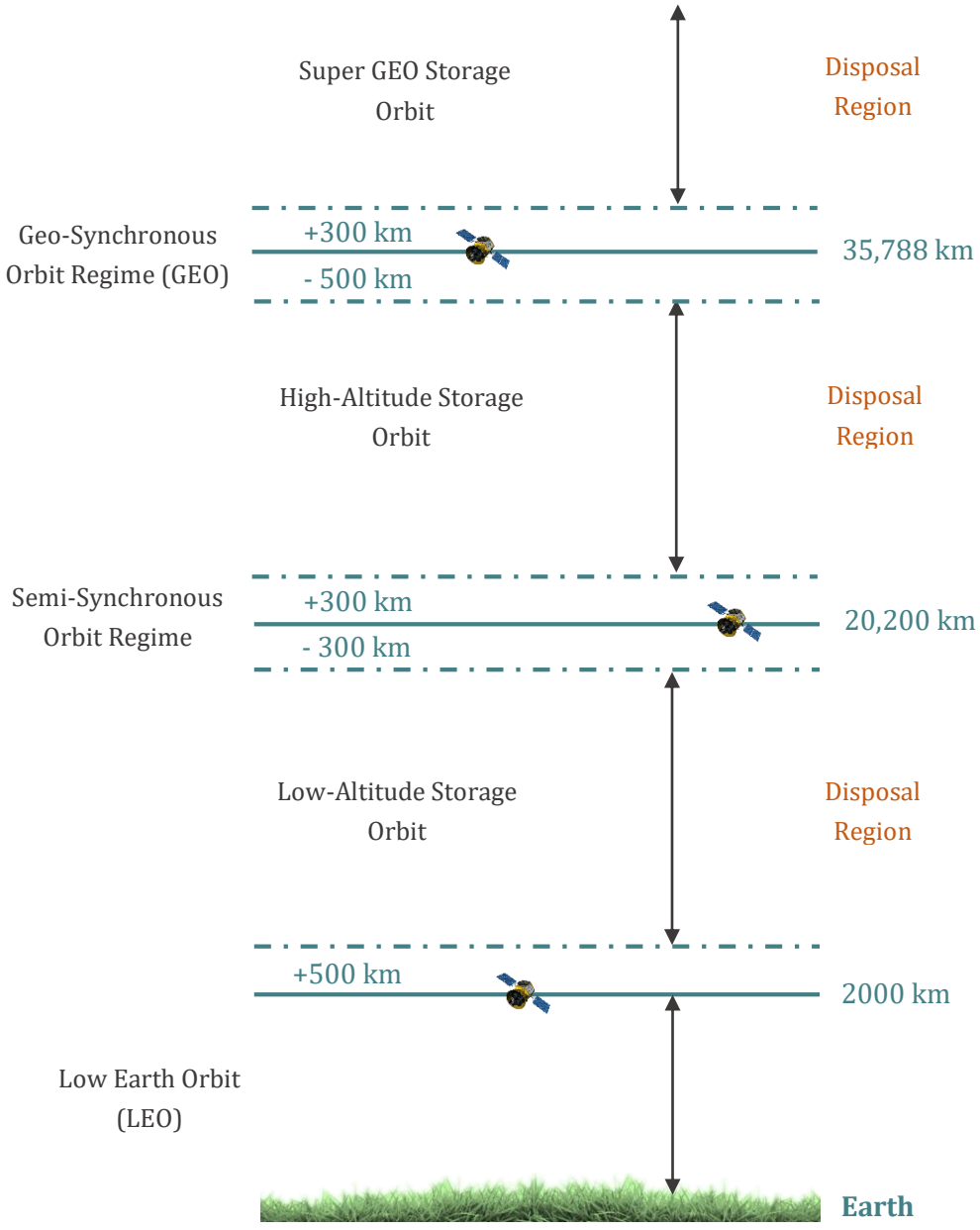

***Fig. 16** Storage orbits and disposal regions options for end-of-life disposal operations.*

Consequently, the most suitable post-mission strategy consists of moving the spacecraft to a high disposal orbit. This is the common maneuver for eccentric highly-inclined geosynchronous orbits. Also, it is considerably attractive from an energetic point of view. This strategy aims at

moving the spacecraft to this specific disposal area in which the satellite will not be an obstacle for upcoming space operations. A useful solution is the circularization or almost circularization of the disposal orbit.

4.1. Circularization using an impulse maneuver

Starting from an eccentric orbit with the apoapsis placed at the desired final altitude, to achieve a circular orbit at such altitude, the periapsis must be raised until the selected altitude while the apoapsis is kept fixed. Typically, to perform a circularization, one or a few thruster burns are used with a total duration shorter than the orbital period. To keep the apoapsis unchanged and raise the periapsis altitude, the impulse must be applied at apoapsis, must be orthogonal to the line of apsides in the direction of motion. This maneuver increases the orbital energy and reduces the eccentricity. Once the maneuver is finalised, a circular orbit at the original apoapsis altitude is obtained. Figure 17 outlines a circularization maneuver by one impulse.

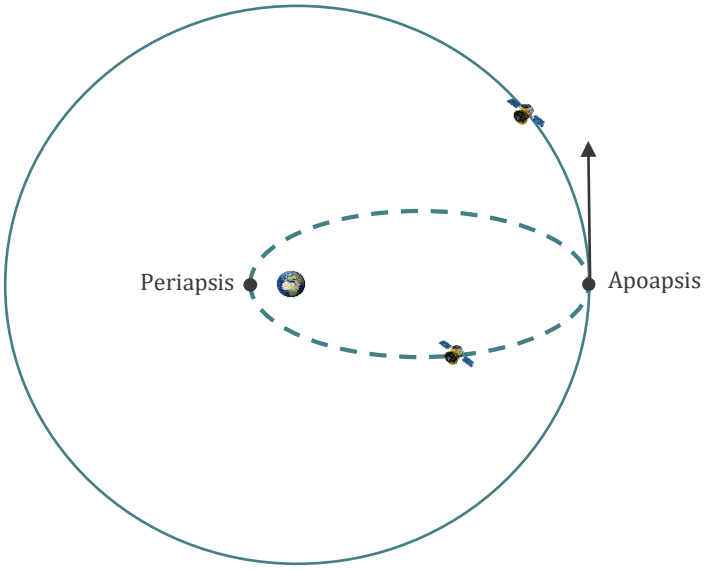

Fig. 17 Circularization maneuver.

If the initial eccentricity is moderate to high, the Δv required in the one-impulse circularization is very high. In order for the maneuver to have a short duration, the thrust provided must be large, and this can only be achieved with chemical engines. To give an approximated idea of the propellant cost used to perform this disposal strategy, this strategy is simulated using a script programmed in Matlab and the data of the initial orbit from Section 2.1.

4.1.1. Algorithm of an impulse disposal maneuver

This section aims at computing the increment of velocity and the propellant mass required to perform the described circularization. Firstly, we are going to apply the conservation of mechanical energy in order to find an expression for the specific mechanical energy, which will allow us to calculate the spacecraft velocity.

The gravitational force $\boldsymbol{F}$ experienced by the satellite in the relative orbit is:

$$\boldsymbol{F} = m\,\boldsymbol{a_{rel}} = -m\,\frac{G(m+M)}{r^3}\,\boldsymbol{r} \cong -\frac{m\mu}{r^3}\,\boldsymbol{r}. \tag{37}$$

The elementary work dW made by **F** over a displacement $d\boldsymbol{r}$ is:

$$dW = \boldsymbol{F} \cdot d\boldsymbol{r}\,. \tag{38}$$

$\boldsymbol{F}$ can be expressed by means of the potential energy per unit mass Φ, hence:

$$\boldsymbol{F} = -m\nabla\Phi\,, \tag{39}$$

where:

$$\Phi = -\frac{G(m+M)}{r} \cong -\frac{\mu}{r}. \tag{40}$$

By applying the theorem of kinetic energy:

$$dW = dE_k\,, \tag{41}$$

where:

$$dE_k = d\left(\frac{mv^2}{2}\right), \tag{42}$$

we obtain:

$$-m\,d\left(-\frac{\mu}{r}\right) = d\left(\frac{mv^2}{2}\right) \Longrightarrow d\left(\frac{mv^2}{2} - m\frac{\mu}{r}\right) = 0\,. \tag{43}$$

The total mechanical energy E_0 is:

$$E_0 = \frac{mv^2}{2} - m\frac{\mu}{r} = constant. \tag{44}$$

Dividing this energy by the mass yields:

$$E = \frac{E_0}{m} = \frac{v^2}{2} - \frac{\mu}{r}, \tag{45}$$

which is the specific mechanical energy E. This quantity is conserved along a Keplerian orbit, and as such it can be computed at any point. It can be computed at any point on the orbit. In the case of an elliptical orbit of semimajor a and eccentricity e, the evaluation of E at periapsis (r_π, v_π) gives:

$$E = \frac{v_\pi^2}{2} - \frac{\mu}{r_\pi}, \tag{46}$$

where:

$$r_\pi = \frac{a(1-e^2)}{1+e\cos(\theta)} \Longrightarrow \theta = 0^o \Longrightarrow r_\pi = \frac{a(1-e^2)}{1+e} = \frac{h^2}{1+e}\ ; \tag{47}$$

$$\boldsymbol{v_\pi} = r\dot{\theta}\boldsymbol{u_\theta} \Longrightarrow v_\pi = \frac{\left(\frac{h^2}{\mu}\right)\dot{\theta}}{1+e} = \frac{\left(\frac{h^2}{\mu}\right)\left(\frac{h}{r_\pi^2}\right)}{1+e} = \frac{\left(\frac{h^3}{\mu r_\pi^2}\right)}{1+e} = \frac{\mu(1+e)}{h}. \tag{48}$$

Here, $\boldsymbol{h} = \boldsymbol{r} \times \boldsymbol{v}$ and is the specific angular momentum vector, and $\dot{\theta}$ is the local orbital angular velocity of the satellite. Therefore:

$$E = \frac{1}{2}\frac{\mu^2(1+e)^2}{h^2} - \frac{\mu^2(1+e)}{h^2} = -\frac{\mu^2(1-e^2)}{2h^2}, \tag{49}$$

Upon substituting:

$$a(1-e^2) = \frac{h^2}{\mu} \Longrightarrow \frac{h^2}{\mu(1-e^2)} = a, \tag{50}$$

we obtain:

$$E = -\frac{\mu}{2a}. \tag{51}$$

If the orbit is circular, then $a = r$, and:

$$E = -\frac{\mu}{2r}. \tag{52}$$

Equating Eqs. 44 and 49 written for the apogee (r_α, v_α) yields:

$$-\frac{\mu}{2a}=\frac{v_\alpha^2}{2}-\frac{\mu}{r_\alpha} \implies \boxed{v_\alpha=\sqrt{\frac{2\mu}{r_\alpha}-\frac{\mu}{a}}}, \tag{53}$$

in which:

$$r_\alpha=\frac{a(1-e^2)}{1+e\cos(\theta)} \Longrightarrow \theta=180^o \Longrightarrow r_\alpha=\frac{a(1-e^2)}{1-e}. \tag{54}$$

Equating Eqs. 44 and 50 allows to find the speed v_c in the circular orbit of radius r:

$$-\frac{\mu}{2r}=\frac{v_c^2}{2}-\frac{\mu}{r} \implies v_c=\sqrt{\frac{2\mu}{r}-\frac{\mu}{r}} \implies \boxed{v_c=\sqrt{\frac{\mu}{r}}}. \tag{55}$$

Setting $r=r_\alpha$, Eq. 56 provides the velocity of the final circular orbit at apogee altitude.

Finally, the velocity variation Δv is the magnitude of the difference between the velocity vectors of the satellite after and before the maneuver, i.e., respectively on the final circular orbit and at the apogee of the ellipse. Now, given that these two vectors are parallel, the magnitude of their difference equals the difference of their magnitudes.

$$\boxed{\Delta v=v_c-v_\alpha=\sqrt{\frac{\mu}{r}}-\sqrt{\frac{2\mu}{r_\alpha}-\frac{\mu}{a}}}. \tag{56}$$

Once Δv is obtained, it is possible to compute the required propellant mass m_p. This is done by means of the rocket equation (formula of Tsiolkovski):

$$\Delta v=I_{sp}\,g_0\ln\left(\frac{m_i}{m_f}\right), \tag{57}$$

where:

- I_{sp} is the specific impulse of the propulsion system. Typical values of this parameter for chemical engines range between 250 and 300 s.
- g_0 is a factor used to change the dimensions, from velocity to time. Its value is $g_0=9.81\ m/s^2$.
- m_i is the spacecraft initial mass, which means it is the mass prior to burn. Therefore:

$$m_i = m_{dry} + m_p\,, \tag{58}$$

where m_{dry} is the dry mass of the spacecraft, and m_p is the propellant mass required to execute the maneuver. Here we are adopting the simplifying assumption that all the available propellants is spent in the maneuver.

- m_f is the spacecraft final mass, which means it is the mass after burn. Therefore:

$$m_f = m_{dry}\,. \tag{59}$$

Eventually, Eqs. 57 can be written as:

$$\Delta v = I_{sp}\, g_0 \ln\left(\frac{m_{dry} + m_p}{m_{dry}}\right). \tag{60}$$

By isolating m_p, it is possible to compute its value:

$$\boxed{m_p = m_{dry} \cdot \left(e^{\frac{\Delta v}{I_{sp} g_0}} - 1\right)}. \tag{61}$$

4.1.2. Propellant budget of impulsive maneuvers

A script programmed in Matlab is used to compute the propellant mass used to execute this disposal strategy by means of an impulsive maneuver. This script follows the steps described in the previous algorithm (Section 4.1.1.). The script starts by using the orbital elements of the initial orbit, specifically semi-major axis and eccentricity. Bearing in mind the 45 suitable sets of initial orbital elements reported in Section 2.1., it is possible to determine all the possible disposal maneuvers and their corresponding costs.

The semi-major axis is fixed and its value is $a_0 = 42164.6\ km$. The values of the eccentricity appearing in Table 5 are:

$$e_0 = 0.25; 0.30; 0.35; 0.40. \tag{62}$$

The algorithm does not depend on the orbital inclination, since the intention is to perform a circularization in the initial orbital plane. In case a change-of-plane maneuver is required by the specific disposal strategy, then parameters like the inclination and the right ascension of the ascending node will be involved in the determination of the maneuver.

To compute the propellant mass, the dry mass and specific impulse must be known. Communications satellites have typical dry mass of 3000 kg. To validate this value, a research on some communications satellites and their launch mass has been carried out. Table 9 reports the outcomes of the research.

Communications satellite name	Launch date	Launch mass (kg)	Orbit type
GSAT-15	Nov 11, 2015	3164	Geosynchronous
GSAT-6	Aug 27, 2015	2117	Geosynchronous
GSAT-16	Dec 07, 2014	3182	Geosynchronous
GSAT-14	Jan 05, 2014	1982	Geosynchronous
GSAT-7	Aug 30, 2013	2650	Geosynchronous
INSAT-3D	Jul 26, 2013	2060	Geosynchronous
GSAT-10	Sep 29, 2012	3400	Geosynchronous
INSAT-4CR	Sep 02, 2007	2130	Geosynchronous
INSAT-4B	Mar 12, 2007	3025	Geosynchronous
EDUSAT	Sep 20, 2004	1951	Geosynchronous

Table 9 List of communications satellites [41].

By using the described data and algorithm, it is possible to compute the propellant mass needed to perform this disposal strategy. Table 10 shows the results obtained from the Matlab script.

Combinations	1	2	3	4
Eccentricity e_0	0.25	0.30	0.35	0.40
Apoapsis radius r_α (km)	52767.38	54878.08	56988.78	59099.47
Velocity variation Δv (km/s)	0.369	0.441	0.513	0.586
Propellant cost m_p (kg)	486.91	590.97	698.54	810.34

Table 10 Propellant cost of the disposal maneuver according to the selected eccentricity.

The propellant mass cost of this disposal maneuver is between 500 and 1000 kg depending on the eccentricity of the initial orbit. To bring this amount of propellant mass, an extra fuel tank is needed. This means the whole satellite mass increases and, consequently, satellite's structure will probably need to be modified according to the new mass requirements. Therefore, an impulse maneuver is not affordable because the required extra mass and cost are overly high.

4.1.3. Sketch of the impulsive maneuver

A Matlab script is programed to plot the disposal maneuver. To show an example, if we select the data:

$$a_0 = 42164.6km; e_0 = 0.25; i_0 = 55^o;\ \omega_0 = 270^o;\ \Omega_0 = 0^o, \qquad (63)$$

which describe one of the studied orbits, Figure 18 and 19 are obtained. These plots show the initial orbit in blue and the final orbit in green. The initial orbit is an eccentric highly-inclined geosynchronous orbit with the selected data and the final orbit resulting from the circularization is a circular orbit at apogee altitude. Moreover, the point of application of the impulsive maneuver, which corresponds to the apogee point of the initial orbit, is also shown. This point belongs to both orbits and it is indicated with a red circle. The position of the Earth is represented with a black dot in the origin of the reference system used.

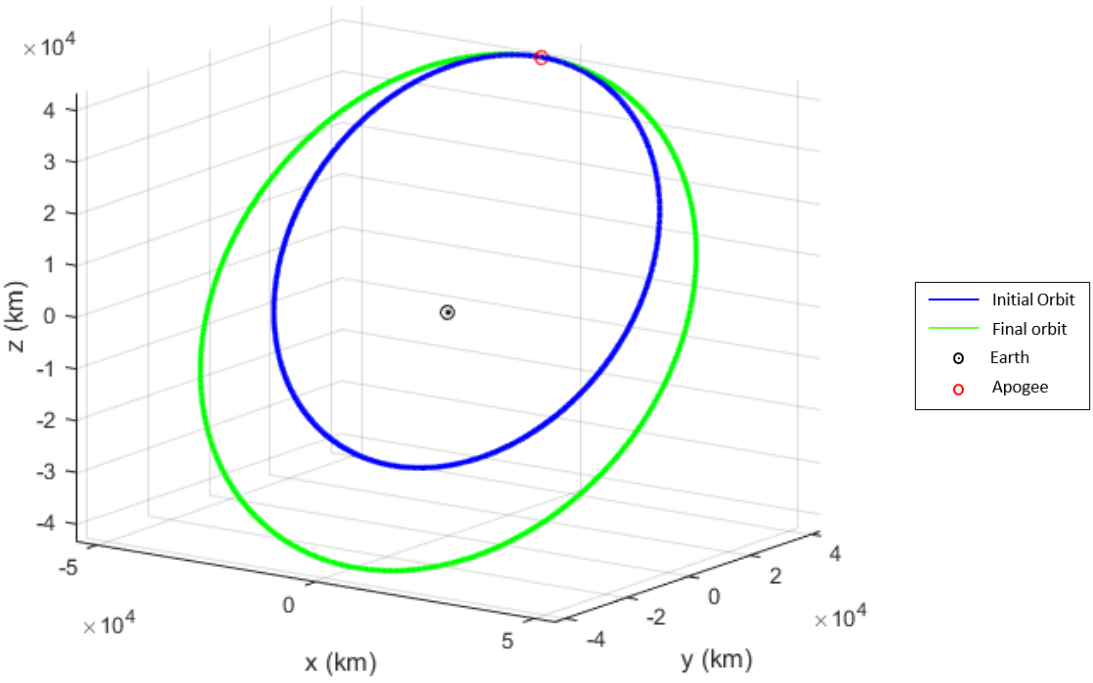

Fig. 18 3D view of the initial and final orbit.

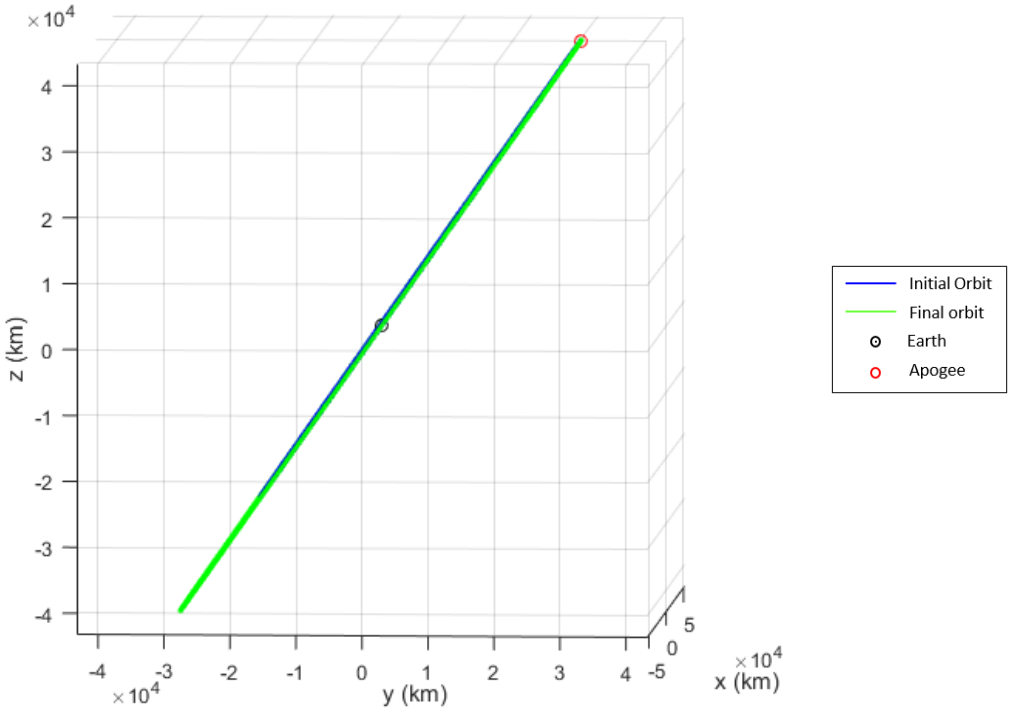

Fig. 19 3D view of the initial and final orbit, both with the same inclination.

4.2. Performance of a disposal maneuver

Although the circularisation by means of an impulsive maneuver is a possible strategy to circularise an orbit, it is not the most efficient way to do it. The variation of energy produced by changing the orbit is a useful measure of the performance of a particular space maneuver. As it has been mentioned, the specific energy of an elliptic orbit E is:

$$E = \frac{v^2}{2} - \frac{\mu}{r} = -\frac{\mu}{2a}. \qquad (64)$$

To study the correlation between the parameters that affect the change in orbital energy ΔE, it is needed to linearize Eqs. 64:

$$\Delta E = v\,\Delta v + \frac{\mu}{r^2}\,\Delta r\,. \qquad (65)$$

Eqs. 65 shows the direct correlation of the change in energy ΔE with the variation in the instantaneous position Δr and/or velocity Δv. However, in the described disposal strategy, the change in the instantaneous spacecraft position is physically impossible, consequently, the change in orbital energy is only produced by a modification of the instantaneous velocity by

means of some impulses. Therefore, in an impulsive maneuver, the change in the specific energy can be approximated as:

$$\Delta E = v\,\Delta v\,. \tag{66}$$

The change in energy increases with the velocity of the spacecraft v and the velocity variation Δv. To obtain the largest change in energy, the impulse should be applied at the point where the satellite has maximum velocity. For elliptic orbits, this site corresponds to periapsis. Nevertheless, a circularization made through an impulsive maneuver requires a considerably amount of propellant. The propellant mass needed increases with Δv, and Δv increases with v. Consequently, a circularisation by means of an impulsive maneuver carried out at perigee (r_π, v_π) consume much more propellant than such performed at apogee (r_α, v_α). Table 11 reports the outcomes of this study.

Moreover, the final orbit shares the point of application of the impulse with the initial orbit. Bearing in mind that the purpose of this disposal strategy is to perform a circularization while raising the periapsis, the fastest solution is the one analysed, which consist of applying the impulse at apogee.

The change in the energy ΔE is the difference between the energy in the almost circular orbit E_c and the energy in the elliptical orbit E_e:

$$\Delta E = E_c - E_e = -\frac{\mu}{2r_e} - \left(-\frac{\mu}{2a}\right) = \frac{\mu}{2a} - \frac{\mu}{2r_e}, \tag{67}$$

where r_e is the radius of the application spot of the impulsive maneuver. By using a Matlab script, the change in energy, for each of the combinations shown in Table 10, is computed. The outcomes are shown in Table 11.

Eccentricity e_0	**0.25**	**0.30**	**0.35**	**0.40**
Change in specific energy ΔE_α (km^2/s^2)	*0.95*	*1.09*	*1.23*	*1.35*
Propellant cost m_{p_α} (kg)	*486.91*	*590.97*	*698.54*	*810.34*
Change in specific energy ΔE_π (km^2/s^2)	*-1.58*	*-2.03*	*-2.55*	*-3.16*
Propellant cost m_{p_π} (kg)	*1935.04*	*2519.30*	*3216.52*	*4064.52*

Table 11 *Change in orbit energy ΔE needed to carry out an impulse maneuver at apogee.*

Table 11 shows that the magnitude of ΔE increases with the eccentricity, as it happened with the propellant mass required to carry out the space maneuver. Therefore, if the initial orbit has high eccentricity, the change in orbit energy will be also large.

Considering the obtained results, the analysed disposal maneuver is effective, because it achieves the goal without losing time and the final altitude obtained is considerably high. However, it requires too many propellant, which is a big drawback because, amongst others disadvantages, this greatly increases the initial spacecraft weight. For this reason, it is interesting to investigate another strategy which needs less propellant, although this means spending long time to reach the disposal orbit.

One useful and efficient strategy that has become considerably popular in recent years and could provide an appropriate disposal strategy is low-thrust propulsion. When considering continuous maneuvers and multiple impulsive maneuvers, the regions or spots of application of these impulses produce several consequences. Therefore, the decision between carrying out the burn closer to perigee, where the orbit velocity is maximised, and applying it at apogee, where the perigee raises directly, becomes increasingly important to optimise the maneuver.

4.3. Circularization using a low-thrust maneuver

Propulsion systems such as electric ion engines, laser engines and solar sails systems are gaining popularity in the space maneuver industry. This is mainly because these technologies allow the execution of low-thrust maneuvers, which are the present and, with high probabilities, the future of controlling satellites. Low-thrust propulsion systems open the door to a huge variety of maneuvers and space profiles that were impossible to imagine in the past. Although they are characterized by low thrust, they usually have extremely high values of specific impulse and they provide adaptive and continuous thrust control. These features are responsible of the spacecraft performance during different orbital maneuvers. This satellites use less propellant mass than if, for example, the maneuver is executed by means of a chemical thruster. By reducing the propellant mass, the payload mass fraction is increased in comparison with the case of chemical propulsion systems. Consequently, low-thrust maneuvers have considerably high efficiency. However, they require more time than chemical engines to reach the final orbit.

The design of a transfer maneuver by means of a low-thrust system is a challenging task, specifically if the maneuver includes propulsion and trajectory optimization. However, in this

FDP, the proposed low-thrust disposal strategy will not dive into the world of optimal low-thrust, because it escapes from the project aims.

4.3.1. Description of the low-thrust maneuver

The aim of this section is to design, by means of a continuous thrust maneuver, the disposal orbit of a satellite, which is operating in one of the eccentric highly-inclined geosynchronous orbits described in Section II. Moreover, the purpose is to carry out this maneuver by using the minimum propellant mass. The final disposal orbit will be a circular or almost circular orbit placed at a distance enough far from the GEO ring to avoid any possible collision or dangerous situation. To take into account some interesting data, Figure 16 shows that the geosynchronous orbit regime was established as 300 km above and 500 km below the GEO altitude, which is at 35788 km.

During the disposal maneuver, the satellite shall not cross this protected region. Therefore, the decision of selecting the spot at which the first burn is applied has considerably importance. This is because, since the first time the satellite crosses the zero latitude, it shall be flying at an altitude enough far from the GEO protected area. In some initial orbits, this requirement may remove the chance to start the disposal strategy in a point close to perigee, which is an interesting option from the point of view of the performance. As it was explained in Section 4.2: as faster is the satellite, as larger will be the change in the orbital energy. Considering the orbits studied in this FDP and by means of a Matlab script, it is possible to compute the perigee and apogee altitudes, which are shown in Table 12. These values will be interesting to select the spot at which the maneuver is started.

Combinations	**1**	**2**	**3**	**4**
Eccentricity e_0	0.25	0.30	0.35	0.40
Apogee radius r_α (km)	52767.38	54878.08	56988.78	59099.47
Perigee radius r_π (km)	31660.43	29549.74	27439.04	25328.34

***Table 12** Apogee and perigee radius.*

Table 12 shows that, in all of the combinations, perigee is located at an altitude lower than the GEO altitude. Therefore, if the low-thrust maneuver is started at this place, there will be a period of time during which the satellite has an altitude equal to the GEO protected area. The spacecraft can reach and surpass this altitude before it crosses the zero latitude, in that case, there would

be no problem to carry out this strategy. If the satellite has an altitude considerably lower than GEO altitude when it crosses the zero latitude, there would not be any trouble. However, if in the zero latitude it has an altitude similar to the altitude of the GEO ring, this maneuver cannot be executed. In such case, we have to move the starting spot far from perigee to gain altitude.

It is possible to know if the spacecraft will cross the GEO protected area at zero latitude before precisely know the low-thrust maneuver it will describe. This can be achieved by plotting the selected initial orbit and, in the same Figure, the GEO ring. Then, we have to focus on the zero latitude and look if the spacecraft altitude in the initial orbit at such point is higher or lower than the GEO altitude or equal to it. To achieve this goal, a Matlab script was programmed.

Firstly, the Earth's parameters and the GEO altitude are defined in the script. To plot the initial orbit, the first step is writing the values of the six orbital elements of the studied orbit. Also, this script uses the same function used in Section 2.2.2, which computes the state vector which contains orbital position and velocity in geocentric equatorial frame. To plot the whole orbit, a loop is programmed. This loop goes through all the true anomaly values, from $\theta = 0\ rad$ to $\theta = 2\pi\ rad$, and, for each value, computes the mentioned state vector by means of the commented function. From this we obtain the Cartesian coordinates of the satellite at each point and we plot it to obtain the complete curve envelope. Moreover, if the script detects that the computed coordinates are the ones of the zero latitude, the script plots this point in order to highlight it. The script follows the same steps to plot the GEO ring, which is situated at zero latitude during the whole orbit, because GEO orbits are equatorial, which means zero inclination.

The figure obtained by using this Matlab script shows the initial orbit in blue, the two points at zero latitude are highlighted with a red circle, the GEO altitude orbit in red and the limits of the GEO protected area are plotted in yellow. The position of the Earth is represented with a black dot in the origin of the reference system used.

To show an example, if we select the data:

$$a_0 = 42164.6km; e_0 = 0.25; i_0 = 55^o;\ \omega_0 = 270^o;\ \Omega_0 = 0^o, \qquad (68)$$

which describe one of the studied orbits, Figure 20 and 21 are obtained.

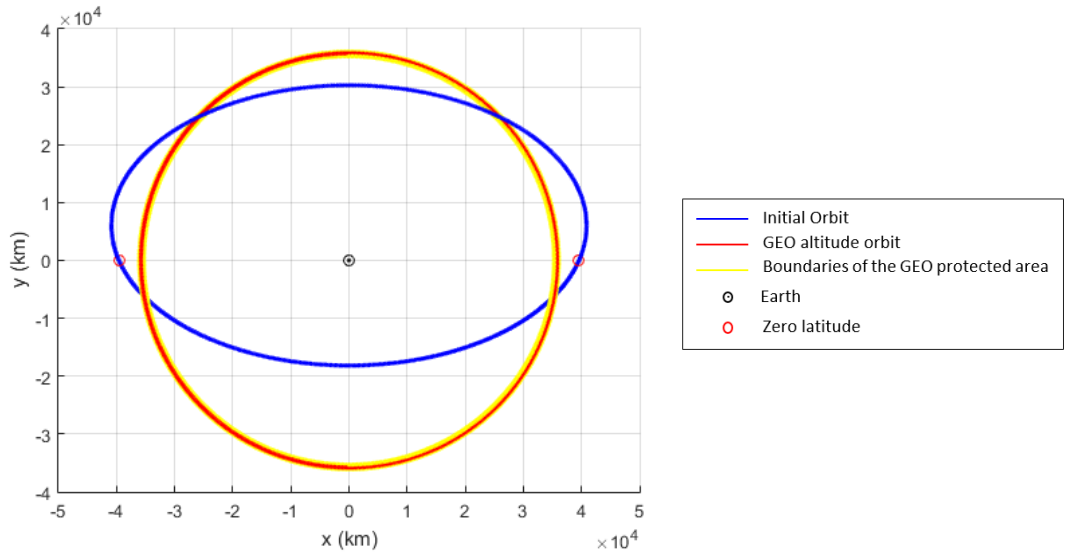

***Fig. 20** x-y view of the initial orbit and the GEO protected area for $e_0 = 0.25, i_0 = 55^o$ and $\Omega_0 = 0^o$.*

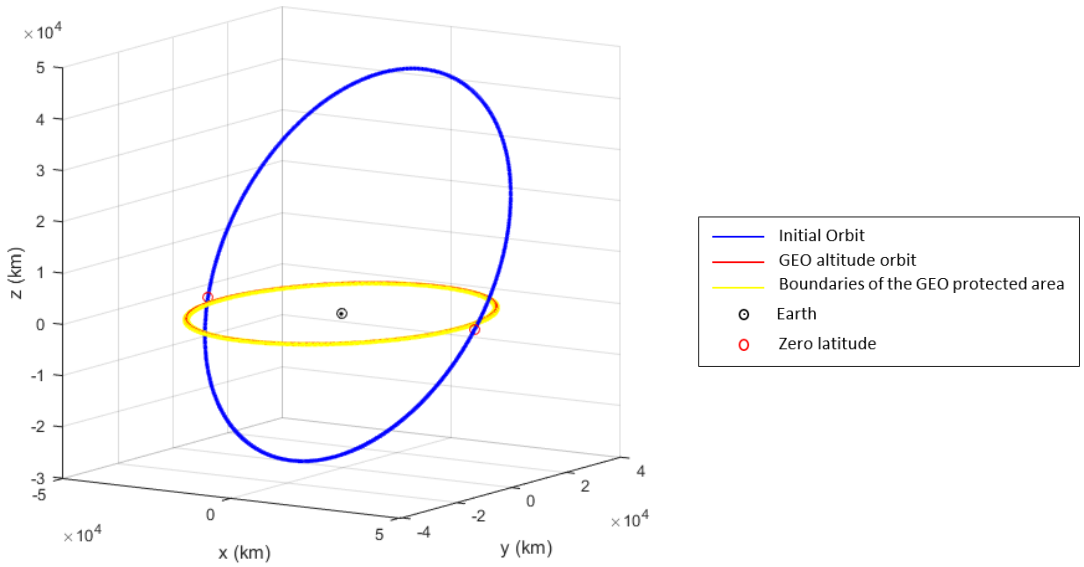

***Fig. 21** 3D view of the initial orbit and the GEO protected area for $e_0 = 0.25, i_0 = 55^o$ and $\Omega_0 = 0^o$.*

Figure 20 perfectly shows that the spacecraft at zero latitude will not cross the GEO ring, because it is flying at a higher altitude than the superior boundary of this protected region. Figure 21 provides a clear 3D view in order to show that the GEO protected area has zero inclination, therefore if the satellite is flying at GEO altitude but a latitude different from zero, it will not cross this area.

By plotting the figures of the 45 sets of initial orbits described at Section 2.1., it is possible to recognize which orbits cross the GEO protected area or pass really close to it at zero latitude. Figure 22 shows four orbits with the same inclination and RAAN, but different eccentricities.

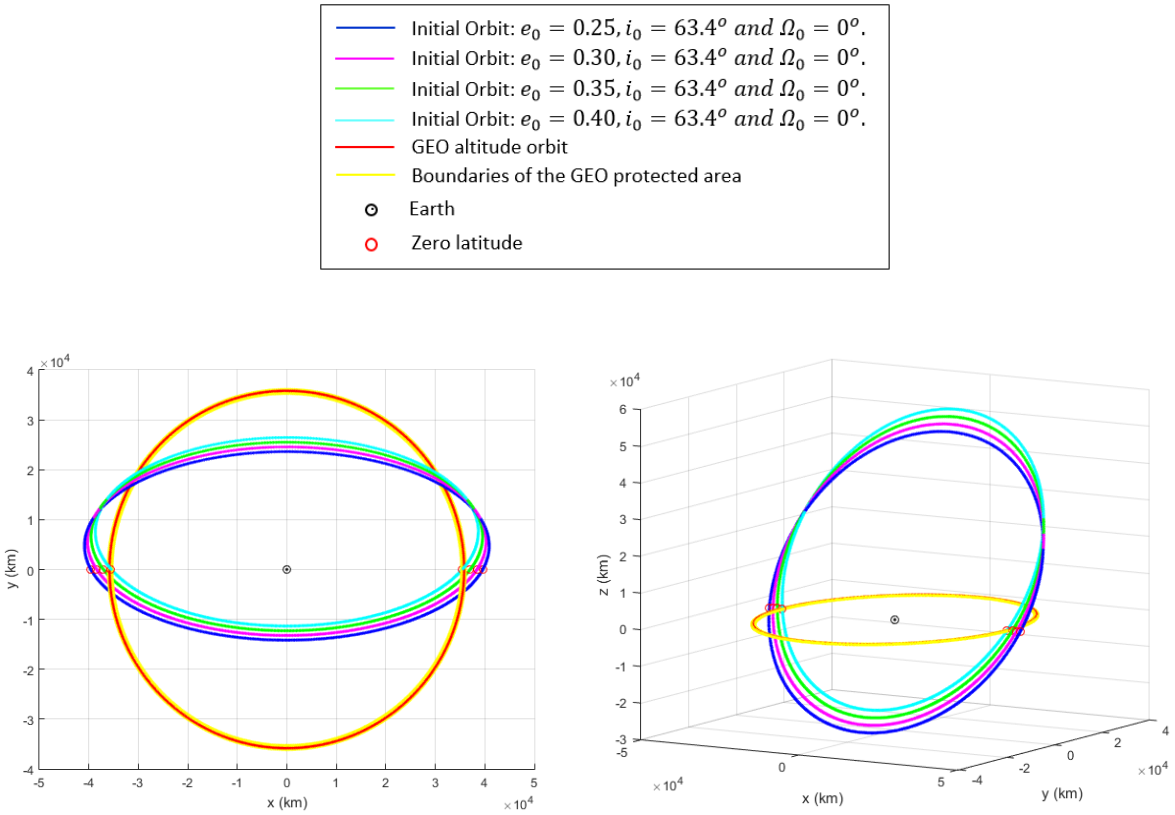

***Fig. 22** x-y view (left) and 3D view (right) of the GEO protected area and various initial orbit with different eccentricities*.

The GEO protected area was established between 35288 and 36088 km. Figure 22 shows that the orbit with $e_0 = 0.35$ passes considerably close to the GEO ring at zero latitude. Specifically, in the case of $e_0 = 0.35, i_0 = 63.4^o$ and $\Omega_0 = 0^o$, the satellites operating at such orbit have an altitude of:

$$r = 37074\ km, \tag{69}$$

at zero latitude. Figure 22 also shows that the orbit with $e_0 = 0.40$ crosses the GEO protected area. Specifically, in the case of $e_0 = 0.40, i_0 = 63.4^o$ and $\Omega_0 = 0^o$, the satellites operating at such orbit have an altitude of:

$$r = 35494\ km, \tag{70}$$

at zero latitude. If the inclination changes (i.e., the orbit with $e_0 = 0.40, i_0 = 70.0^o$ and $\Omega_0 = 0^o$), the orbit has the same altitude at zero latitude. If the RAAN is changed, the spots of the orbit with zero latitude may change their location in space, but they have the same altitude. Figure 23 outlines these outcomes with the critical case of orbits with $e_0 = 0.40$. Consequently, the orbits of the 45 sets of initial orbits described at Section 2.1 that have $e_0 = 0.40$ cross the GEO protected area.

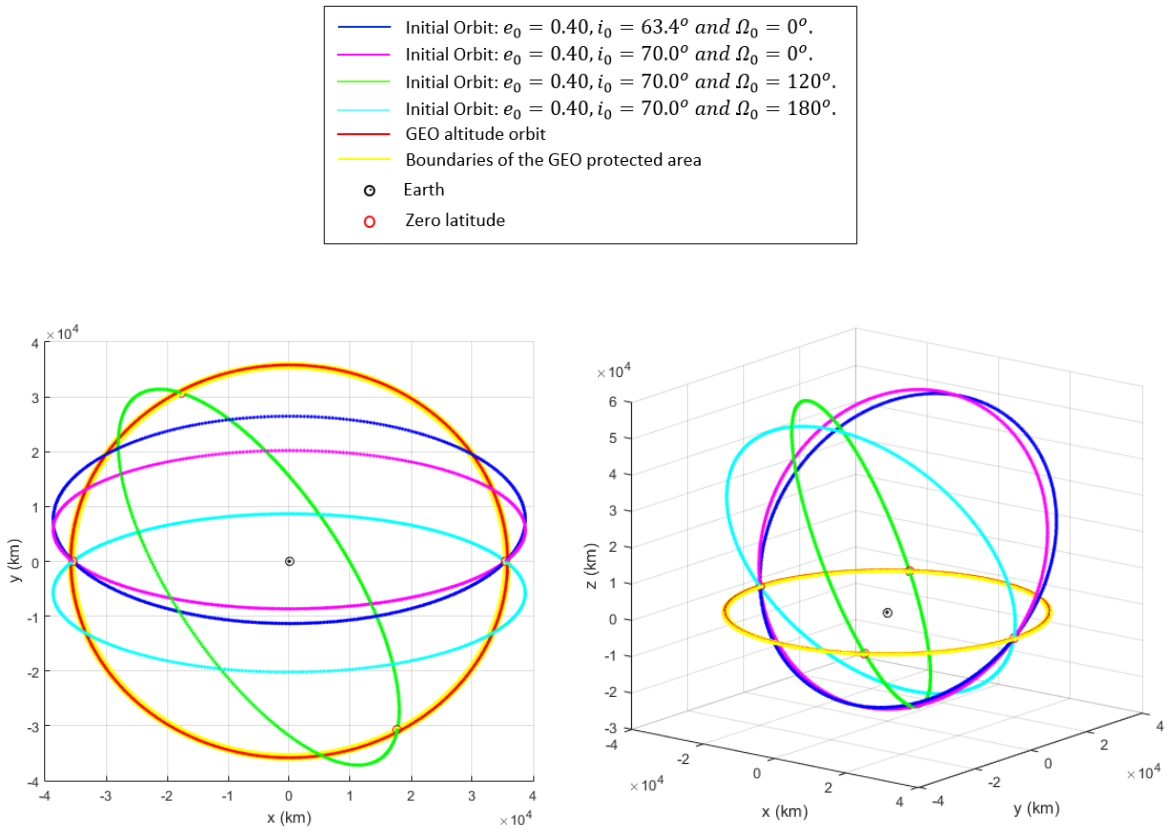

Fig. 23 *x-y view (left) and 3D view (right) of the GEO protected area and various initial orbit with* $e_0 = 0.40$.

When performing the disposal maneuver, if the starting application burn is at perigee or at a point close to it and the orbit has $e_0 = 0.40$, it is important to develop a further study to guarantee that the transfer maneuver does not cross the GEO protected area at zero latitude. If the starting burn of the disposal maneuver is carried out at any spot of an orbit with an eccentricity different from $e_0 = 0.40$, any satellite flying at such transfer maneuver will not cross the GEO protected area. This is because, as it has been analysed, at the zero latitude the initial orbit has more altitude than this region and, since the low-thrust disposal maneuver increases the altitude of the transfer curve, the satellite increases its altitude and the distance to the GEO ring.

The inclination of the final orbit and that of the trajectory maneuver are equal to the inclination of the initial orbit, because the maneuver will be performed at the same plane. To design a suitable circularization by means of a low-thrust strategy it is needed to define the execution times, the velocity variation made at each section and the propellant mass required to carry out the whole maneuver. To give an approximated idea of these unknown variables, this strategy is simulated using a script programmed in Matlab and the data of the initial orbit from Section 2.1.

4.3.2. Algorithm of the low-thrust maneuver

The most efficient way to execute the disposal maneuver is by means of the implementation of the optimal control theory. Precise numerical methods to optimally design low-thrust maneuvers, and determine the magnitude and the direction of the thrust vector at each spot, require high computational cost. Consequently, if the mission needs this level of optimization, the analysis are usually left as a further study to be developed during the most advanced phases of the mission design. Optimal control theory escapes from the aims of this FDP. The algorithm presented in this study allows a quick evaluation of several low-thrust disposal strategies, prior to a complete optimization using more complex steering programs.

The algorithm aims at computing the state vector of six elements (position $\boldsymbol{r}$ and velocity $\boldsymbol{v}$) at each spot of the low-thrust maneuver. The algorithm starts with the Second Newton's law of dynamics:

$$m\,\ddot{\boldsymbol{r}} = -\frac{\mu m}{r^3}\boldsymbol{r} + m\,\boldsymbol{a_T}, \tag{71}$$

where $\boldsymbol{a_T}$ is the acceleration produced by thrust and $\ddot{\boldsymbol{r}}$ is the satellite acceleration vector expressed as the second derivative of $\boldsymbol{r}$ with respect to time t:

$$\ddot{\boldsymbol{r}} = \frac{d^2\boldsymbol{r}}{dt^2} = \frac{d}{dt}\left(\frac{d\boldsymbol{r}}{dt}\right). \tag{72}$$

The left side of the equality in Eqs. 71 is the force experienced by the satellite. The first term in the right side refers to the gravitational force produced by the Earth and experienced by the satellite. The second term in the right side is the thrust $\boldsymbol{T}$. The spacecraft mass m can be expressed as a function of time:

$$m = m_i + \dot{m}\,(t - t_i), \tag{73}$$

where m_i is the spacecraft initial mass as defined in Eqs. 58, $\dot{m}$ is the mass flow expulsed through the satellite nozzle and t_i is the initial time. In Eqs. 73 the variation produced by $\dot{m}$ is added to the initial mass, as the satellite loses mass, $\dot{m}$ shall be negative.

The dry mass m_{dry} used in this algorithm is equal to the value obtained in the study outlined in Table 9 $\left(m_{dry} = 3000\ kg\right)$. The propellant mass m_p required to execute the maneuver is an unknown variable, consequently, the satellite mass is also unknown. The mass variable appears in all terms of Eqs. 71, therefore, it can be removed. This leads to:

$$\ddot{\boldsymbol{r}} = -\frac{\mu}{r^3}\boldsymbol{r} + \boldsymbol{a_T}, \tag{74}$$

Eqs. 74 is a system of three differential equations, one per each direction of the Cartesian coordinates system:

$$\begin{cases} \ddot{x} = -\dfrac{\mu}{r^3}x + a_{T_x}\,, \\ \ddot{y} = -\dfrac{\mu}{r^3}y + a_{T_y}\,, \\ \ddot{z} = -\dfrac{\mu}{r^3}z + a_{T_z}\,. \end{cases} \tag{75}$$

The acceleration produced by thrust $\boldsymbol{a_T}$ and its components $(a_{T_x}, a_{T_y}, a_{T_z})$ can be expressed as:

$$\boldsymbol{a_T} = \frac{\boldsymbol{T}}{m} \Longrightarrow \begin{cases} a_{T_x} = \dfrac{T}{m}\dfrac{\dot{x}}{v}\,, \\ a_{T_y} = \dfrac{T}{m}\dfrac{\dot{y}}{v}\,, \\ a_{T_z} = \dfrac{T}{m}\dfrac{\dot{z}}{v}\,, \end{cases} \tag{76}$$

where v is the magnitude of the spacecraft velocity, which can be expressed as:

$$v = \sqrt{\dot{x}^2 + \dot{y}^2 + \dot{z}^2}\,. \tag{77}$$

The state vector consist of 6 elements. Therefore, to solve the system, three more equations are required. These equations are the three differential equations to compute the spacecraft velocity components. By using Newton's notation, it can be expressed as:

$$\frac{d\boldsymbol{r}}{dt} = \dot{\boldsymbol{r}} \,. \tag{78}$$

And its components are:

$$\begin{cases} \dot{x} = \dfrac{dx}{dt} = v_x \,, \\ \dot{y} = \dfrac{dy}{dt} = v_y \,, \\ \dot{z} = \dfrac{dz}{dt} = v_z \,. \end{cases} \tag{79}$$

By integrating numerically the 6 differential equations (Eqs. 75 and 79), it is possible to obtain the state vector at each spot of the disposal maneuver. The implemented Matlab script uses the function "odeset", which allows to select some options and pass them as an argument to the ODE (Ordinary Differential Equations) solver. Specifically, the relative and absolute tolerance values are fixed to select a threshold for the admitted error. The function "ode113" is the ODE solver used to integrate the system of differential equations from the initial time t_0 to the final time with initial conditions (IC). Mathematically, it can be expressed as:

$$\left.\begin{aligned} \text{ODE: } \ddot{\boldsymbol{r}} = -\frac{\mu}{|r|^3}\boldsymbol{r} + \boldsymbol{a_T}(\boldsymbol{r}, \dot{\boldsymbol{r}}, t) \\ \text{IC: } t_0, \boldsymbol{r}_0, \dot{\boldsymbol{r}}_0 \end{aligned}\right\} \Longrightarrow \boldsymbol{r} = \boldsymbol{r}(t, t_0, \boldsymbol{r}_0, \dot{\boldsymbol{r}}_0) \,. \tag{80}$$

The solver is used to solve an equations system with the form:

$$\dot{\boldsymbol{x}} = f(\boldsymbol{x}, t) \,, \tag{81}$$

where $\boldsymbol{x}$ is the state vector:

$$\boldsymbol{x} = \begin{Bmatrix} x \\ y \\ z \\ v_x \\ v_y \\ v_z \end{Bmatrix}, \tag{82}$$

and $\dot{\boldsymbol{x}}$ its derivative with respect to time:

$$\dot{\boldsymbol{x}} = \begin{Bmatrix} v_x \\ v_y \\ v_z \\ -\frac{\mu}{r^3}x + a_{T_x} \\ -\frac{\mu}{r^3}y + a_{T_y} \\ -\frac{\mu}{r^3}z + a_{T_z} \end{Bmatrix} . \tag{83}$$

The spacecraft mass m is unknown, therefore $\boldsymbol{a_T}$ is also unknown. To start with the computations, we can impose $\boldsymbol{a_T}$ as a vector with a constant magnitude and select a particular value for it. To do so, the typical values of thrust T of electrical engines, the dry mass m_{dry} of communications satellites and the propellant mass m_p required to carry out the maneuver have to be considered. a_T is imposed to be constant and m_p is reduced during the maneuver, consequently, T must change throughout the trajectory to keep a_T constant. The electric propulsion system that will be used in the mission is not known. However, it is possible to do the calculations by means of a characteristic value of the electrical engines family. In view of the data from Table 8, a suitable value of thrust can be:

$$T < 100 \text{ mN} . \tag{84}$$

The dry mass is $m_{dry} = 3000\ kg$ (Table 9). The propellant mass m_p is an unknown variable which will be obtained at the end of the low-thrust study. To define the quotient T/m, m_p can be approximated as:

$$m_p = 150\ kg , \tag{85}$$

which is a value excessively large considering the requirements of any disposal space mission, hence, it should not be overpassed. Bearing in mind all this contemplations, the quotient T/m can be approximated as:

$$a_T = \frac{T}{m} < \frac{100 \cdot 10^{-3}\ N}{3000\ kg + 150\ kg} = 3.17 \cdot 10^{-5}\ m/s^2 . \tag{86}$$

Once a_T is established, the initial conditions and the time needed to execute the disposal maneuver must be determined. A practical formulation to design a low-thrust strategy was developed by Burt [50]. It is based on the supposition that thrust produces a marginal variation in each orbital element during one orbital period of the initial orbit. Consequently, the secular rates of change of any orbital element can be computed by keeping the rest of elements constant

throughout the maneuver. To design the low-thrust disposal maneuver, we can base on the study developed by Pollard [49], which extends Burt's methodology to the situation of discontinuous thrusting with the aim at studying apogee- and perigee-centered burns arcs. This approach to the problem can be really useful to the study presented in this FDP because it provides a suitable strategy to raise the perigee of an elliptical orbit and circularize it by means of a continuous thrust. In Burt's nomenclature, the thrust per unit mass $\boldsymbol{a_T}$ is defined as $\boldsymbol{f}$, hence:

$$\boldsymbol{f} = \frac{\boldsymbol{T}}{m}. \qquad (87)$$

It has three components f_1, f_2 and f_3, which are shown in Figure 24. Bearing in mind the satellite coordinate system RSW, f_1 is directed radially outward from the Earth centre to the satellite, f_2 is orthogonal to the radius vector in the orbital plane and in the direction of motion, and f_3 is normal to the orbital plane in the direction of the angular momentum vector.

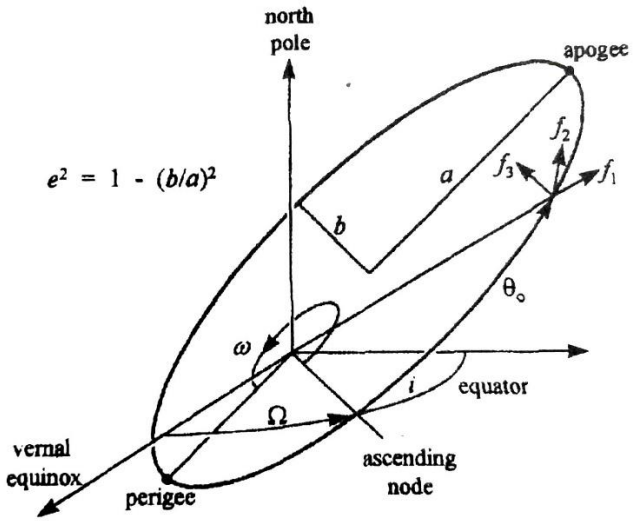

Fig. 24 Orbital elements and components of the acceleration $\boldsymbol{f}$ in satellite coordinate system RSW [49].

The magnitude of the acceleration remains constant throughout the disposal mission. Considering Eqs. 86 and its components, it can be expressed as:

$$f = \sqrt{(f_1)^2 + (f_2)^2 + (f_3)^2} < 3.17 \cdot 10^{-5}\ m/s^2\,. \qquad (88)$$

The in-plane and out-of-plane components of the acceleration $\boldsymbol{f}$ are:

$$f_{12} = \sqrt{(f_1)^2 + (f_2)^2} = f\ cos|\beta|\,, \qquad f_3 = f\ sin|\beta|\,, \qquad (89)$$

where β is the magnitude of the out-of-plane thrust angle. It is taken to be constant during each burn. The low-thrust maneuver presented in this FDP is carried out in the same plane, therefore $\beta = 0$. By putting this result into Eqs. 89, it is obtained:

$$f_{12} = f\ , \qquad f_3 = 0\ . \tag{90}$$

By deriving from the Lagrange planetary equations it is possible to obtain the expressions of the rates of change of the orbital elements $(a, e, i, \Omega, \omega)$ as functions of eccentric anomaly E:

$$\frac{da}{dE} = \frac{2a^3}{\mu}\left(f_1\, e\, sinE + f_2\, \sqrt{1-e^2}\ \right), \tag{91}$$

$$\frac{de}{dE} = \frac{a^2}{\mu}\left[f_1\, (1-e^2)\, sinE + f_2\, \sqrt{1-e^2}\ (2\, cosE - e - e\cos^2 E)\right], \tag{92}$$

$$\frac{di}{dE} = \frac{a^2}{\mu}\, f_3\, (1 - e\, cosE)\, \left[\frac{(cosE - e)cos\omega}{\sqrt{1-e^2}} - sinE\, sin\omega\right], \tag{93}$$

$$\frac{d\Omega}{dE} = \frac{a^2}{\mu}\, f_3 \frac{1 - e\, cosE}{\sin i}\, \left[\frac{(cosE - e)sin\omega}{\sqrt{1-e^2}} + sinE\, cos\omega\right], \tag{94}$$

$$\frac{d\omega}{dE} = \frac{a^2}{\mu}\left\{\begin{array}{l}\frac{1}{e}\left[-f_1\, \sqrt{1-e^2}\ (cosE - e) + f_2\, (2 - e^2 - e\, cosE) sinE\right] \\ -f_3\, (1 - e\, cosE)\cot i\, \left[\frac{(cosE - e)sin\omega}{\sqrt{1-e^2}} + sinE\, cos\omega\right]\end{array}\right\}. \tag{95}$$

These expressions have been directly obtained from Pollard study [49]. Eqs. 91 and 92 show that the semimajor axis a and the eccentricity e of the orbit are affected by the in-plane components of the acceleration f_1 and f_2. Eqs. 93 and 94 outline that the inclination i and the right ascension of the ascending node Ω are affected by the out-of-plane component f_3. The low-thrust maneuver presented in this FDP is carried out in the same plane, therefore $f_3 = 0$. Consequently, i and Ω do not experience any variation. Eqs. 95 shows that the argument of perigee ω is affected by all the components of the acceleration (f_1, f_2 and f_3), hence ω changes due to the execution of the disposal maneuver. However, its changes do not have to be monitored because the satellite is inoperative when it carries out the disposal maneuver. Additionally, when the orbit is circularized, the argument of perigee is meaningless. Taking into account these considerations,

the variation of the semimajor axis a and the eccentricity e are the only ones that must be analysed. Specifically, it is essential to monitor the distance between the spacecraft and the forbidden region (GEO ring).

To compute the relative rates of variation of the semimajor axis and the eccentricity, it is needed to define the steering guidelines. To do so, the components of the acceleration f_1 and f_2 must be specified as functions of E, which means that they are also functions of time. The direction of the in-plane acceleration vector $\boldsymbol{f_{12}}$ is not yet established. To select the most suitable one, the four cases presented in Pollard study [49] are going to be analysed. The four different pitch steering options are:

- Case 1: $\boldsymbol{f_{12}}$ is perpendicular to the orbit radius vector.
- Case 2: $\boldsymbol{f_{12}}$ is tangent to the orbit path.
- Case 3: $\boldsymbol{f_{12}}$ is perpendicular to the semimajor axis of the ellipse.
- Case 4: $\boldsymbol{f_{12}}$ is parallel to the semimajor axis of the ellipse.

It is needed to find an expression for f_1 and f_2 as functions of E in the four steering cases. Discontinuous acceleration can be simulated by means of perigee- or apogee-centered burns. Figure 25 outlines the representation of a burn arc centered at apogee and another centered at perigee.

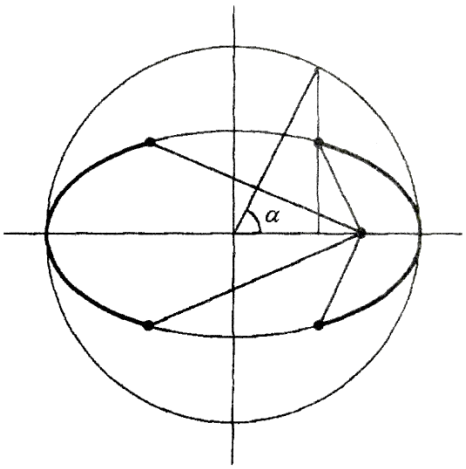

Fig. 25 Apogee and perigee centered burn arcs defined in units of eccentric anomaly [49].

The burn arc centered at perigee is defined as:

$$-\alpha \leq E \leq +\alpha, \tag{96}$$

and the burn arc centered at apogee is defined as:

$$\pi - \alpha \leq E \leq \pi + \alpha. \tag{97}$$

If we select $\alpha = \pi$ in the case expressed in Eqs. 96, a continuous thrust during all the orbital period is obtained. In the case studied in this FDP, to reduce the propellant mass required, a good option to analyse is execute the maneuver in an arc centered at apogee, because the maneuver aims at raising the perigee altitude.

Once the expressions of $f_1(E)$ and $f_2(E)$ are determined, it is possible to compute the secular rate of change of any orbital element. Specifically, in the present case, it is interesting to obtain the secular rate of change of the eccentricity. To do so, after inserting $f_1(E)$ and $f_2(E)$ into Eqs. 92, it is possible to integrate the obtained expression over a particular burn arc, which is defined by selecting a specific value of α. The result of this integration provides the change of eccentricity produced during one revolution Δe. To compute the secular rate of change of the eccentricity, it is only needed to multiply Δe times the orbit frequency. Mathematically, this can be expressed as:

$$\frac{d\tilde{e}}{dt} = \frac{1}{2\pi}\sqrt{\frac{\mu}{a^3}}\,\Delta e\,. \tag{98}$$

The secular rates of change of the other orbital elements (a, i, Ω and ω) can be also obtained by applying the same procedure described above. However, in this study, they are not needed. To obtain the algorithm to design the disposal maneuver, it is only required to determine the expressions of the secular rate of change of the eccentricity for each of the four proposed steering cases.

Once they are known, by fixing the eccentricities of the initial and final orbit for each steering case, it is possible to compute analytically the velocity variation Δv, the trip time Δt and the propellant mass m_p required to carry out the whole maneuver. In all the steering cases, the velocity variation can be computed as:

$$\Delta v = f\,\Delta t\,, \tag{99}$$

and the propellant mass m_p can be computed by using the same equation obtained in Section 3.1:

$$m_p = m_{dry} \cdot \left(e^{\frac{\Delta v}{I_{sp} g_0}} - 1 \right). \tag{100}$$

4.3.2.1. Case 1: f_{12} perpendicular to the orbit radius vector

Firstly, it is needed to find an expression for f_1 and f_2 as functions of E. By observing the sketch shown in Figure 26, they can be directly determined.

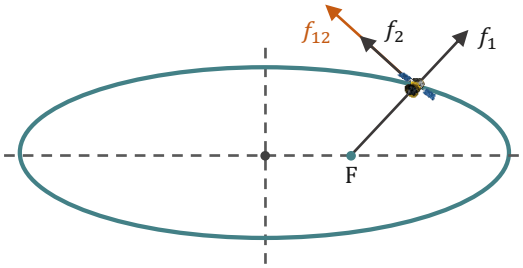

Fig. 26 Sketch of the steering case 1: f_{12} perpendicular to the orbit radius vector.

The expressions of $f_1(E)$ and $f_2(E)$ are:

$$f_1(E) = 0, \qquad f_2(E) = f_{12}\,. \tag{101}$$

The next step aims at computing the change of eccentricity produced during one revolution Δe. To determine it, $f_1(E)$ and $f_2(E)$ are inserted into Eqs. 92 and the obtained expression is integrated over a particular burn arc:

$$\frac{de}{dE} = \frac{a^2}{\mu}\left[f_{12}\sqrt{1-e^2}\,(2\,cosE - e - e\cos^2 E)\right], \tag{102}$$

$$\Delta e = \int_{-\alpha}^{\alpha} \frac{a^2}{\mu} f_{12}\sqrt{1-e^2}\,(2\,cosE - e - e\cos^2 E)\,dE\,, \tag{103}$$

$$\begin{aligned}\Delta e = \frac{a^2}{\mu} f_{12}\sqrt{1-e^2}\Big(&2sin\alpha - 2\sin(-\alpha) - 2e\alpha \\ &-\frac{e}{2}[2\alpha + sin\alpha\,cos\alpha - \sin(-\alpha)\cos(-\alpha)]\Big).\end{aligned} \tag{104}$$

Upon substituting:

$$\sin(-\alpha) = -sin\alpha \quad and \quad \cos(-\alpha) = cos\alpha\,, \tag{105}$$

we obtain:

$$\Delta e = \frac{a^2}{\mu} f_{12}\sqrt{1-e^2}\,(4sin\alpha - 3e\alpha - e\,cos\alpha\sin\alpha)\,. \tag{106}$$

To compute the secular rate of change of the eccentricity $d\tilde{e}/dt$, it is only needed to multiply Δe times the orbit frequency:

$$\frac{d\tilde{e}}{dt} = \frac{f_{12}}{2\pi}\sqrt{\frac{a}{\mu}(1-e^2)}\ (4sin\alpha - 3e\alpha - e\,cos\alpha\,\sin\alpha)\,. \qquad (107)$$

To include the apogee case ($\pi - \alpha \leq E \leq \pi + \alpha$), we modify Eqs. 107 by adding the σ parameter, which is:

$$\boxed{\sigma = \begin{cases} +1 \text{ (Apogee case)} \\ -1 \text{ (Perigee case)} \end{cases}}\,. \qquad (108)$$

By including σ, we obtain:

$$\frac{d\tilde{e}}{dt} = -\frac{f_{12}}{2\pi}\sqrt{\frac{a}{\mu}(1-e^2)}\ (4\sigma sin\alpha + 3e\alpha + e\,cos\alpha\,\sin\alpha)\,. \qquad (109)$$

To determine the trip time Δt required to carry out the whole disposal maneuver, we integrate Eqs. 109:

$$\Delta t = -\frac{2\pi}{f_{12}}\sqrt{\frac{\mu}{a}}\int_{e_1}^{e_2}\frac{d\tilde{e}}{\sqrt{1-e^2}\,(4\sigma sin\alpha + 3e\alpha + e\,cos\alpha\,\sin\alpha)}\,, \qquad (110)$$

The semimajor axis a experiences considerable variations during the evolution of the disposal maneuver due to the raise of perigee altitude. Consequently, it must be expressed as a function of the eccentricity and must be integrated. Considering that the apogee does not raise its altitude, or at least it does not change too many, a suitable hypothesis is keep the apogee altitude constant. With this assumption, the semimajor axis is obtained as a function of the eccentricity and the apogee altitude:

$$a = \frac{r_\alpha}{1+e}\,, \qquad (111)$$

where:

$$r_\alpha = \frac{a(1-e_1^2)}{1-e_1}\,. \qquad (112)$$

By including Eqs. 111 into Eqs.110, we obtain:

$$\Delta t = -\frac{2\pi}{f_{12}}\sqrt{\mu}\int_{e_1}^{e_2}\frac{d\tilde{e}}{\sqrt{\frac{r_\alpha}{1+e}}\ \sqrt{1-e^2}\left(4\sigma sin\alpha + e(3\alpha + cos\alpha\,\sin\alpha)\right)} \qquad (113)$$

where: $A = 4\sigma\ sin\alpha$, and $B = 3\alpha + sin\alpha\ cos\alpha$. By integrating Eqs. 113, we obtain the trip time Δt required to carry out the whole disposal maneuver:

$$\boxed{\Delta t = -\frac{2\pi}{f_{12}}\sqrt{\mu}\left[\frac{2\sqrt{e-1}\tan^{-1}\left(\frac{\sqrt{B}\sqrt{e-1}}{\sqrt{A+B}}\right)}{\sqrt{B}\sqrt{1-e^2}\sqrt{A+B}\sqrt{\frac{r_\alpha}{e+1}}}\right]_{e_1}^{e_2}}. \qquad (114)$$

The function $\tan^{-1}(x)$ is the inverse tangent function. Finally, by applying Eqs. 99 and 100, it is possible to compute the velocity variation Δv and the propellant mass m_p required to carry out the whole maneuver.

4.3.2.2. Case 2: f_{12} tangent to the orbit path

To find an expression for f_1 and f_2 as functions of E, it is needed to find the position (x, y) and the velocity $(\dot{x},\ \dot{y})$ of the spacecraft as functions of the eccentric anomaly E.

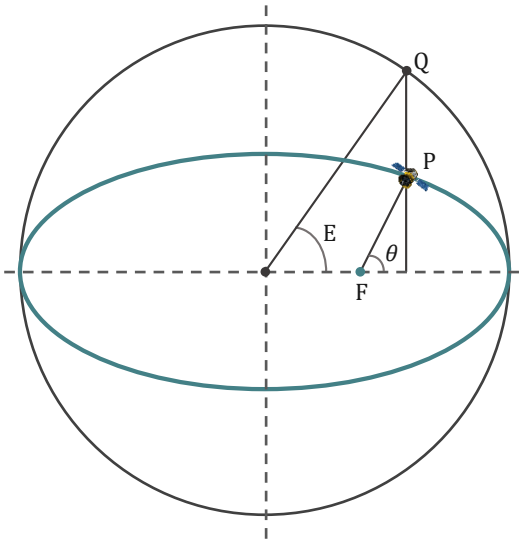

Fig. 27 *Sketch to show the relation between eccentric anomaly and true anomaly.*

By observing the sketch shown in Figure 27, it is possible to determine the coordinates of the point Q, which are:

$$x_Q = a\,cosE - ae\,, \tag{115}$$

$$y_Q = a\sin E\,. \tag{116}$$

The y coordinate of point P on the ellipse is $b/a\left(=\sqrt{1-e^2}\right)$ times the y coordinate of the corresponding point Q on the auxiliary circle. The coordinates of point P, which are equally to the coordinates of the spacecraft, are:

$$x = a\,cosE - ae\,, \tag{117}$$

$$y = a\sqrt{1-e^2}\sin E\,. \tag{118}$$

The velocity components of the spacecraft can be obtained by deriving Eqs. 117 and 118 with respect to time:

$$\dot{x} = -a\,\dot{E}\,sinE\,, \tag{119}$$

$$\dot{y} = a\sqrt{1-e^2}\,\dot{E}\cos E\,. \tag{120}$$

The components a_{T_x} and a_{T_y} of the acceleration produced by thrust can be expressed as:

$$a_{T_x} = \frac{T}{m}\frac{\dot{x}}{v} = f_{12}\frac{\dot{x}}{v}\,, \tag{121}$$

$$a_{T_y} = \frac{T}{m}\frac{\dot{y}}{v} = f_{12}\frac{\dot{y}}{v}\,, \tag{122}$$

where:

$$v = \sqrt{\dot{x}^2+\dot{y}^2} = \sqrt{\left(-a\,\dot{E}\,sinE\right)^2 + \left(a\sqrt{1-e^2}\,\dot{E}\cos E\right)^2} = \tag{123}$$

$$= \sqrt{a^2\,\dot{E}^2\left((\sin^2 E + \cos^2 E) - e^2\cos^2 E\right)} = a\dot{E}\sqrt{1-e^2\cos^2 E}\,. \tag{124}$$

Upon introducing Eqs. 124, 119 and 120 into Eqs. 121 and 122, we obtain:

$$a_{T_x} = f_{12}\frac{-a\,\dot{E}\,sinE}{a\dot{E}\sqrt{1-e^2\cos^2 E}} = -f_{12}\frac{\sin E}{\sqrt{1-e^2\cos^2 E}}\,, \tag{125}$$

$$a_{T_y} = f_{12}\frac{a\sqrt{1-e^2}\,\dot{E}\cos E}{a\dot{E}\sqrt{1-e^2\cos^2 E}} = f_{12}\frac{\sqrt{1-e^2}\cos E}{\sqrt{1-e^2\cos^2 E}}\,. \tag{126}$$

a_{T_x} and a_{T_y} are the acceleration components in the Cartesian coordinate reference system as functions of E. We have to pass them into the satellite coordinate system RSW to obtain $f_1(E)$ and $f_2(E)$. By observing Figure 28, we can determine the expressions:

$$f_1 = a_{T_x}\, cos\theta + a_{T_y}\, sin\theta \ , \tag{127}$$

$$f_2 = -a_{T_x}\, sin\theta + a_{T_y}\, cos\theta \ . \tag{128}$$

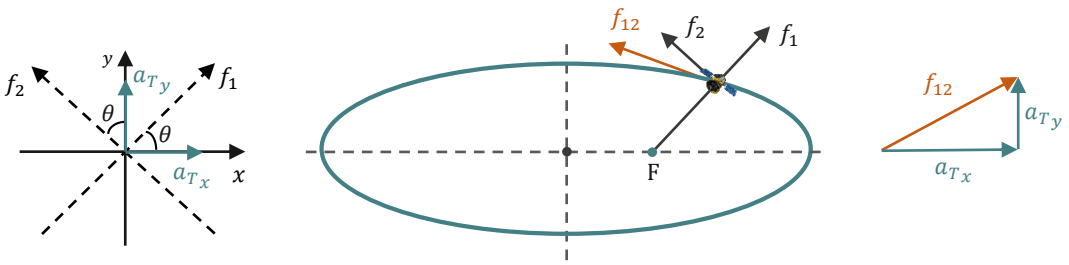

Fig. 28 Sketch of the steering case 2: f_{12} tangent to the orbit path.

Upon substituting:

$$\cos\theta = \frac{e - \cos E}{e\cos E - 1} \quad \text{and} \quad \sin\theta = \frac{\sqrt{1-e^2}\sin E}{1 - e\cos E} \ , \tag{129}$$

and introducing Eqs. 125 and 126, we obtain:

$$f_1 = -f_{12}\frac{\sin E}{\sqrt{1-e^2\cos^2 E}}\frac{e-\cos E}{e\cos E - 1} + f_{12}\frac{\sqrt{1-e^2}\cos E}{\sqrt{1-e^2\cos^2 E}}\frac{\sqrt{1-e^2}\sin E}{1-e\cos E} \ , \tag{130}$$

$$f_1 = f_{12}\frac{\sin E}{\sqrt{1-e^2\cos^2 E}}\left[\frac{-e + \cos E - (1-e^2)\cos E}{e\cos E - 1}\right] , \tag{131}$$

$$f_1 = f_{12}\frac{\sin E}{\sqrt{1-e^2\cos^2 E}}\left[\frac{-e + e^2\cos E}{e\cos E - 1}\right] , \tag{132}$$

$$\boxed{f_1 = \frac{f_{12}\, e\ \sin E}{\sqrt{1-e^2\cos^2 E}}} \ , \tag{133}$$

$$f_2 = f_{12}\frac{\sin E}{\sqrt{1-e^2\cos^2 E}}\frac{\sqrt{1-e^2}\sin E}{1-e\cos E} + f_{12}\frac{\sqrt{1-e^2}\cos E}{\sqrt{1-e^2\cos^2 E}}\frac{e-\cos E}{e\cos E - 1} \ , \tag{134}$$

$$f_2 = f_{12}\frac{\sqrt{1-e^2}}{\sqrt{1-e^2\cos^2 E}}\left[\frac{\sin^2 E}{1-e\cos E}+\frac{\cos E\,(e-\cos E)}{e\cos E-1}\right], \tag{135}$$

$$f_2 = f_{12}\frac{\sqrt{1-e^2}}{\sqrt{1-e^2\cos^2 E}}\left[\frac{(\sin^2 E+\cos^2 E)-e\cos E}{1-e\cos E}\right], \tag{136}$$

$$\boxed{f_2 = f_{12}\sqrt{\frac{1-e^2}{1-e^2\cos^2 E}}}\,. \tag{137}$$

Once the expressions of $f_1(E)$ and $f_2(E)$ are determined, the next step aims at computing the change of eccentricity produced during one revolution Δe. To determine it, Eqs. 133 and 137 are inserted into Eqs. 92 and the obtained expression is integrated over a particular burn arc:

$$\frac{de}{dE} = \frac{a^2}{\mu}\left[\frac{f_{12}\,e\,\sin E}{\sqrt{1-e^2\cos^2 E}}\,(1-e^2)\,sinE + f_{12}\sqrt{\frac{1-e^2}{1-e^2\cos^2 E}}\,\sqrt{1-e^2}\,(2\,cosE-e-e\cos^2 E)\right], \tag{138}$$

$$\frac{de}{dE} = \frac{a^2}{\mu}\frac{f_{12}\,(1-e^2)}{\sqrt{1-e^2\cos^2 E}}\,[e\sin^2 E+2\,cosE-e-e\cos^2 E]\,, \tag{139}$$

$$\frac{de}{dE} = \frac{a^2}{\mu}\frac{f_{12}\,(1-e^2)}{\sqrt{1-e^2\cos^2 E}}\,[2\,cosE-2\,e\cos^2 E]\,, \tag{140}$$

$$\Delta e = \frac{2a^2}{\mu}f_{12}(1-e^2)\int_{-\alpha}^{\alpha}\frac{\cos E\,(1-e\cos E)}{\sqrt{1-e^2\cos^2 E}}\,dE\,. \tag{141}$$

To compute the secular rate of change of the eccentricity $d\tilde{e}/dt$, we multiply Δe times the orbit frequency:

$$\frac{d\tilde{e}}{dt} = \frac{2f_{12}}{\pi}\sqrt{\frac{a}{\mu}}\,(1-e^2)\,H(\sigma,\alpha)\,, \tag{142}$$

where:

$$H(\sigma=-1,\alpha) = \int_0^{\alpha}\frac{\cos E\,(1-e\cos E)}{\sqrt{1-e^2\cos^2 E}}\,dE \implies \text{Perigee}, \tag{143}$$

$$H(\sigma = +1, \alpha) = \int_{\pi}^{\pi+\alpha} \frac{\cos E\,(1 - e\cos E)}{\sqrt{1 - e^2\cos^2 E}}\,dE \implies \text{Apogee.} \qquad (144)$$

To solve numerically the definite integral $H(\sigma, \alpha)$, some complex analytical calculations have to be done. To simplify the computations, we can apply a well-known fundamental theorem of calculus related to the anti-derivative of a function. This states that given a function g of a real variable x and an interval of integration $[a, b]$, the definite integral can be approximated as the specific area of the region in the plane xy which is bounded by the function $g(x)$, the x axis and the two vertical lines $x = a$ and $x = b$. Considering this statement, if the numerical integration of $H(\sigma, \alpha)$ is overly complex, we can approximate its solution by computing the area. To do so, a Matlab script is programmed which approximates the area by means of two methods. The first one computes the area of each trapezium subtended by the curve and the other uses a simple step function. The first one is more precise than the other, although, by reducing step size, both procedures shall provide the same outcome.

Once $H(\sigma, \alpha)$ is determined, to compute the trip time Δt required to carry out the whole disposal maneuver, we have to integrate numerically the differential equation (Eqs. 142). Firstly, by introducing the semimajor axis as a function of the eccentricity and the apogee altitude (Eqs. 111), we obtain:

$$\frac{d\tilde{e}}{dt} = \frac{2f_{12}}{\pi}\sqrt{\frac{r_\alpha}{\mu\,(1+e)}}\,(1 - e^2)\,H(\sigma, \alpha)\ . \qquad (145)$$

To solve this differential equation, a Matlab script is implemented. It uses the function "odeset", which allows to select some options and pass them as an argument to the ODE solver. Specifically, the relative and absolute tolerance values are fixed to select a threshold for the admitted error. The function "ode113" is the ODE solver used. Finally, by applying Eqs. 99 and 100, it is possible to compute the velocity variation Δv and the propellant mass m_p required to carry out the whole maneuver.

4.3.2.3. Case 3: f_{12} perpendicular to the semimajor axis of the ellipse

Firstly, it is needed to find an expression for $f_1(E)$ and $f_2(E)$. Considering the Cartesian coordinates reference, the components a_{T_x} and a_{T_y} of the acceleration produced by thrust are:

$$a_{T_x} = 0 \quad \text{and} \quad a_{T_y} = f_{12}\,. \qquad (146)$$

By observing Figure 29 and inserting Eqs. 129, the expressions of $f_1(E)$ and $f_2(E)$ can be directly determined:

$$f_1 = a_{T_y} \sin\theta = f_{12} \frac{\sqrt{1-e^2}\sin E}{1-e\cos E} , \tag{147}$$

$$f_2 = a_{T_y} \cos\theta = f_{12} \frac{e-\cos E}{e\cos E - 1} = \frac{f_{12}(\cos E - e)}{1-e\cos E} . \tag{148}$$

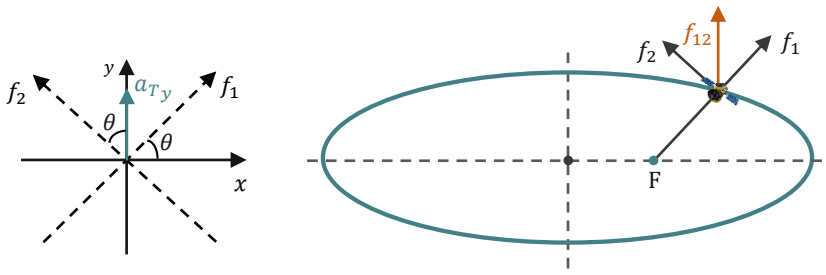

Fig. 29 Sketch of the steering case 3: f_{12} perpendicular to the semimajor axis of the ellipse.

To determine the change of eccentricity produced during one revolution Δe, $f_1(E)$ and $f_2(E)$ are inserted into Eqs. 92 and the obtained expression is integrated over a particular burn arc:

$$\frac{de}{dE} = \frac{a^2}{\mu}\left[f_{12} \frac{\sqrt{1-e^2}\sin E}{1-e\cos E} (1-e^2)\, sinE + \frac{f_{12}(\cos E - e)}{1-e\cos E} \sqrt{1-e^2}\, (2\, cosE - e - e\cos^2 E)\right] , \tag{149}$$

$$\frac{de}{dE} = \frac{a^2}{\mu}\frac{f_{12}\sqrt{1-e^2}}{1-e\cos E}\left[1+\cos^2 E + 2e^2\cos^2 E - 3e\cos E - e\cos^3 E\right] , \tag{150}$$

$$\Delta e = \frac{a^2}{\mu} f_{12}\sqrt{1-e^2} \int_{-\alpha}^{\alpha} \frac{1+\cos^2 E + 2e^2\cos^2 E - 3e\cos E - e\cos^3 E}{1-e\cos E}\, dE , \tag{151}$$

$$\Delta e = \frac{a^2}{\mu} f_{12}\sqrt{1-e^2} \left[\frac{-8e\, sinE + 6E + sin2E}{4}\right]_{-\alpha}^{\alpha} , \tag{152}$$

$$\Delta e = \frac{a^2}{\mu} f_{12}\sqrt{1-e^2}\, (-4e\, sin\alpha + 3\alpha + sin\alpha\, cos\alpha) . \tag{153}$$

To include the apogee case ($\pi - \alpha \leq E \leq \pi + \alpha$), we modify the obtained expression by including the σ parameter, which is defined in Eqs. 108. To compute the secular rate of change of the eccentricity $d\tilde{e}/dt$, we multiply Δe times the orbit frequency:

$$\frac{d\tilde{e}}{dt} = \frac{f_{12}}{2\pi}\sqrt{\frac{a}{\mu}\,(1-e^2)}\,(4e\,\sigma\,sin\alpha + 3\alpha + sin\alpha\,cos\alpha)\,. \qquad (154)$$

By integrating Eqs. 154, we obtain the trip time Δt required to carry out the whole disposal maneuver:

$$\Delta t = \frac{2\pi}{f_{12}}\sqrt{\frac{\mu}{a}}\int_{e_1}^{e_2}\frac{d\tilde{e}}{\sqrt{1-e^2}\,(Ae+B)}\,, \qquad (155)$$

where: $A = 4\sigma\,sin\alpha$ and $B = 3\alpha + sin\alpha\,cos\alpha$. By including Eqs. 111 into Eqs. 155, we obtain:

$$\Delta t = \frac{2\pi}{f_{12}}\sqrt{\mu}\int_{e_1}^{e_2}\frac{d\tilde{e}}{\sqrt{\frac{r_\alpha}{1+e}}\sqrt{1-e^2}\,(Ae+B)}\,, \qquad (156)$$

$$\boxed{\Delta t = \frac{2\pi}{f_{12}}\sqrt{\mu}\left[\frac{2\sqrt{e-1}\,\tan^{-1}\left(\frac{\sqrt{A}\sqrt{e-1}}{\sqrt{A+B}}\right)}{\sqrt{A}\sqrt{1-e^2}\sqrt{A+B}\sqrt{\frac{r_\alpha}{e+1}}}\right]_{e_1}^{e_2}}\,. \qquad (157)$$

Finally, by applying Eqs. 99 and 100, we compute the velocity variation Δv and the propellant mass m_p required to carry out the whole maneuver.

4.3.2.4. Case 4: f_{12} parallel to the semimajor axis of the ellipse

Considering the Cartesian coordinates reference, the components a_{T_x} and a_{T_y} of the acceleration produced by thrust are:

$$a_{T_x} = f_{12} \quad \text{and} \quad a_{T_y} = 0\,. \qquad (158)$$

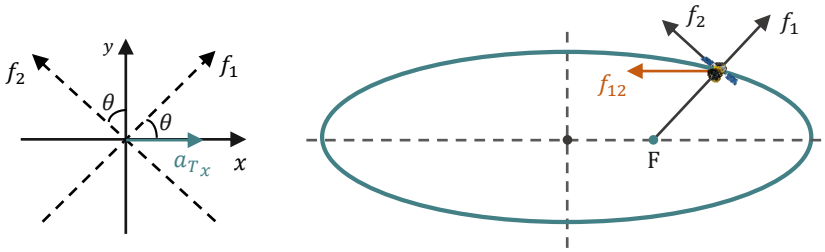

Fig. 30 Sketch of the steering case 4: f_{12} parallel to the semimajor axis of the ellipse.

By observing Figure 30 and inserting Eqs. 129, the expressions of $f_1(E)$ and $f_2(E)$ can be directly determined:

$$f_1 = a_{T_x}\cos\theta = f_{12}\,\frac{e-\cos E}{e\cos E - 1} = \frac{f_{12}(\cos E - e)}{1 - e\cos E}\,, \qquad (159)$$

$$f_2 = -a_{T_x} \sin\theta = -f_{12} \frac{\sqrt{1-e^2}\sin E}{1-e\cos E} \quad . \tag{160}$$

To determine the change of eccentricity produced during one revolution Δe, $f_1(E)$ and $f_2(E)$ are inserted into Eqs. 92 and the obtained expression is integrated over a particular burn arc:

$$\frac{de}{dE} = \frac{a^2}{\mu}\frac{f_{12}(1-e^2)}{1-e\,cosE}[(\cos E - e)\,sinE - sinE\,(2\,cosE - e - e\cos^2 E)]\,, \tag{161}$$

$$\frac{de}{dE} = \frac{a^2}{\mu}\frac{f_{12}(1-e^2)}{1-e\,cosE}[-cosE\,\sin E + e\,cos^2 E\,\sin E]\,, \tag{162}$$

$$\Delta e = -\frac{a^2}{\mu}\,f_{12}(1-e^2)\int_{-\alpha}^{\alpha} cosE\,\sin E\;dE\,, \tag{163}$$

$$\Delta e = \frac{a^2}{\mu}\,f_{12}(1-e^2)\left[\frac{1}{2}\cos^2 E\right]_{-\alpha}^{\alpha}, \tag{164}$$

$$\boxed{\Delta e = 0}\,. \tag{165}$$

Considering the obtained result, case 4, which has the in-plane acceleration parallel to the semimajor axis of the ellipse, gives no change in e. Consequently, this steering case cannot be used to circularize the initial orbit.

4.3.3. Possible low-thrust disposal strategies

To design a suitable disposal strategy by means of a low-thrust maneuver, the described algorithm for cases 1, 2 and 3 are going to be used. Moreover, for each case, several burn arc extensions are going to be analysed. The purpose is to find the maneuver which requires less propellant mass to carry out the whole disposal strategy.

If a continuous thrust with an arc extension of $\alpha = \pi$ is applied, all the points of the initial orbit will change. Consequently, the apogee and perigee will change their altitudes. The purpose is to obtain a circular or almost circular disposal orbit. Considering that the perigee has an altitude significantly lower than the apogee, if the apogee also raises its altitude, it is difficult to obtain a circularisation in a short time.

In some sections there is no need to apply a continuous impulse, because there is no need to raise the altitude in the sections closer to apogee. It is important to bear in mind that the maneuver

aims at raising the perigee altitude, therefore a good option to analyse is the one which executes the maneuver in an arc centered at apogee. Instead of having the engine fired during all the maneuver, the engine is fired during a certain duration. It is possible to carry out some burns and stops of the engine until reaching the final disposal orbit. By means of this strategy, the apogee does not raise its altitude, or at least it does not change too many. Consequently, it is possible to obtain the desirable circularisation faster. This is a simple way to simulate an impulsive maneuver by means of an electrical engine. Moreover, if the continuous impulse is applied at arcs centered at the apogee, there is no risk of crossing the GEO protected area.

The extension of the arc α, the trip time Δt, the velocity variation Δv and the propellant mass m_p required to carry out the circularisation by means of a low-thrust propulsion, must be computed. To give an approximated idea of these unknown variables, this strategy is simulated using a script programmed in Matlab, the algorithm presented in Section 4.3.2 and the data of the initial orbit from Section 2.1.

Each of the disposal strategies obtained by considering each of the proposed initial orbit eccentricities, which are 0.25; 0.30; 0.35; 0.40, and each of the steering cases, are analysed. The algorithm does not depend on the orbital inclination, since the intention is to perform a circularization in the initial orbital plane. In case a change-of-plane maneuver is required by the specific disposal strategy, then parameters like the inclination and the right ascension of the ascending node will be involved in the determination of the maneuver. Moreover, the changes of argument of perigee do not have to be monitored because the satellite is inoperative when it carries out the disposal maneuver.

We impose the eccentricity of the final orbit to be zero because the purpose is to obtain a circular disposal orbit. The results presented use the maximum possible value of the magnitude of the in-plane acceleration vector f_{12}, which is established in Eqs. 88: $f_{12} = 3.17 \cdot 10^{-8}\ km/s^2$. The burn arc is centered at apogee, therefore $\sigma = +1$. The used dry mass is 3000 kg and the specific impulse is 3000 s, which is a realistic value for an electric propulsion system. To select which is the adequate arc extension, expressed by means of α, to execute the low thrust disposal maneuver by using the minimum propellant mass, all the possible values of α , which are ranged between $\alpha = 0^o$ (apogee) and $\alpha = 180^o$ (perigee), are analysed.

The results obtained by means of steering case 2 are not realistic and may have some computational mistakes. For reasons of time and complexity, this steering case is left as a further study. The outcomes of steering case 1 and 3 are illustrated in the following figures.

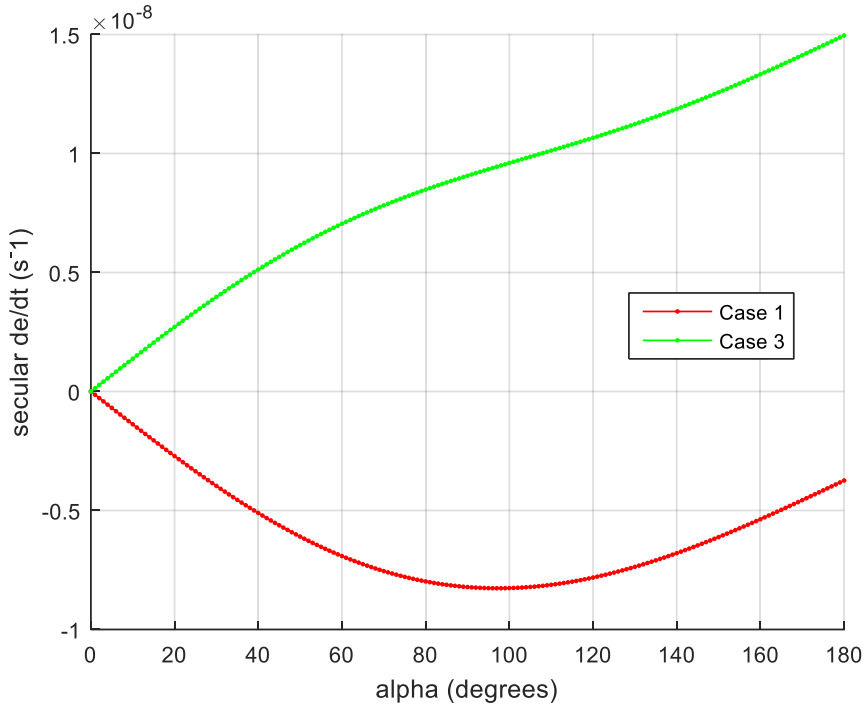

Fig. 31 Secular rates of change of eccentricity for e = 0.25.

Figure 31 outlines the secular rate of change of eccentricity against the arc extension for the analysed steering cases. Both curves start with a zero secular rate, which makes sense considering that if no impulse is applied (the arc extension is zero), it is impossible to modify the eccentricity of the orbit. Case 1 experiences a negative secular rate with a maximum in absolute value situated approximately at $\alpha = 96^o$. Case 3 experiences a positive secular rate which increases continuously, achieving its maximum at $\alpha = 180^o$.

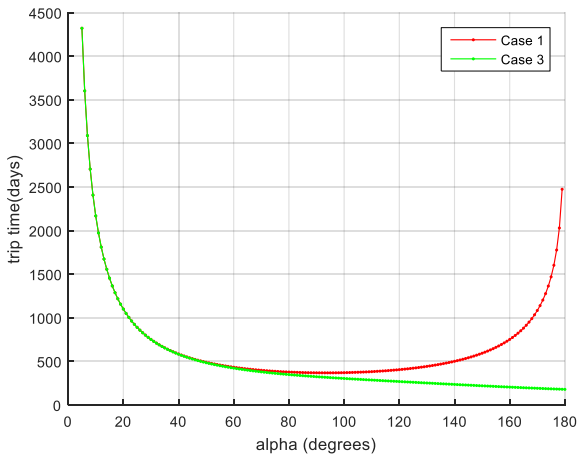

Fig. 32 Trip time e = 0.25.

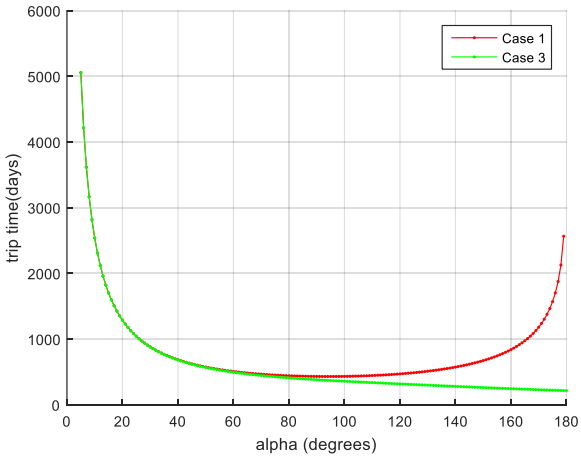

Fig. 33 Trip time e = 0.30.

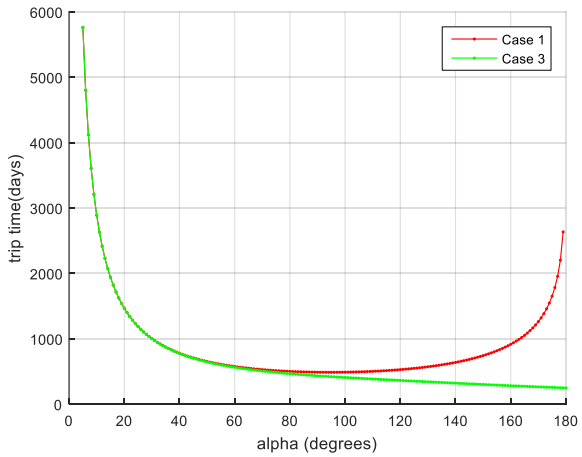

Fig. 34 Trip time e = 0.35.

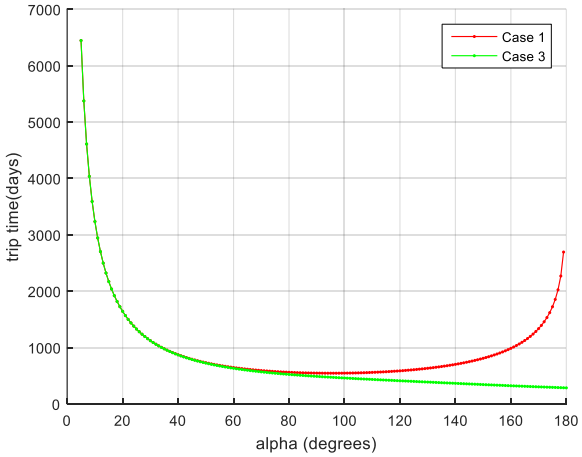

Fig. 35 Trip time e = 0.40.

Figures 32, 33, 34 and 35 show the trip time against the arc extension for both steering cases and for each initial eccentricity. It is observed that while the eccentricity of the initial orbit increases, the trip time increases too, which means that the curves are moved upwards following the ordinate axis. For small arc extensions, the trip time is extremely high. This makes sense considering that the thrust provided by an electric propulsion system is considerable small, therefore, to modify the orbit, a continuous thrust with a suitable arc extension is needed. If the arc extension is overly short, several burns and stops of the engine will be required to perform the whole maneuver, and since the burn is only carried out during a short time of the orbital period, the trip time will be high.

Case 1 has a minimum approximately at $\alpha = 96^o$ and then the trip time increases again. This is because the secular rate of change of eccentricity, described in Figure 31, has a maximum in absolute value approximately at $\alpha = 96^o$ and, then, it starts to decrease. The rate of change of eccentricity obtained by means of steering case 3 increases continuously, therefore the trip time decreases continuously until $\alpha = 180^o$. Consequently, the minimum trip time is obtained at such arc extension.

Figures 36, 37, 38 and 39 illustrate the velocity variation against the arc extension for both steering cases and for each initial eccentricity. Considering that velocity variation is proportional to trip time, as it is expressed mathematically by means of Eqs. 99, the evolution of the velocity variation curve against the arc extension for both steering cases is equal to that described for the trip time.

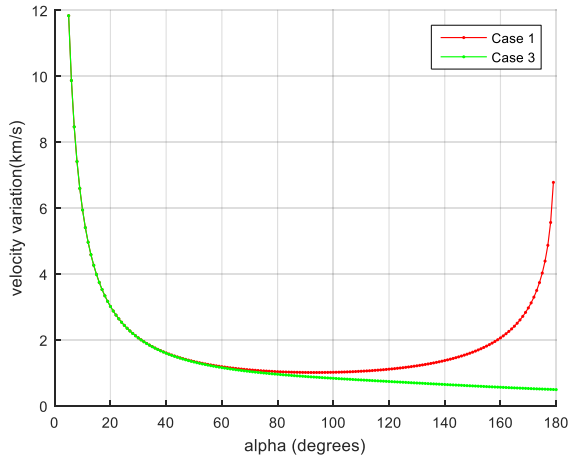

Fig. 36 Velocity variation e = 0.25.

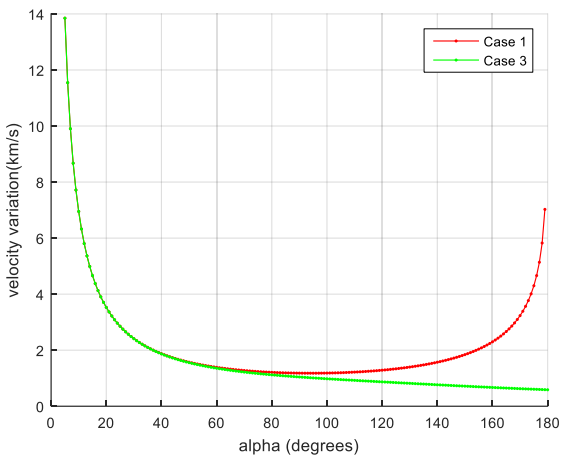

Fig. 37 Velocity variation e = 0.30.

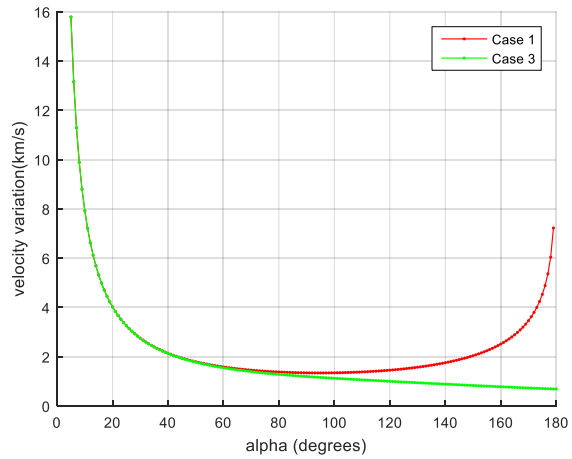

Fig. 38 Velocity variation e = 0.35.

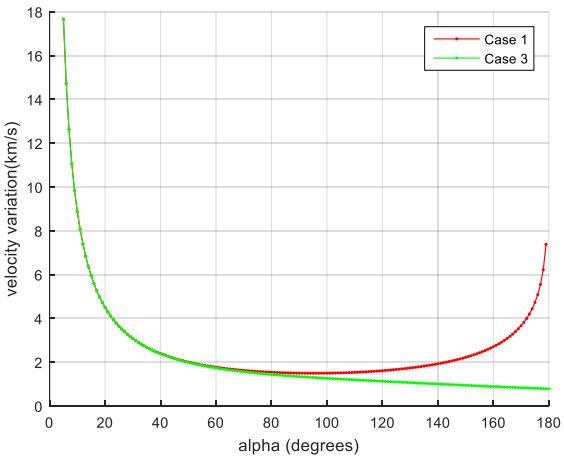

Fig. 39 Velocity variation e = 0.40.

Figures 40, 41, 42 and 43 show the propellant mass against the arc extension for both steering cases and for each initial eccentricity. The evolution of the curves for each steering case is extremely similar to the evolution described for trip time and velocity variation. It is interesting to highlight that for an arc extension larger than $\alpha = 20^o$, the propellant mass needed to execute the low thrust disposal maneuver is considerable lower than that required to obtain the circularization by means of an impulse maneuver. Nevertheless, the trip time is much bigger with the low-thrust strategy.

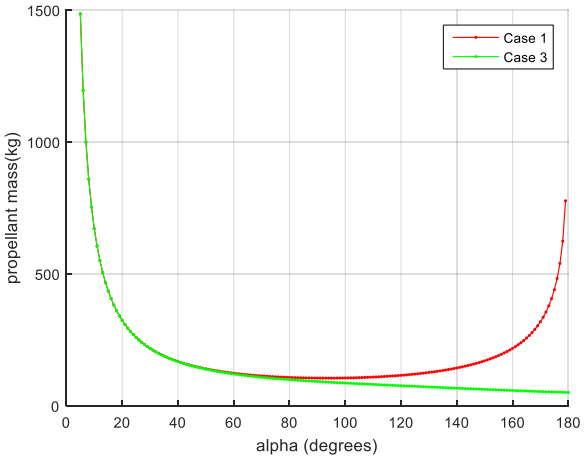

Fig. 40 Propellant mass for e = 0.25.

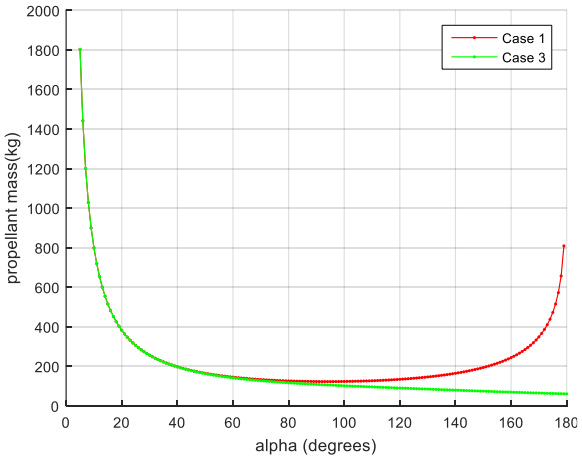

Fig. 41 Propellant mass for e = 0.30.

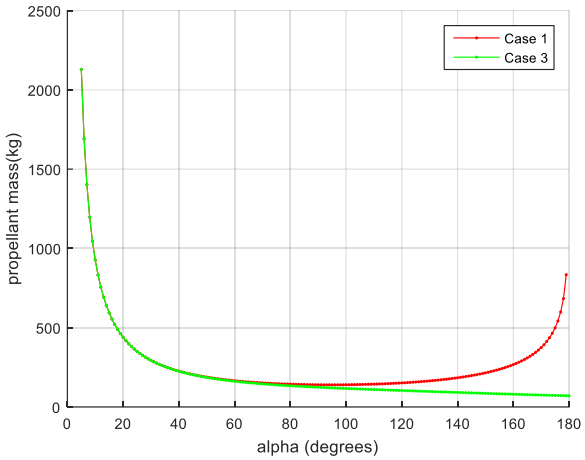

Fig. 42 Propellant mass for e = 0.35.

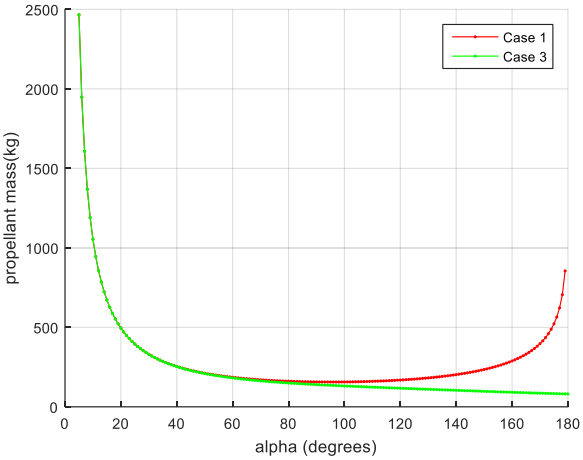

Fig. 43 Propellant mass for e = 0.40.

4.3.4. Propellant budget of low thrust maneuvers

The figures presented in Section 4.3.3 are really useful because they allow to find the suitable arc extension to carry out the disposal maneuver by using the minimum propellant mass. Ones the adequate arc extension is encountered, it is possible to find the trip time and the velocity variation by means of the other presented figures.

Table 13 shows the extension of the arc, the trip time and the velocity variation needed to obtain the low-thrust strategy that circularizes the orbit by means of the steering case 1 while using the minimum propellant mass. The mentioned useful data is detailed for each of the four initial eccentricities. Table 14 provides the same data but for the steering case 3.

Case 1 - Combinations	1	2	3	4
Eccentricity e_0	0.25	0.30	0.35	0.40
Extension of the arc α *(deg)*	92	92	94	96
Trip time *(days)*	369.2	430.5	488.7	544.8
Velocity variation Δv (km/s)	1.01	1.18	1.34	1.49
Propellant cost m_p (kg)	104.9	122.6	139.6	156.0

Table 13 *Minimum propellant cost of the disposal maneuver by means of the steering case 1.*

Case 3 - Combinations	1	2	3	4
Eccentricity e_0	0.25	0.30	0.35	0.40
Extension of the arc α *(deg)*	180	180	180	180
Trip time *(days)*	179.6	214.7	249.9	285.5
Velocity variation Δv (km/s)	0.49	0.59	0.68	0.78
Propellant *cost* m_p (kg)	50.6	60.54	70.6	80.8

Table 14 *Minimum propellant cost of the disposal maneuver by means of the steering case 3.*

By comparing the results obtained by means of the low thrust strategy and the results of the impulse maneuver presented in Table 10, the low thrust disposal strategy that uses the steering case 3 (f_{12} tangent to the orbit path) with a burn arc centered at apogee and an arc extension of $\alpha = 180^o$ is the most suitable disposal maneuver to circularize any of the eccentric highly-inclined geosynchronous orbits studied in this TFG. This is because it carries out the maneuver with the minimum propellant mass and also the minimum time in comparison with the other low-thrust strategies.

The propellant mass of this disposal maneuver is estimated between 50 and 100 kg. This means a reduction of 90% the propellant mass used in the impulse maneuver. This significant reduction allows the satellite to keep approximately constant the mass estimated without the disposal strategy. Therefore, an extra fuel tank is not required and the satellite's structure will not need to be modified.

4.3.5. Sketch of the low-thrust maneuver

A Matlab script is programed to plot the disposal maneuver. To show an example, if we select the data:

$$a_0 = 42164.6km; e_0 = 0.25; i_0 = 55^o;\ \omega_0 = 270^o;\ \Omega_0 = 0^o, \qquad (166)$$

which describe one of the studied orbits, Figure 44 and 45 are obtained. These plots show the initial orbit in blue and the final orbit in magenta. The initial orbit is an eccentric highly-inclined geosynchronous orbit with the selected data and the final orbit resulting from the circularization is a circular orbit with an inclination equal to that of the initial orbit, as seen in Figure 44. The low thrust maneuver is illustrated in red and the position of the Earth is represented with a black dot in the origin of the reference system used.

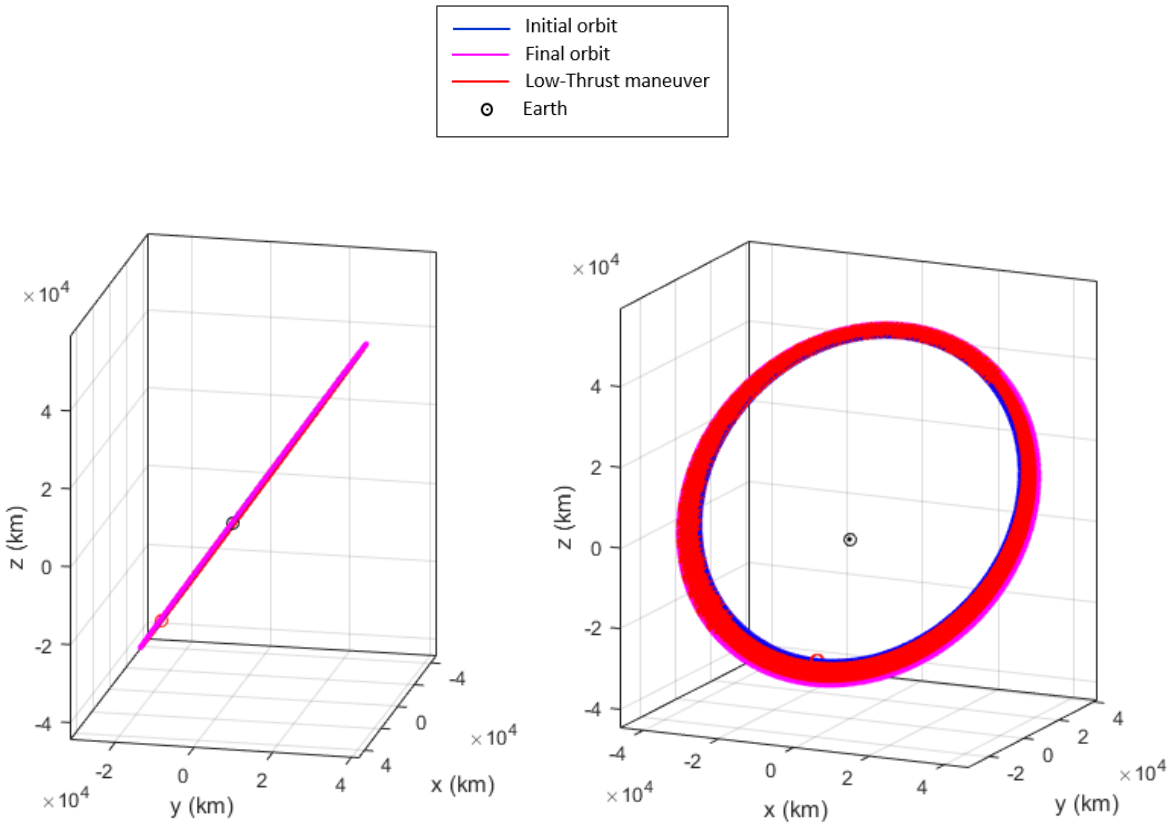

Fig. 44 3D view of the initial and final orbit, both with the same inclination.

Fig. 45 3D view of the initial and final orbit and the low thrust maneuver.

The low-thrust maneuver outlined in Figure 45 has a trip time of 179.6 days. Although it cannot be seen in Figure 45 because the zoom is not enough, the trajectory followed by the spacecraft when it is executing this low thrust maneuver can be described as some coplanar almost circular

arcs which are increasing its altitude in order to reach the altitude of the final orbit. To illustrate this concept, another simulation of another low-thrust maneuver with a larger trip time has been implemented. Figure 46 shows the same initial orbit, whose orbital elements are described in Eqs. 166, in blue; a random final orbit in magenta and the trajectory of the low-thrust maneuver in red. This maneuver has a trip time of 538.8 days. Although it is not a realistic low-thrust disposal maneuver, it perfectly shows the typical trajectory followed by spacecraft while carrying out a low thrust maneuver.

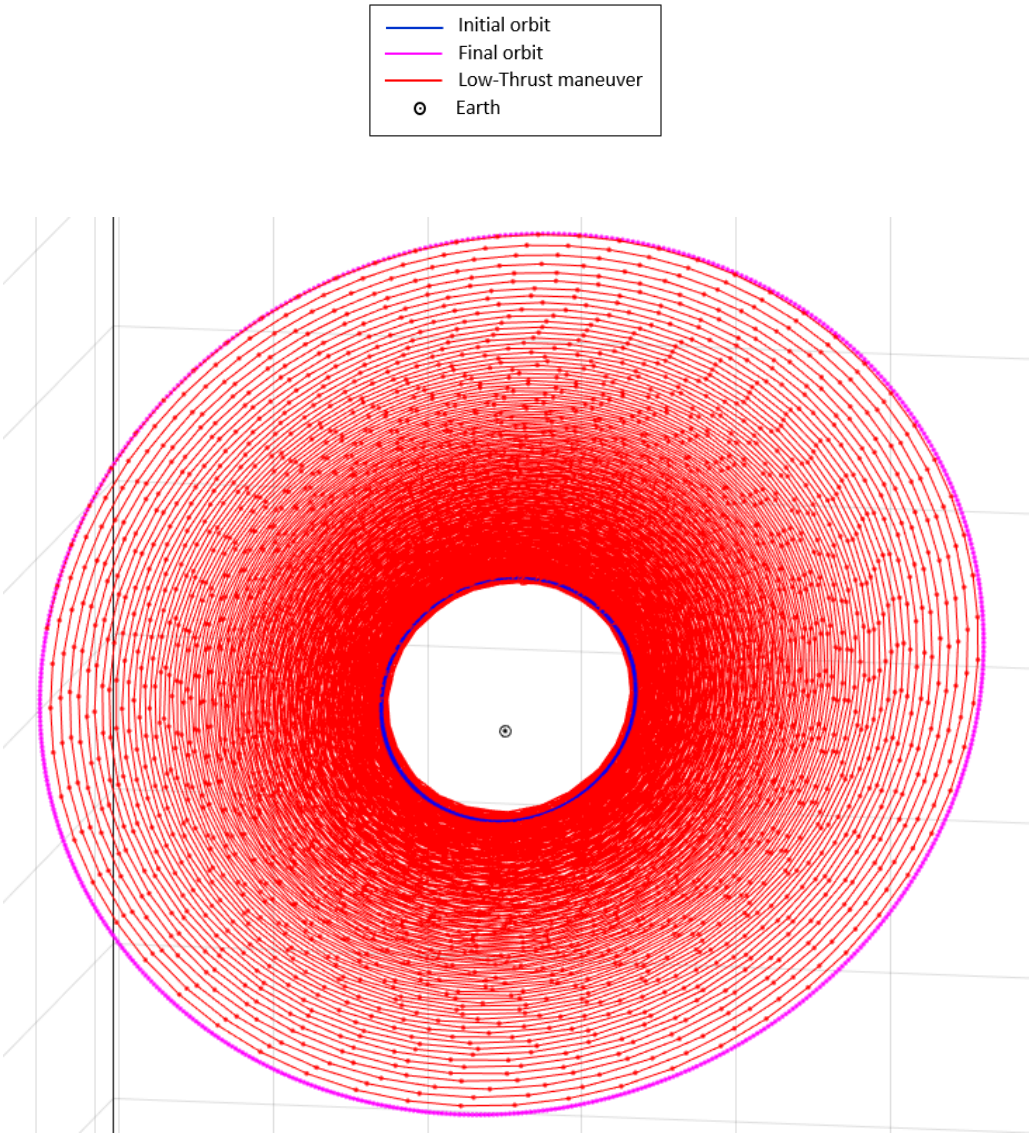

***Fig. 46** Sketch of the typical trajectory followed by spacecraft while carrying out a low thrust maneuver.*

V. Safety

To keep the rate of progress of space missions and guarantee the security of space environment and all spacecraft flying in it, it is essential to carry out the operations fulfilling the space safety requirements. Space safety can be defined as freedom from natural or man-made damaging situations. These damaging situations are those conditions that can be responsible of injury, death, illness, damage to or loss of equipment, systems, property or facilities, or damage to the space environment. Additionally, space safety includes the security of human on-board, personnel involved with the mission and general public. For unmanned satellites, degradation or loss of mission intentions are also considered harmful conditions.

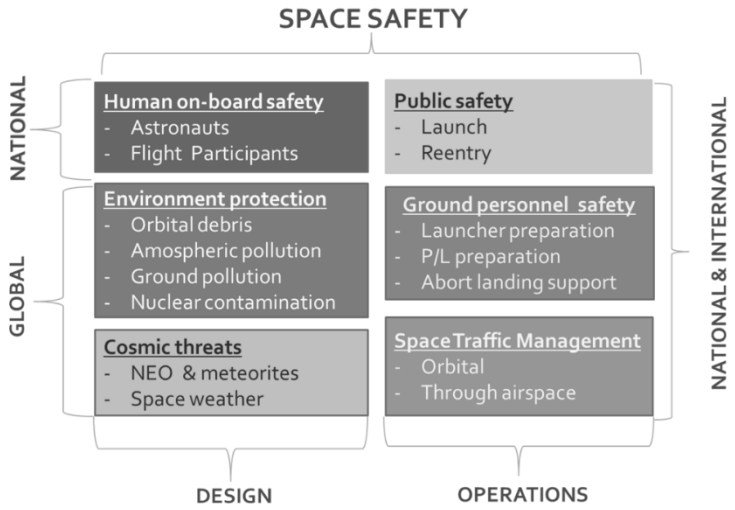

Fig. 47 Fields of space safety [51].

Figure 47 shows some fields of space safety; its main areas of interest, which can be national, international or global; and the principal ways for guaranteeing safety, which is by means of design and operations. To consider an environment or spacecraft absolutely safe, it should never cause or have the potential to cause a harmful condition. Consequently, complete freedom from damaging situations is impossible to achieve. Safety generally means acceptable risk level, not absolute safety conditions. To make a system safe, it is needed to test and implement the best practices at state-of-art, which are traditionally determined by government regulations and industrial standards. The acceptable risk level of any space system can be represented by the accomplishment of regulations, norms and standards.

Undesirable collision of a satellite with space debris or with another spacecraft is one of the most harmful situations in space. The risk of collision increases when an inoperative satellite is left in its operational orbit. In such case, the orbit will develop freely under the perturbations, it can suffer modifications which cannot be predicted and it can cross other satellites or space debris orbits. The potential danger grows when the orbit is near the GEO ring, where a huge amount of satellites are orbiting, which is the present case in this TFG. The probability that the satellite crosses the GEO ring has to be considered. The study identifies and evaluates alternative options for satellite end-of-life disposal from an eccentric highly-inclined geosynchronous orbit. By means of performing a disposal strategy, the study aims at reducing collision risk. To design the disposal maneuver, the regulations, norms and standards established by UNOOSA, which is the main organization responsible for space law, are fulfilled.

VI. Environmental Implication

Current engineering, besides considering the functional and economic aspects of the mission, has to minimize the environmental impact. It has a considerable importance in industries that design and manufacture systems and devices which, during their regular working cycle, can release harmful substances for the environment. This is also the case of space industry, which has invested a significantly amount of resources to innovate, design and develop environmentally friendly technologies and propellant. For instance, NASA has developed alternative propellant for rockets in order to throw away the tremendously risky solid rocket engines.

Additionally, as it has been explained in Section 1, space debris is the main problem in the space surroundings of the Earth. An impact with even a miniscule fragment can be catastrophic at orbital speeds. Some disposal strategies have been promoted over the years for several means of removing inoperative satellites and debris from the Earth space environment. In a smaller impact scale, another issue that can affect the environment is the computational energetic cost used for aerospace simulations.

6.1. Fuel emissions reduction

The overall weight of any spacecraft is a characteristic parameter of its mission and it is responsible of the amount of fuel emissions. During the launch, if the weight of the satellite increases, more propellant mass is needed to put the satellite on orbit. Therefore, any method or technology that provides a solution to minimize the mass of a spacecraft directly decreases the propellant consumption of the launcher, which leads to a reduction of emissions.

The study developed in this TFG aims at analysing several disposal strategies to find the maneuver which requires less propellant mass to carry out the whole disposal strategy. If the propellant mass needed to execute this maneuver is reduced, the total mass of the satellite can be reduced too, which decreases fuel emissions during the launch. Moreover, if the disposal strategy is developed by using the minimum fuel, the propellant emissions released during this phase of the mission are also reduced.

6.2. Space debris and collision risk reduction

The purpose is to avoid an accumulation of inoperative satellites, and the associated growth in population density and potential risk of collision that this situation would lead to. Considering the limitations of space propulsion systems, a re-entry maneuver hardly can be carried out from an eccentric highly-inclined geosynchronous orbit, such those studied in this TFG. This is mainly because the propellant costs to perform a de-orbiting maneuver from this family of orbits are extremely high. Moreover, these un-functional objects cannot be moved to orbits below the GEO protected area because, in such case, they can be a collision hazard for future spacecraft injected into the geosynchronous region. Consequently, a disposal region must be established above and at an altitude sufficiently high that under the influence of perturbing forces, the satellite cannot interfere with existing operational satellites in the GSO region. This TFG considers all these problems and provide an efficient solution to avoid them.

6.3. Computational energetic cost reduction

Aerospace simulations can reach excessive levels of electricity consumption. To develop large simulations, companies and research centres consume high amounts of electricity. Mathematical and physical models can optimize the computations and reduce energy consumption. Consequently, in more advanced investigations of the strategies analysed in this TFG, computational models should be implemented.

VII. Future Lines of Investigation

The study developed in this TFG aims at identifying and evaluating alternative options for satellite end-of-life disposal from an eccentric highly-inclined geosynchronous orbit. Bearing in mind the disposal requirements, the study searches for the most efficient option between all the analysed. Specifically, it aims at minimizing the propellant mass needed to perform the disposal maneuver. By using the low thrust maneuver, the disposal strategies presented in the results provide a fairly good solution from the point of view of efficiency. However, the proposed strategy can be improved in future investigations.

Considering that, in the present low thrust strategy, the apogee does not raise its altitude, or at least it does not change too many, the hypothesis used to obtain the semimajor axis as a function of the eccentricity and the apogee altitude, which is taken to be constant, provides realistic results. However, an interesting option to improve the algorithm is consider the apogee radius variations.

Moreover, low thrust disposal strategies can be optimized by means of the implementation of optimal control theory and calculus of variation. The focus of future studies will be to apply the classical methods of optimal control theory to the problem of circularizing an eccentric highly-inclined geosynchronous orbit using low thrust propulsion systems. It will be interesting to minimize the shift of the apogee altitude during each apoapsis pass. Additionally, some mathematical and physical models will be implemented to reduce the computational cost.

VIII. Planning and Scheduling

In this section it is detailed the planning and scheduling followed to organize and develop the project in order to finish all tasks on time. Additionally, bearing in mind the future lines of investigation presented in Section 7, a possible planning to continue with the study is presented.

8.1. Planning and scheduling followed

The planning and scheduling followed to develop this study is described in this section. No substantial scheduling problems have been experienced and a few rescheduling tasks have been done to introduce new sections.

8.1.1. Brief task description

To achieve the goal of the project, the following work packages and tasks have been developed:

1. **Introduction**

   Brief introduction of the project including a description of the need that is being covered and an analysis of its usefulness. Study of the advantages or disadvantages of this approach. Identification of the critical elements of the research and description of some previous experiences in the context.

2. **State of art**

   To have a preliminary idea of the current situation and the aims to achieve, a bibliographic study of the previous disposal missions in GEO and geosynchronous orbits will be considered.

3. **Certifications and regulations**

   To ensure that the recommendations for end-of-life disposal strategies follow the specific requirements, a research on space satellite navigation regulations will be carried out. The main organisation that normalises space navigation is UNOOSA.

4. **Description of the orbits**

   Highly-inclined geosynchronous orbits will be studied and characterized in order to establish a base to begin with the analysis of end-of-life disposal strategies considering also the possible troubles that may appear due to the operational environment where the maneuvers will be performed. The following points will be covered:

4.1. Characterization of the orbit

Description of the orbit elements and selection of their range of values for these specific solutions.

4.2. Operational environment

Some external problems may occur during the execution of the maneuvers, to prevent them, a study of the operational environment must be developed. However, too many risks can occur in space and the time to develop the TFG is overly little to evaluate all the possible troubles. For this reason, this point will be a brief description of the operational environment and an introduction to the future work that should be done. The main concern is space debris.

5. Possible types of propulsion systems

To perform the disposal maneuvers, a propulsion system must be selected. First, a comparison between the main thrusters will be developed considering their suitability to operate in the mentioned orbit and advantages and drawbacks. In a first step, two options will be contemplated:

5.1. Chemical engines.

5.2. Electrical engines.

6. Possible end-of-life disposal strategies

To ensure the selection of a suitable, effective and efficient maneuver, an analysis of the possible strategies will be developed, highlighting the positive and negative effects of each case. The main end-of-life disposal strategies that will be studied are the following ones:

6.1. De-orbiting

A study of the feasibility of this post-mission disposal option considering the initial orbit. If this strategy is possible, a deeper analysis will be developed considering two options:

6.1.1. Uncontrolled de-orbiting

6.1.2. Controlled de-orbiting

6.2. Maneuvers to disposal regions

It consist on the study of a suitable maneuver to move the spacecraft to a specific disposal area in which it will not be an obstacle for upcoming space operations. A useful solution is the circularization, which will also be analysed.

6.2.1. Impulse maneuver

6.2.2. Low thrust maneuver

7. Detailed description of the maneuver strategy

Once chosen the appropriate end-of-life disposal strategy, a deeper analysis will be developed, taking into account all the details which are necessary to fully define the maneuver.

7.1. Maneuver description

7.2. Cost and requirements on the propellant mass

7.3. Execution times

8. Simulation of the disposal maneuver

By using Matlab software, a simulation of the satellite end-of-life disposal from an eccentric highly-inclined geosynchronous orbit will be implemented. The availability of a visual tool will be useful in the development of the project.

9. Report

Elaboration of the document that summarizes all the general aspects of the research and includes the study and the computations to obtain the suitable satellite end-of-life disposal strategy.

10. Presentation

Preparation a talk and graphical support in order to show the work done throughout the project and the results obtained.

8.1.2. Interdependency relationship amongst tasks

Code	Task identification	Preceding task(s)
IN	Introduction	-
SA	State of art	-
CR	Certifications and regulations	-
DO	Description of the orbits	DO.1, DO.2
DO.1	Characterization of the orbit	-
DO.2	Operational environment	DO.1
PS	Possible types of propulsion systems	PS.1, PS.2
PS.1	Chemical engines	SA, DO, CR
PS.2	Electrical engines	SA, DO, CR
DS	Possible end-of-life disposal strategies	DS.1, DS.2
DS.1	De-orbiting	DS.1.1, DS.1.2
DS.1.1	Uncontrolled de-orbiting	SA, IN, DO, CR, PS
DS.1.2	Controlled de-orbiting	SA, IN, DO, CR, PS
DS.2	Maneuvers to disposal regions	DS.2.1, DS.2.2
DS.2.1	Impulse maneuver	SA, IN, DO, CR, PS
DS.2.2	Low thrust maneuver	SA, IN, DO, CR, PS
DMS	Detailed description of the maneuver strategy	DMS.1, DMS.2, DMS.3
DMS.1	Maneuver description	DO, PS
DMS.2	Cost and requirements of the propellant mass	DO, PS
DMS.3	Execution times	DO, PS
SDM	Simulation of the disposal maneuver	DMS
RT	Report	IN, SA, CR, DO, PS, DS, DMS
PT	Presentation	RT, SDM

Table 15 *Interdependency relationship amongst tasks.*

8.1.3. Level of effort (hours) to develop each task

Code	Task identification	Level of effort (h)
IN	Introduction	16
SA	State of art	18
CR	Certifications and regulations	22
DO	Description of the orbits	8
DO.1	Characterization of the orbit	52
DO.2	Operational environment	36
PS	Possible types of propulsion systems	-
PS.1	Chemical engines	12
PS.2	Electrical engines	12
DS	Possible end-of-life disposal strategies	-
DS.1	De-orbiting	-
DS.1.1	Uncontrolled de-orbiting	5
DS.1.2	Controlled de-orbiting	5
DS.2	Maneuvers to disposal regions	-
DS.2.1	Impulse maneuver	36
DS.2.2	Low thrust maneuver	122
DMS	Detailed description of the maneuver strategy	-
DMS.1	Maneuver description	12
DMS.2	Cost and requirements of the propellant mass	32
DMS.3	Execution times	22
SDM	Simulation of the disposal maneuver	32
RT	Report	50
PT	Presentation	20
FDP	**Final degree project**	**512**

Table 16 *Level of effort (hours) to develop each task.*

8.1.4. Preliminary Gantt chart

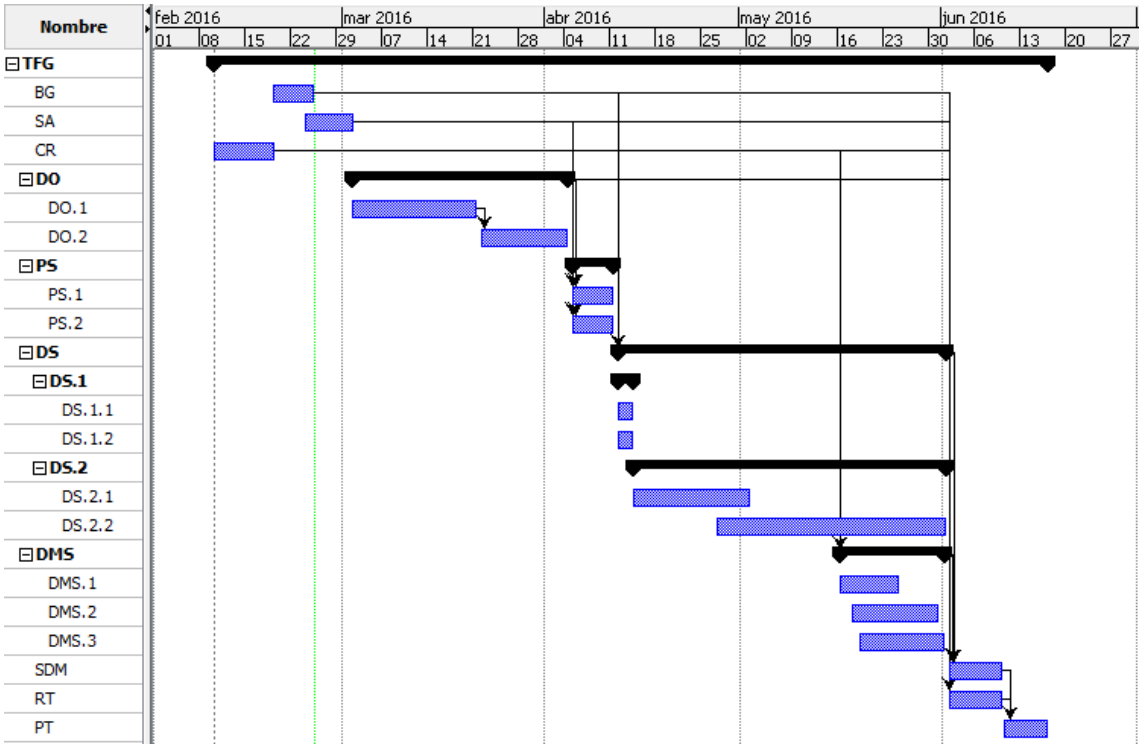

Fig. 48 Followed Gantt Chart.

8.2. Future planning and scheduling

In this section it is described a possible planning and scheduling for further studies related with the issues presented in this TFG. Considering the objectives proposed in Section 7, the main reference used to obtain some ideas of the tasks to be done is the thesis developed by Brenton John Duffy [48]. A brief explanation of the proposed tasks is presented in Section 8.1 and a possible schedule starting on 1st September 2016 is shown by means of a Gantt chart.

8.2.1. Brief task description

1. **Introduction**

   Brief introduction of the project including a description of the need that is being covered and an analysis of its usefulness. Study of the advantages or disadvantages of this approach. Identification of the critical elements of the research and description of some previous experiences in the context.

2. State of art

To have a preliminary idea of the current situation and the aims to achieve, a bibliographic study of the previous disposal missions will be considered.

3. Orbital mechanics

This section will explain the dynamics of orbital mechanics. Specifically the purpose will be to analyse the simplest case, which is the two-body problem in which a satellite is under the gravitational influence of a central body. Once this concept is well defined, the circularization maneuver will be introduced.

4. Low-thrust propulsion

An introduction to low-thrust disposal maneuvers will be presented. Moreover, a description of the possible strategies by means of continuous low-thrust will be analysed, highlighting the main advantages and disadvantages of each option.

5. Notation

Description of the notation used to develop the algorithm of this project. It is based on the common notation used in optimal control texts.

6. Optimal control theory for low-thrust propulsion

The purpose of this section is to describe the optimal control theory, which is derived from the Calculus of Variations. This applied theory deals with the problem of finding a control law for a given space system. The following points will be covered:

6.1. Problem formulation

Formulation of the needed equations to control a shift over time of the orbital elements due to an acceleration provided by the propulsion system. The dynamics of low-thrust propulsion will be described using Lagrange's planetary equations.

6.2. Necessary conditions for optimality

A description of the required conditions to optimally control the disposal maneuver will be presented. These conditions for optimality can be:

6.2.1. First-order conditions.

6.2.2. Second-order conditions.

6.3. Control law

This section will provide an introduction to the optimal control law, which is based on the weak form of Pontryagin's minimum principle.

6.4. Numerical solution to the terminally constrained TPBVP

By means of the control law, a numerical solution for the Two-Point Boundary Value Problem (TPBVP) will be implemented.

6.5. Interior point constraints

In this section, the optimal control problem is presented with regard to constraining the apoapsis altitude. One interesting approach consist of applying one or more interior point constraints whenever the satellite flies near apoapsis. The following points will be covered:

6.5.1. First-order necessary conditions for a single orbit

6.5.2. First-order necessary conditions for multiple orbits

6.5.3. Second-order necessary conditions

6.5.4. Numerical solution to the interior constrained MPBVP

The required conditions for an optimal control solution to the constrained interior point optimal control problem need the result of a first-order multi-point boundary value problem (MPBVP). Therefore, a numerical solution to the interior constrained MPBVP will be implemented.

6.6. Performance measures

The velocity variation and the propellant mass required to carry out the desirable circularization maneuver will be computed in order to measure the performance of the low-thrust strategy.

7. Algorithm validation

To validate the algorithm, the following validation problems will be presented:

7.1. Maximize semimajor axis

7.2. Minimize eccentricity

8. Optimizing the circularization maneuver

In this section, the optimal control problem for circularizing an eccentric highly-inclined geosynchronous orbit will be considered. The following three formulations are presented:

8.1. Unconstrained apoapsis

8.2. Terminally constrained apoapsis

8.3. Interior and terminally constrained apoapsis

The first two problems must be solved by means of a numerical solution for the TPBVP whereas the last case requires a MPBVP. All three cases will be analysed in detail for single and multiple orbit maneuvers.

9. Report

Elaboration of the document that summarizes all the general aspects of the research and includes the study and the computations to obtain the suitable disposal strategy.

8.2.2. Interdependency relationship amongst tasks

Code	*Task identification*	*Preceding task(s)*
IN	Introduction	-
SA	State of art	-
OM	Orbital mechanics	-
LT	Low-thrust propulsion	-
NT	Notation	LT
OC	Optimal control theory	OC.1, OC.2, OC.3, OC.4, OC.5, OC.6
OC.1	Problem formulation	IN, SA, OM, LT, NT
OC.2	Necessary conditions for optimality	OC.2.1, OC.2.2
OC.2.1	First-order conditions	LT, NT, OC.1
OC.2.2	Second-order conditions	LT, NT, OC.1
OC.3	Control law	LT, NT, OC.1
OC.4	Numerical solution to the terminally constrained TPBVP	LT, NT, OC.1, OC.3
OC.5	Interior point constraints	OC.5.1, OC.5.2, OC.5.3, OC.5.4
OC.5.1	First-order necessary conditions for a single orbit	LT, NT, OC.1, OC.3
OC.5.2	First-order necessary conditions for multiple orbits	LT, NT, OC.1, OC.3
OC.5.3	Second-order necessary conditions	LT, NT, OC.1, OC.3
OC.5.4	Numerical solution to the interior constrained MPBVP	LT, NT, OC.1, OC.3
OC.6	Performance measures	OC.3, OC.4, OC.5
AV	Algorithm validation	AV.1, AV.2
AV.1	Maximize semimajor axis	OC
AV.2	Minimize eccentricity	OC
OCM	Optimizing the circularization maneuver	OCM.1, OCM.2, OCM.3
OCM.1	Unconstrained apoapsis	OC, AV
OCM.2	Terminally constrained apoapsis	OC, AV
OCM.3	Interior and terminally constrained apoapsis	OC, AV
RT	Report	IN, SA, OM, LT, NT, OC, AV, OCM

Table 17 Interdependency relationship amongst tasks.

8.2.3. Proposed Gantt chart

A possible schedule starting on 1st September 2016 is presented in Figure 49.

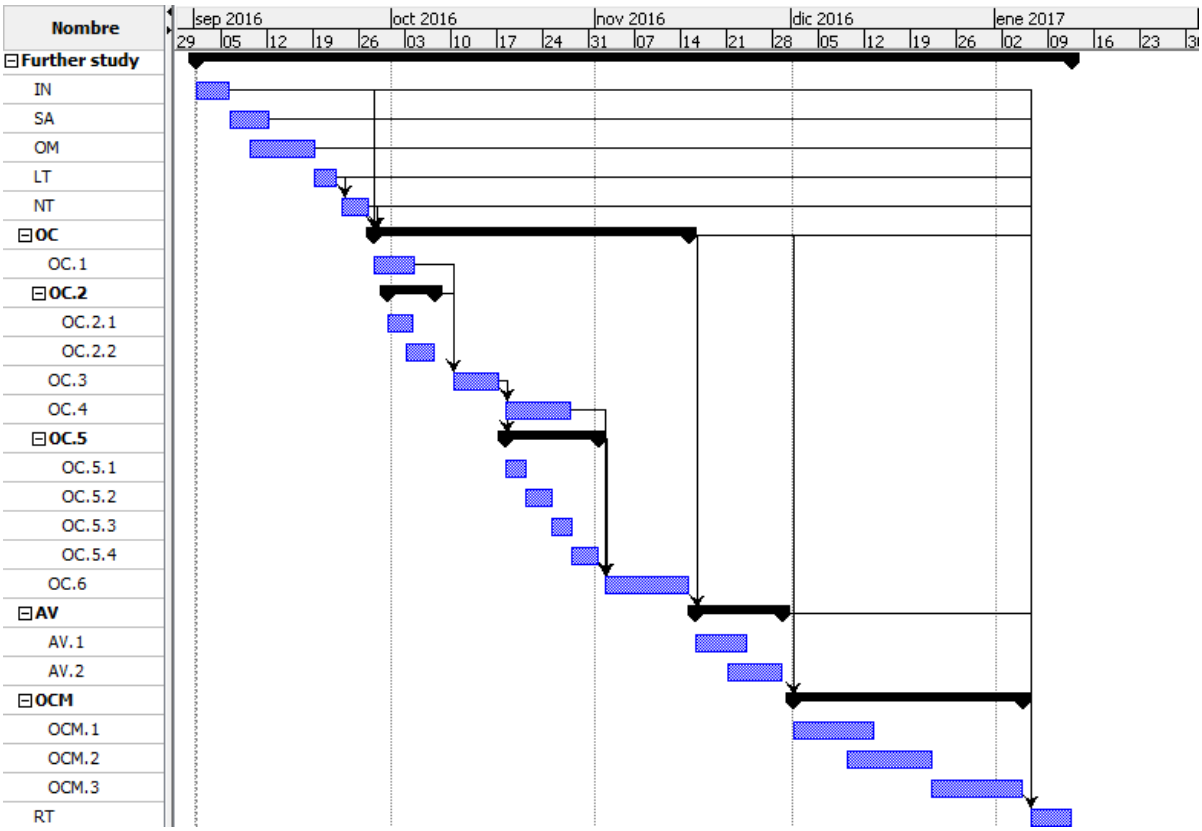

***Fig. 49** Proposed Gantt chart.*

IX. Budget

The budget is presented in detail in a separate document. This section gives a small overview of the budget of the Study of end-of-life disposal options for highly-inclined geosynchronous satellites. The costs are divided into:

- Engineering work, which can be estimated in 7680.00 €.
- Hardware, which is the price of the equipment invested in the study. The subtotal of hardware components can be estimated in 162.60 €.
- Software, which includes all the licenses of the software used to carry out the study. The subtotal of software licenses can be estimated in 580.00 €.
- Electric power consumption, which is a result of the processing time required by the project. The subtotal of simulation hours can be estimated in 15.51 €.

An overhead of 10% has been applied to the engineering work cost estimation and to the processing costs. No overhead has been applied to hardware and software expenses, as their cost is considered to be already established. The total cost of the study is estimated to 9207.66 €.

X. Economic Viability

As it was presented in Section 2.3.3, once the mission is ended, the station-keeping maneuvers are no longer applied. Consequently, if the satellite is left in its operational orbit, the orbit will develop freely under the perturbations described in Section 2.3.1. In general, the likelihood that it crosses the GEO ring is not small and has to be considered. Therefore, an evaluation of alternative options for satellite end-of-life disposal from an eccentric highly-inclined geosynchronous orbit is required.

The most suitable and common post-mission strategy consists of moving the spacecraft to a high disposal orbit. A useful solution is the circularization or almost circularization of the disposal orbit. If this circularization is carried out at apoapsis by means of an impulse maneuver that uses a chemical propulsion system, the required propellant mass is estimated between 500 and 1000 kg, depending on the eccentricity of the initial orbit. To bring this amount of propellant mass, an extra fuel tank is needed. This means the whole satellite mass increases and, consequently, satellite's structure will probably need to be modified according to the new mass requirements. Therefore, an impulse maneuver is not affordable because the required extra mass and cost are overly high.

This study proposes an alternative strategy by means of a low-thrust system. The presented low-thrust disposal strategy uses an electrical propulsion system with the in-plane acceleration thrust vector perpendicular to the semimajor axis of the orbit. The propellant mass of this disposal maneuver is estimated between 50 and 100 kg. This means a reduction of 90% the propellant mass used in the impulse maneuver. This significant reduction allows the satellite to keep approximately constant the mass estimated without the disposal strategy. Therefore, an extra fuel tank is not required and the satellite's structure will not need to be modified. Consequently, the economic savings are considerable.

The total cost of the study is estimated to 9207.66 €. Considering the remarkable propellant mass reduction and the economic savings, the costs of the study will be compensated and will make affordable the disposal strategy.

XI. Conclusions

In this chapter, we draw the conclusions of the study. The objective of this work was to identify and evaluate alternative options for satellite end-of-life disposal from an eccentric highly-inclined geosynchronous orbit.

Numerous studies [1, 2, 3, 4] have identified telecommunications gaps in the northern regions, specifically in the Artic zone, Canada and northern Russia. The lack of radio and satellite communications for data and voice transmission in this area, the noticeable intensification of aircraft operations at high latitudes and the increase of the commercial shipping activity in the North East Passage, create the need for enhancing aeronautical traffic services and operational communications. These points show the increased demand for communications services in the Arctic. In previous studies [8], a family of eccentric, highly-inclined geosynchronous orbits have been investigated to achieve the present and upcoming goals.

Once the mission is completed, the station-keeping maneuvers are no longer applied. Consequently, due to natural evolution, these orbits are pulled to cross the geostationary ring. This movement is extremely dangerous due to the high probability of impact with the many satellites operating at such altitudes. Therefore, an end-of-life disposal strategy is required.

The performance of the propulsion system is typically the key factor to design and select the suitable maneuver. Conventional chemical thrusters are characterized by fairly high thrust, but low exhaust velocities, consequently, they give a high specific power. In contrast, electrical rockets are characterised by high exhaust speeds, which means operating at high specific impulse, therefore they use much less propellant in comparison with classical propulsion systems. This comparison between space propulsion systems leads us to two possible disposal strategies, one by means of a chemical engine and the other by using an electrical rocket.

The most suitable and common post-mission strategy for such orbits consists of moving the spacecraft to a high disposal orbit. A useful solution is the circularization. The circularization can be carried out by means of an impulse maneuver, which uses a chemical propulsion system. The results obtained in this study estimate the required propellant mass between 500 and 1000 kg, depending on the eccentricity of the initial orbit. To bring this amount of propellant mass, an extra fuel tank is needed. Therefore, an impulse maneuver is not affordable because the required extra mass and cost are overly high.

One useful and efficient strategy that has become considerably popular in recent years and provides an appropriate disposal strategy is low-thrust propulsion. This is a complex problem, whose solution requires mathematical tools related to calculus of variation. Additionally, with the massive introduction of electric motors, it is a very current problem. The presented investigation has studied different low-thrust disposal strategies, which use an electrical propulsion system. Specifically it has analysed four different steering cases in which the direction of the in-plane acceleration vector can be perpendicular to the orbit radius vector, tangent to the orbit path, perpendicular and parallel to the semimajor axis of the ellipse. The outcomes are analytical solutions based on the Lagrange planetary equations.

For each steering case, several burn arc extensions centered at apogee were studied. To select the most suitable solution, the study has defined the extension of the arc, the trip time and the velocity variation required to carry out the circularisation by using the minimum propellant mass.

Steering case 3, with the in-plane acceleration thrust vector perpendicular to the semimajor axis of the orbit, provides the most efficient and adequate solution. The propellant mass of this disposal maneuver has been estimated between 50 and 100 kg. This means a reduction of 90% the propellant mass used in the impulse maneuver. This significant reduction allows the satellite to keep approximately constant the mass estimated without the disposal strategy. Consequently, the economic savings are considerable. Moreover, if the disposal strategy is developed by using the minimum fuel, the propellant emissions released during this phase of the mission are also reduced.

The total cost of the study is estimated to 9207.66 €. Considering the remarkable propellant mass reduction and the economic savings, the costs of the study will be compensated and will make affordable the disposal strategy.

The focus of future studies will be to apply the classical methods of optimal control theory to the problem of circularizing an eccentric highly-inclined geosynchronous orbit using low thrust propulsion systems. It will be interesting to minimize the shift of the apogee altitude during each apoapsis pass. Additionally, some mathematical and physical models will be implemented to reduce the computational cost.

XII. Bibliography

12.1. Introduction

[1] CHAN, Joseph, SHANNON, Mark, KOKKALAKIS, Michael. *Search for Stable Decommission Orbits for SXM HIEO Satellites*. Washington DC.

[2] Anonymous author. *Arctic Communications System Utilizing Satellites in Highly Elliptical Orbits*. Thesis for the degree of Philosophiae Doctor. Norwegian University of Science and Technology. Faculty of Information Technology, Mathematics and Electrical Engineering. Department of Electronics and Telecommunications. Trondheim, March 2013.

[3] CAVALLARO, G., PHAM-MINH, D., BOUSQUET, M. *HEO Constellation Design for Tactical Communications*. Toulouse, France.

[4] ZEPPENFELDT, Frank. *ESA activities on satellite communications for high latitude regions*.

[5] BURKHARDT, Holger, SIPPEL, Martin, FRITSCHE, Bent. *Evaluation of propulsion systems for satellite end-of-life de-orbiting*. Cologne, Aidlingen, Bremen, Katlenburg-Lindau: American Institute of Aeronautics and Astronautics. AIAA-2002-4208.

[6] CANADIAN SPACE AGENCY. *Polar Communications and Weather mission*. http://www.asc-csa.gc.ca/eng/satellites/pcw/. Checked on 12/02/2016.

[7] MORAND, Vincent, FRAYSSE, Hubert, LAMY, Alain. *End of life disposal of satellites in the GEO region, the issue of high inclinations*. Toulouse.

[8] FANTINO, E., FLORES, R., DI SALVO, A., DI CARLO, M. *Analysis of perturbations and station-keeping requirements in highly-inclined geosynchronous orbits*. Munich, Germany: October 2015.

[9] MERZ, K., KRAG, H., LEMMENS, S. *Orbit Aspects of End-Of-Life Disposal from Highly Eccentric Orbits*. Darmstadt, Germany: ESA/ESOC.

[10] AMSA. *Arctic Marine Shipping Assessment 2009 Report*.

[11] KAY, E., KVAMSTAD, Beate, BEKKADAL, Fritz. *Maritime communications to support safe navigation*. Trondheim, Norway.

[12] WOOD, Lloyd, LOU, Yuxuan. *Revisiting elliptical satellite orbits to enhance the O3b constellation*. University of Surrey.

12.2. State of the art

[13] EUROPEAN SPACE AGENCY. *Geostationary Orbit Impact Detector*. http://space-env.esa.int/R_and_D/gorid/gorid_web.html. Checked on 24/02/2016.

[14] JOHNSON, Nicholas L. *A New Look at the GEO and Near-GEO Regimes: Operations, Disposals, and Debris*. NASA Johnson Space Center.

[15] CROCKETT, Derick Alan. *Geosynchronous earth orbit/low earth orbit space object inspection and debris disposal: a preliminary analysis using a carrier satellite with deployable small satellites*. Utah State University. Logan, Utah.

[16] INTER-AGENCY SPACE DEBRIS COORDINATION COMMITTEE (IADC). *Space debris issues in the geostationary orbit and the geostationary transfer orbits.* Vienna, February.

[17] NASA. *Syncom 2*. NASA Space Science Data Coordinated Archive. http://nssdc.gsfc.nasa.gov/nmc/spacecraftDisplay.do?id=1963-031A. Checked on 24/02/2016.

[18] ESA. *The story of space debris*. http://www.esa.int/spaceinvideos/Videos/2013/04/Space_debris_story. Checked on 26/02/2016.

[19] INTERNATIONAL TELECOMMUNICATIONS UNION (ITU). *Recommendation ITU-R S.580-6. Radiation diagrams for use as design objectives for antennas of earth stations operating with geostationary satellites*. From 1982 to 2003.

[20] NASA. *Process for Limiting Orbital Debris*. NASA technical standard. NASA-STD-8719.14A. Washington, DC.

In this section, bibliography [7 and 8] were also used.

12.3. Legal specifications

[21] COPUOS/SCST - LTS Workshop. *Eutelsat practice & views on long term sustainability*. Vienna: Eutelsat communications, February 2013.

[22] BONNAL, Christophe. *Requirements for Debris Mitigation*. IISL-ECSL Space Law Symposium 2014. Vienna: IAA Space Debris Committee, March 2014.

[23] MARIEZ, Julien, HUCTEAU, Mario. *Overview on space debris activities in France*. Centre National d'Etudes Spatiales. COPUOS LSC, March 2012.

[24] UNOOSA. *United Nations Treaties and Principles On Outer Space, related General Assembly resolutions and other documents*. UNOOSA, V.14-00496 (E). 90p.

[25] VIIKARI, Lotta. *The environmental element in Space Law. Assessing the Present and Charting the Future*. Leiden-Boston: Martinus Nijhoff Publishers, 2008.

[26] BÖCKSTIEGEL, Karl-Heinz, BENKÖ, Marietta, HOBE, Stephan. *Space Law, Basic Legal Documents.* Institute of air and space law at Cologne University. Cologne: Eleven international publishing, May 2005. Volume 1.

12.4. Description of the orbit

[27] AGRAWAIT, Brij N. *High Latitude Communications Satellite*. Naval Postgraduate School. Monterey. California.

[28] BOCCIA, V., GRASSI, M., MARCOZZI, M, NOTARANTONIO, A., SOLLAZZO, L. *Mission analysis and orbit control strategy for a space mission on a polar tundra orbit*. 63rd International Astronautical Congress, Naples, Italy.

[29] BRUNO, Michael Joseph. *Tundra constellation design and station-keeping*. San Jose State University. May 2004.

[30] LIU, Xiaodong, BAOYIN, Hexi, MA, Xingrui. *Extension of the critical inclination*. School of Aerospace, Tsinghua University. Beijing, China.

[31] WERTZ, James R. *Coverage, responsiveness and accessibility for various responsive orbits*. 3rd Responsive Space Conference. Los Angeles, CA. April 25–28, 2005.

[32] Anonymous author. *Overhead system of inclined eccentric geosynchronous orbiting satellites*. *http://www.google.com/patents/US6389336*. Checked on 9/03/2016.

[33] Anonymous author. *Visual Satellite Observing*. *http://www.satobs.org/faq/Chapter-04.txt*. Checked on 9/03/2016.

[34] Anonymous author. *Orbit Perturbations*. *http://aerospacengineering.net/?p=537.* Checked on 23/03/2016.

[35] FRIESEN, Larry J., JACKSON, Albert A., ZOOK, Herbert A., KESSLER, Donald J. *Analysis of orbital perturbations acting on objects in orbits near geosynchronous earth orbit*. NASA Johnson Space Center, Houston, TX, United States. Mar 25, 1992.

[36] SELLERS, Jerry Jon. *Orbit perturbations. https://www.agi.com/resources /educational-alliance-program/astroprimer/primer97.htm.* Checked on 3/03/2016.

[37] Population histograms. *http://www.radicalcartography.net/*. Checked on 11/03/2016.

[38] ESA. EO Portal Directory. *https://directory.eoportal.org/web/eoportal/satellite-missions/q/qzss*. Checked on 13/04/2016.

In this section, bibliography [3, 7, 8 and 14] were also used.

12.5. Possible types of propulsion systems

[39] JANOVSKY, R., KASSEBOM, M., LÜBBERSTEDT, H. *End-of-life de-orbiting strategies for satellites.* OHB System AG, Bremen, Germany.

[40] FANTINO, Elena. *In-Space Propulsion*. University class notes. Polytechnic University of Catalonia (UPC). Barcelona, Spain.

In this section, bibliography [5] was also used.

12.6. Possible end-of-life disposal strategies

[41] INDIAN SPACE RESEARCH ORGANISATION. *List of Communication Satellites*. http://www.isro.gov.in/spacecraft/list-of-communication-satellites. Checked on 24/04 /2016.

[42] EDELBAUM, Theodore N. *Applications of Ion Propulsion to NASA Missions*. ARS Space Flight Report to the Nation, 1961.

[43] EDELBAUM, Theodore N. *The Use of High- and Low-Thrust Propulsion in Combination for Space Missions.* Journal of the Astronautical Sciences, 1962.

[44] EDELBAUM, Theodore N. *Optimum Low-Thrust Rendezvous and Station Keep- ing*. AIAA Journal, July 1964.

[45] KECHICHIAN, J.A. *Low-Thrust Eccentricity-Constrained Orbit Raising*. Journal of Spacecraft and Rockets, 1998.

[46] KECHICHIAN, J.A. *Constrained Circularization in Elliptic Orbits Using Low Thrust with Shadowing Effect.* Journal of Guidance, Control, and Dynamics, 2003.

[47] IRVING, Jack H. *Low thrust Flight: Variable Exhaust Velocity in Gravitational Fields*. Space Technology. New York, 1959.

[48] DUFFY, Brenton John. *A Study of Eccentric Orbit Circularization using Low-Thrust Propulsion*. B.S. in Aerospace Engineering, North Carolina State University. Dec. 2005.

[49] POLLARD, James E. *Simplified Approach for Assessment of Low-Thrust Elliptical Orbit Transfers.* The Aerospace Corporation, Los Angeles.

[50] E.G.C. Burt. *On space manoeuvres with continuous thrust*. Planet. Space Sci. 15, 103-122. 1967.

12.7. Safety

[51] IAASS. *International Association for the Advancement of Space Safety*. http://iaass.space-safety.org/. Checked on 1/06/2016.

12.8. Environmental implication

[52] TATE, Karl. Space Junk Explained: How Orbital Debris Threatens Future of Spaceflight (Infographic). October 1, 2013. *http://www.space.com/23039-space-junk-explained-orbital-debris-infographic.html.* Checked on 1/06/2016.

[53] THE CONVERSATION. *Space junk and the environment: it's a very dark picture indeed.* July 6, 2011. *http://theconversation.com/space-junk-and-the-environment-its-a-very-dark-picture-indeed-2187*. Checked on 1/06/2016.

[54] NASA. Space Debris and Human Spacecraft. Sept. 27, 2013. *http://www.nasa.gov/mission_pages/station/news/orbital_debris.html.* Checked on 1/06/2016.

[55] NASA. Orbital Debris Frequently Asked Questions. *http://orbitaldebris.jsc.nasa.gov/faqs.html.* Checked on 1/06/2016.

Bibliographic style: UNE-ISO 690